Nuclear Science
NEA/NSC/DOC(2015)9
www.oecd-nea.org

Primary Radiation Damage in Materials

OECD
BETTER POLICIES FOR BETTER LIVES

NEA
NUCLEAR ENERGY AGENCY

Nuclear Science

Primary Radiation Damage in Materials

Review of Current Understanding and Proposed
New Standard Displacement Damage Model to Incorporate
in Cascade Defect Production Efficiency
and Mixing Effects

Report prepared by the OECD/NEA
Working Party on Multiscale Modelling of Fuels and Structural Materials for Nuclear Systems,
Expert Group on Primary Radiation Damage

ORGANISATION FOR ECONOMIC CO-OPERATION AND DEVELOPMENT

The OECD is a unique forum where the governments of 34 democracies work together to address the economic, social and environmental challenges of globalisation. The OECD is also at the forefront of efforts to understand and to help governments respond to new developments and concerns, such as corporate governance, the information economy and the challenges of an ageing population. The Organisation provides a setting where governments can compare policy experiences, seek answers to common problems, identify good practice and work to co-ordinate domestic and international policies.

The OECD member countries are: Australia, Austria, Belgium, Canada, Chile, the Czech Republic, Denmark, Estonia, Finland, France, Germany, Greece, Hungary, Iceland, Ireland, Israel, Italy, Japan, Luxembourg, Mexico, the Netherlands, New Zealand, Norway, Poland, Portugal, the Republic of Korea, the Slovak Republic, Slovenia, Spain, Sweden, Switzerland, Turkey, the United Kingdom and the United States. The European Commission takes part in the work of the OECD.

OECD Publishing disseminates widely the results of the Organisation's statistics gathering and research on economic, social and environmental issues, as well as the conventions, guidelines and standards agreed by its members.

NUCLEAR ENERGY AGENCY

The OECD Nuclear Energy Agency (NEA) was established on 1 February 1958. Current NEA membership consists of 31 countries: Australia, Austria, Belgium, Canada, the Czech Republic, Denmark, Finland, France, Germany, Greece, Hungary, Iceland, Ireland, Italy, Japan, Luxembourg, Mexico, the Netherlands, Norway, Poland, Portugal, the Republic of Korea, the Russian Federation, the Slovak Republic, Slovenia, Spain, Sweden, Switzerland, Turkey, the United Kingdom and the United States. The European Commission also takes part in the work of the Agency.

The mission of the NEA is:

- to assist its member countries in maintaining and further developing, through international co-operation, the scientific, technological and legal bases required for a safe, environmentally friendly and economical use of nuclear energy for peaceful purposes;
- to provide authoritative assessments and to forge common understandings on key issues, as input to government decisions on nuclear energy policy and to broader OECD policy analyses in areas such as energy and sustainable development.

Specific areas of competence of the NEA include the safety and regulation of nuclear activities, radioactive waste management, radiological protection, nuclear science, economic and technical analyses of the nuclear fuel cycle, nuclear law and liability, and public information.

The NEA Data Bank provides nuclear data and computer program services for participating countries. In these and related tasks, the NEA works in close collaboration with the International Atomic Energy Agency in Vienna, with which it has a Co-operation Agreement, as well as with other international organisations in the nuclear field.

This document and any map included herein are without prejudice to the status of or sovereignty over any territory, to the delimitation of international frontiers and boundaries and to the name of any territory, city or area.

Corrigenda to OECD publications may be found online at: *www.oecd.org/publishing/corrigenda*.

© OECD 2015

You can copy, download or print OECD content for your own use, and you can include excerpts from OECD publications, databases and multimedia products in your own documents, presentations, blogs, websites and teaching materials, provided that suitable acknowledgment of the OECD as source and copyright owner is given. All requests for public or commercial use and translation rights should be submitted to *rights@oecd.org*. Requests for permission to photocopy portions of this material for public or commercial use shall be addressed directly to the Copyright Clearance Center (CCC) at *info@copyright.com* or the Centre français d'exploitation du droit de copie (CFC) *contact@cfcopies.com*.

Foreword

Under the auspices of the NEA Nuclear Science Committee (NSC), the Working Party on Multiscale Modelling of Fuels and Structural Materials for Nuclear Systems (WPMM) was established in 2008 to assess the scientific and engineering aspects of fuels and structural materials, aiming at evaluating multi-scale models and simulations as validated predictive tools for the design of nuclear systems, fuel fabrication and performance. The WPMM's objective is to promote the exchange of information on models and simulations of nuclear materials, theoretical and computational methods, experimental validation, and related topics. It also provides member countries with up-to-date information, shared data, models and expertise.

The WPMM Expert Group on Primary Radiation Damage (PRD) was established in 2009 to determine the limitations of the NRT-dpa standard, in the light of both atomistic simulations and known experimental discrepancies, to revisit the NRT-dpa standard and to examine the possibility of proposing a new improved standard of primary damage characteristics.

This report reviews the current understanding of primary radiation damage from neutrons, ions and electrons (excluding photons, atomic clusters and more exotic particles), with emphasis on the range of validity of the "displacement per atom" (dpa) concept in all major classes of materials with the exception of organics. The report also introduces an "athermal recombination-corrected dpa" (arc-dpa) relation that uses a relatively simple functional to address the well-known issue that "displacement per atom" (dpa) overestimates damage production in metals under energetic displacement cascade conditions, as well as a "replacements-per-atom" (rpa) equation, also using a relatively simple functional, that accounts for the fact that dpa is understood to severely underestimate actual atom relocation (ion beam mixing) in metals.

Acknowledgements

The NEA Secretariat would like to express its sincere gratitude to the members of the Expert Group on Primary Radiation Damage for contributing to this report, and in particular to Prof. Kai Nordlund (Finland), Chair of this Expert Group, and to Dr. François Willaime (France), Vice-Chair of this Expert Group and current Vice-Chair of the WPMM.

Special thanks are also due to Dr. Marius Stan (US), Dr. Ted M. Besmann (US), former and current Chair of the WPMM, and to Dr. Carole Valot (France), former Vice-Chair of the WPMM.

List of authors

Kai Nordlund[1], Andrea E. Sand[1], Fredric Granberg[1], Steven J. Zinkle[2], Roger Stoller[3], Robert S. Averback[4], Tomoaki Suzudo[5], Lorenzo Malerba[6], Florian Banhart[7], William J. Weber[3,8], Francois Willaime[9], Sergei Dudarev[10], David Simeone[11,12]

[1] University of Helsinki, Department of Physics, P.O.Box 43, 00014 Finland
[2] University of Tennessee, Department of Nuclear Engineering, Knoxville, TN 37996, United States
[3] Oak Ridge National Laboratory, Division of Materials Science & Technology, P.O. Box 2008, Oak Ridge, TN 37831, United States
[4] University of Illinois, Department of Materials Science & Engineering, Urbana, IL 61801, United States
[5] Japan Atomic Energy Agency, Center for Computational Science and e-Systems, Tokai, Ibaraki 319-1195, Japan
[6] SCK-CEN, Institute for Nuclear Materials Science, B-2400 Mol, Belgium
[7] University of Strasbourg, CNRS, UMR 7504, Institut de Physique et Chimie des Matériaux, F-67034 Strasbourg, France
[8] University of Tennessee, Department of Materials Science and Engineering, Knoxville, TN 37996, United States
[9] CEA, DEN, Service de Recherches de Metallurgie Physique, Gif-sur-Yvette, France
[10] CCFE, EURATOM-CCFE Fusion Assoc., Abingdon OX14 3DB, Oxon, England
[11] École Centrale Paris, CNRS, SPMS, Chatenay-Malabry, France
[12] CEA, DEN, SRMA, LA2M, Gif-sur-Yvette, France

Table of contents

Executive summary

One of the consequences of the interaction of high energy particles (photons, neutrons, ions or electrons) with crystalline materials is the formation of lattice defects resulting from the energy transfer to the atoms. Figure ES.1 illustrates the process of damage creation in a displacement cascade triggered by a neutron or an ion. This damage, and its evolution with time, determines the macroscopic response of a material to radiation, and is thus crucial to understand. The damage production can in most cases be divided into two categories: the primary damage that is formed immediately (within a few picoseconds) after the ion/neutron/electron impact by atomic collision processes far from thermodynamic equilibrium, and the long-time scale (nanoseconds to years) damage evolution caused by thermally activated processes. **This topical review focuses on the primary damage.**

Figure ES.1. Collision cascade induced by a 10 keV recoil in Au at an ambient temperature of 0K

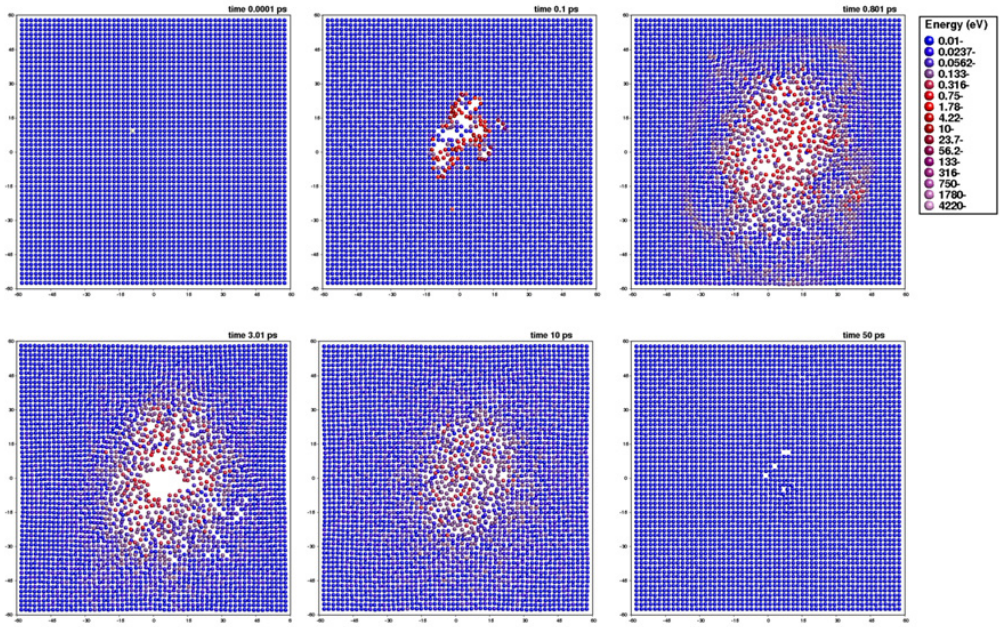

The circles indicate atom positions in a 1 unit cell thick cross-section through the center of the simulation cell, and the color scale the kinetic energy of the atoms. Note: A very large number of atoms is initially displaced, but when the cascade cools down, almost all of them return to perfect crystal positions. This is the *athermal recombination* effect discussed extensively in this report. However, many atoms do not return to the same position they started in, and hence the number of atom *replacements* is much larger than the number of defects produced.

A very useful and widely used standard for estimating the primary damage from neutrons, ions or electrons was proposed by Norgett, Torrens and Robinson in 1975 to evaluate the number of Frenkel pairs formed for a given energy transferred to the primary knock-on atom, and therefore the number of "displacements per atom", or so-called NRT-dpa (or just dpa in short). It is based on the earlier, somewhat simpler, Kinchin-Pease model.

Within this report, we review the current understanding of primary radiation damage from neutrons, ions and electrons (excluding photons, atom clusters, and more exotic particles), with emphasis on the range of validity of the dpa concept in all main classes of materials (except organic ones), and in particular discuss known shortcomings. **We recognise that the current NRT-dpa standard is fully valid in the sense of a scaled radiation exposure measure, as it is essentially proportional to the radiation energy deposited per volume. As such, it is highly recommended to be used in reporting neutron damage results to enable comparison between different nuclear reactor environments and ion irradiations.** However, in the sense of a measure of damage production the NRT-dpa value has several well-known problems, which are discussed at length.

To partially start to alleviate these problems, for the case of metals we present an **"athermal recombination-corrected dpa" (arc-dpa)** equation that accounts in a relatively simple functional for the well-known issue that the dpa overestimates damage production in metals under energetic displacement cascade conditions, as well as a **"replacements-per-atom" (rpa)** equation that accounts in a relatively simple functional for the well-known issue that the dpa severely underestimates the actual atom relocations (ion beam mixing) in metals.

The arc-dpa function presented is:

$$N_{d,arcdpa}(E) = \begin{bmatrix} 0 & \text{when} & E < E_d \\ 1 & \text{when} & E_d < E < 2E_d / 0.8 \\ \dfrac{0.8E}{2E_d}\xi(E) & \text{when} & 2E_d / 0.8 < E < \infty \end{bmatrix}$$

which differs from the NRT-dpa with the efficiency function *ξ(E)* which is given by:

$$\xi(E) = \frac{1 - c_{arcdpa}}{(2E_d / 0.8)^{b_{arcdpa}}} E^{b_{arcdpa}} + c_{arcdpa}$$

where E is the damage energy, E_d the average threshold displacement energy and b_{arcdpa} and c_{arcdpa} unitless fitted parameters with a physical meaning discussed in the article. The original NRT-dpa function is obtained by setting *ξ(E)* =1 for all energies. However, any use should keep in mind that either form is still only a damage exposure parameter that allows comparing different irradiations in a physically motivated way, but cannot predict the exact nature of the microscopic damage which involves many complicated issues such as damage cluster size, thermal mobility and recombination, nonlinear damage buildup at high doses, etc.

Moreover, we present a recommendation for how the dpa value for ion irradiation conditions should be obtained from the widely used SRIM binary collision approximation code.

1. Introduction

Particles with kinetic energies clearly above conventional thermal energies, i.e. with $E_{kin} > 1$ eV, exist in nature due to cosmic radiation and radiation decay, but are nowadays produced in a wide range of man-made devices for basic research and practical applications. For instance, the great accelerators at CERN and other particle physics laboratories in the world attempt to unravel the fundamental nature of the universe [HiggsAtlas; HiggsCMS], and numerous smaller devices are widely used for equally exciting research in physics [Smith], chemistry [Winters, 1992], medicine [Schultz, 2007d] and nanoscience [JAPreview09]. On the application side, ion implantation is one of the key technologies in silicon chip manufacturing, [Chason, 1997], and electron accelerators are one of the key ways to treat cancer. All of these activities make it interesting and important to understand what are the fundamental effects of high-energy particles on matter. Moreover, in nuclear fission reactors, which currently provide about 13% of the world's electricity taking advantage of the fission of uranium nuclei by neutrons, materials degradation associated with neutron irradiation damage is a key factor [Zinkle1].

One of the main consequences of the interaction of high-energy particles (photons, neutrons, ions or electrons) with materials is the formation of lattice defects resulting from the energy transfer towards the atoms (other consequences include production of non-damage-producing phonons, excitons and plasmons, secondary electrons and photons, and heating of the material). Indeed, this consequence is the main reason why radiation has both detrimental and beneficial effects on materials. The damage can take many forms: in a crystal it is easy to understand that an atom can be kicked out from its initial lattice site, leaving an empty site (a vacancy) behind and creating an atom at an interstitial site in front [Kittel, 1968]. It is, however, important to realise the crystal defects formed can also be much more complicated [Zinkle, 2012]: they can for instance be defect clusters [Partyka, 2000], amorphous zones [Ruault, 1984; Zinkle3], dislocation loops [Eyre, 1973] or three-dimensional defects [Silcox, 1959b; Kitagawa, 1985]. On surfaces the damage can also take the form of adatoms [Hashimoto, 2004], craters [Ghaly, 1994; Birtcher, 1999] and ripples [Erlebacher, 1999]. In amorphous materials the generated defects can be over- or under-coordinated atoms [Laaziri, 1999] or empty regions [Roorda, 1992]. Photon irradiation creates damage largely by electronic excitation processes causing bond breaking [Spaepen-Turnbull, 1982], although very high-energy gamma photons can also produce damage by atomic recoil processes [Raman, 1994].

The damage production mechanisms can in most cases be well divided into two categories by time scale. The **primary damage** is formed immediately after the particle impact by atomic collision processes and strong material heating caused by the colliding atoms far from thermodynamic equilibrium. Numerous computer simulation and experimental studies have shown that the time scale for the ballistic atom collision processes is of the order of 0.1-1 ps and the time scale for subsequent thermalisation of the collisions

1–10 ps [Diaz, 1987; Stuchbery, 1999; Stoller, 2012], see Figure 1.1 and e.g. [Zinkle4]. After this athermal (in the sense that equilibrium thermally activated processes are not significant) stage, long-time scale (nanoseconds to years) damage evolution caused by thermally activated processes can occur.

Figure 1.1. Collision cascade induced by a 10 keV recoil in Au at an ambient temperature of 0K

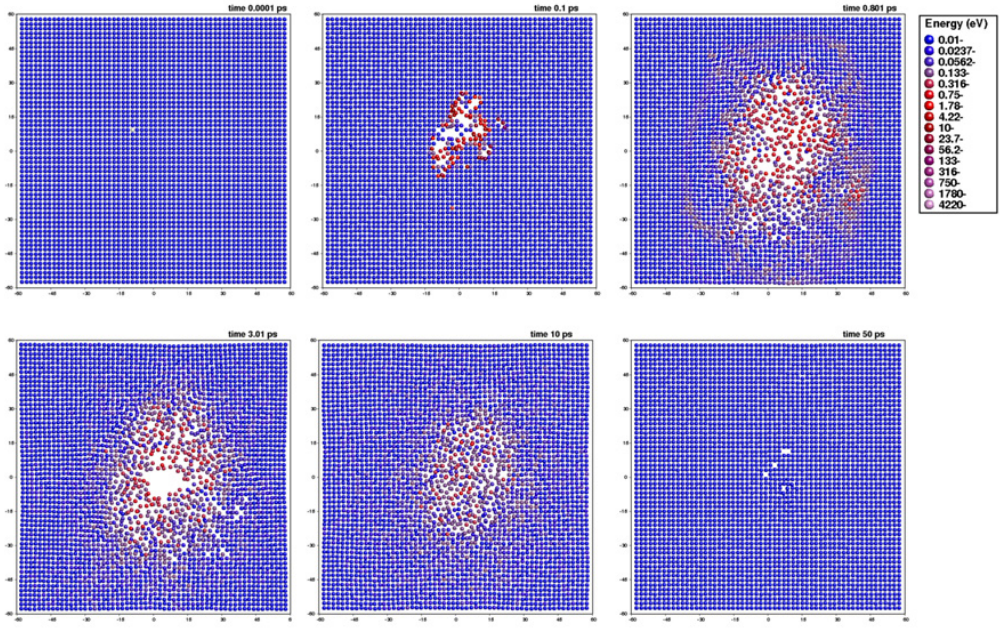

The circles indicate atom positions in a 1 unit cell thick cross section through the center of the simulation cell, and the color scale the kinetic energy of the atoms. Note: A very large number of atoms is initially displaced, but when the cascade cools down, almost all of them return to perfect crystal positions. This is the *athermal recombination* effect discussed extensively in this report. However, many atoms do not return to the same position they started in, and hence the number of atom *replacements* is much larger than the number of defects produced.

In this report, we review the current understanding of primary radiation damage from neutrons, ions and electrons on inorganic materials. We leave out many other important and interesting aspects of radiation damage. Specifically, we exclude from our consideration:

- damage by photons, molecular and nanocluster projectiles;
- more exotic elementary particles (such as muons, positrons, etc.);
- the properties (stability and mobility) of the defects produced;
- damage at elevated temperatures and its consequences (solute segregation and precipitation, void swelling, irradiation creep, embrittlement in all its forms, …);
- response functions, reaction to external driving forces (such as stress, strain or external electromagnetic fields);
- surface effects;
- electronic defect production, including swift heavy ions and ion track production by them;
- organic materials.

1.1 Introduction to the displacements-per-atom concepts

The displacements-per-atom concept was introduced from the original ideas of production of primary point defects [Brinkman, 1954; Kinchin, 1955; PointDefects; Lannoo, 1981; Ehrhart, 1991] in materials. The idea is that the energetic particle travels mostly straight in a material, but occasionally collides strongly in a binary collision and imparts energy to a lattice atom.

For neutrons and electrons this is a very good approximation due to their very small collision cross-sections, while for ions and atomic recoils it is questionable; in many cases these can collide with several nearest-neighbour atoms in sequence, making the process inherently many-body rather than binary in nature. The multiple simultaneous collisions can be described as a "displacement spike" or "heat spike". This concept was already proposed in the 1950's [Brinkman, 1954; Seitz, 1956] and is by now well established [Bacon, 1994; Averback, 1998]. For the remainder of the current section we will ignore these many-body effects, but return to them in the materials-specific sections.

$$N_d(T_d) = \begin{bmatrix} 0 & , & T_d < E_d \\ 1 & , & E_d < T_d < 2E_d \\ \dfrac{T_d}{2E_d} & , & 2E_d < T_d < \infty \end{bmatrix} \quad (1)$$

For a binary collision, it is intuitively clear that if the energy imparted to a lattice atom is less than the cohesive energy of an atom in the lattice, it will not leave its lattice site, and no defect will be produced. On the other hand, if the energy given to the atom is orders of magnitude higher than the cohesive energy, the atom can be expected to become a recoil that moves through the lattice and produces more defects. Such considerations led to the formulation of the Kinchin-Pease (K-P) model, which states that the number of defects produced is [Kinchin, 1955]:

Here the quantity T_d stands for the energy available for damage production. For a single ion it is equal to the nuclear deposited energy $F_{D,n}$ = the total particle energy minus the energy that is lost to electronic stopping power:

$$T_D = F_{D,n} = E_0 - F_{D,e} \quad (2)$$

We note that in the fields of radiation safety, medical physics and damage in particle detectors, the nuclear deposited energy is known as "non-ionising energy loss", NIEL, and the electronic deposited energy as "Linear energy transfer", LET, although depending on the precise definition, these quantities may not be exactly equal.

For many ions one can also give FD,n as the total nuclear deposited energy per volume or depth. In this case, FD,n contains also the energy deposited to sub-threshold atomic recoils and it is not exactly correct to insert FD,n into the last line of Equation 1, as then also the energy given to subthreshold recoils becomes calculated into the damage production. This distinction is illustrated in Figure 1.2. In practice, the fraction of energy deposited to subthreshold recoils is often quite small and this distinction can be ignored.

Figure 1.2. Deposited energy for Fe recoils in Fe as calculated with the SRIM2008.04 binary collision approximation code in the full cascade mode

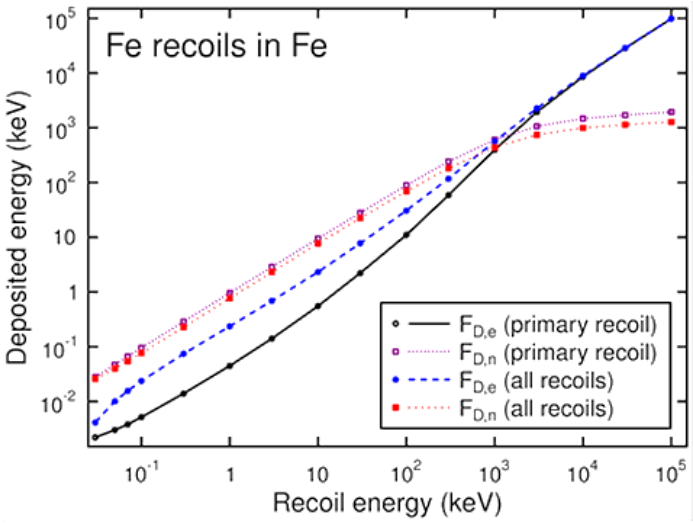

The $F_{D,e}$ data is obtained from the "Ionisation" energy loss percentages given in the SRIM visual outputs, and the $F_{D,n}$ values by summing up the "Vacancies" and "Phonons" energy loss percentages given in the main SRIM window. In both cases the energy loss percentage is multiplied times the recoil energy to get the deposited energy F_D. The "primary recoil" data is obtained by including all the recoil energy loss fractions in the $F_{D,n}$ value of the primary recoil, while for the "all recoils" data the energy loss percentages for electronic and nuclear energy loss are summed up. The difference between the curves illustrates that the total electronic deposited energy $F_{D,e}$ is considerably higher when also electronic stopping of secondary recoils is counted in. Note also that for all energies down to the threshold displacement energy, at least about 20% of the initial recoil energy is lost to electronic stopping.

The only parameter in Equation (1) is the **threshold displacement energy** E_d. This parameter can be expected to be higher than the cohesive energy (which is of the order of 5 eV/atom in typical hard solids [Kittel]), and will be discussed in the next subsection.

Later on, equation (1) was refined by Norgett, Robinson and Torrens based on binary collision approximation (BCA) computer simulations by taking into account the possibility of ballistic processes recombining the defect as it was produced [BCA] [NRT]. This lead to the modified Kinchin-Pease equation, nowadays most often known as the NRT equation, that gives the number of defects produced as:

$$N_d(T_d) = \begin{bmatrix} 0 & , & T_d < E_d \\ 1 & , & E_d < T_d < 2E_d / 0.8 \\ \dfrac{0.8T_d}{2E_d} & , & 2E_d / 0.8 < T_d < \infty \end{bmatrix} \tag{3}$$

where the new factor 0.8 came from the BCA simulations.

Robinson and Oen subsequently published a correction to the above equation to account for energy dissipated in subthreshold displacements [Robinson, 1982]. However, this equation is the basic equation that can be used to calculate the number of displaced atoms in any material for which E_d is known and the damage energy T_d can be calculated. For instance,

neutron transport codes [Greenwook, 1994; NJOY] can calculate the energy given by neutrons to lattice atoms, and tables of nuclear deposited energy can then tell for each atom energy the value of T_d. In this way, one can calculate the number of atoms displaced according to the KP or NRT models in a given volume of material. Furthermore, if this quantity is normalised by the number of atoms in the same volume, one obtains the **displacements-per-atom (dpa)** unitless quantity:

$$\text{dpa} = \text{displacements per atom} = \frac{\text{Number of displaced atoms in volume from NRT equation}}{\text{Number of materials atoms in same volume}} \quad (4)$$

which in this simplified model gives the defect concentration c of primary damage vacancies and interstitials in the material. Assuming no point defects are lost to a surface or other defect sink, naturally the concentrations for vacancies, interstitials and Frenkel pairs (FP's) are equal: $c_v = c_i = c_{FP}$.

The dpa concept and KP/NRT equations are widely used in estimating the amounts of radiation damage in materials. The main reason is of course simplicity: doing the calculation is very easy. Similarly, the "dpa" concept is appealing in that it is easy to understand, and gives an order-of-magnitude estimate of what fraction of atoms are displaced during an irradiation process. For instance, a total radiation dose of, say, 10 kJ/cm3 does not tell a non-expert anything about how many defects such a dosage can be expected to cause, whereas a value of, say, 0.01 dpa would tell any physicists that one atom in a hundred has been displaced (and hence likely to be a defect).

Another major advantage of the dpa concept is that it can be used for scaling radiation doses or fluences between different kinds of irradiations. Since it included implicitly the value of the nuclear deposited energy, which can be reliably calculated, it can be used to estimate how much damage different irradiations cause. For instance, if damage has been produced in a material by a given fluence of 50 keV Ne ions, and one wants to compare with Ar ions, a dpa calculation can tell what energy and fluence for the Ar ions can be expected to produce about the same damage as the 50 keV Ne irradiation did. For cases where the measured accumulated damage does not follow the dpa scaling, this indicates nonlinear behaviour in the damage production [Kucheyev, 2001b; Karaseov, 2009] and/or subsequent defect evolution [Zinkle5].

We note that if the dpa calculation is not interpreted to be directly related to the damage production or actual number of atoms displaced, it can be fully justifiably used as a radiation exposure measure**. Either damage energy or dpa is clearly much better to use than a simple neutron fluence value**, since different neutron spectra can give very different recoil spectra to materials, and hence very different nuclear deposited energy and damage. Moreover, it has the advantage over simple energy deposition (e.g. in the SI units of Gray = J/kg) measures in the sense that it calculates out the electronic stopping, which is known not to cause damage in most inorganic materials (except in the very high-energy swift heavy ion regime [Kanjijal, 2001b]). We strongly recommend using the dpa especially in neutron transport calculations to make for transferable interpretation of different kinds of neutron irradiation conditions. Indeed, the ASTM standard E693-94 promotes and defines how such calculations should be done in Fe and steels [ASTMFe]. **The current review endorses and does not propose a modification of this standard within the framework of dpa used as a displacement damage exposure measure.**

One problem in using the dpa standard is that the name "displacements-per-atom" makes it very tempting to interpret that dpa is equal to defect concentration. Indeed, within the original KP and NRT definitions and the approximations and assumptions built into them, it is fully valid to do so (for conditions where no subsequent defect migration occurs, i.e. near absolute zero temperatures). **However, in many cases current knowledge shows that many of these approximations and assumptions are very problematic, and lead to major (typically half an order of magnitude) errors in equating the dpa value with the number of defects.** As a consequence, some researchers have argued against using a displacement exposure parameter analogous to dpa and instead advocate using a damage correlation parameter (e.g. empirically related to minority carrier lifetime in semiconductors) [Messenger2005]. Such an empirical approach has some pragmatic advantages for developing engineering correlations within a specific experimental regime for cases where sufficient test data are available, but is clearly unsatisfying from a fundamental scientific perspective. The current understanding of defect production and residual defect concentration will be discussed in the remaining sections of this report.

It is historically interesting to note that already Kinchin and Pease recognised that the simple linear formulation, the first equation, may not hold except in a narrow energy interval above the threshold, and proposed several alternatives [Kinchin, 1955]. Also, the "constant" of 0.8 in the NRT equation [NRT] is an approximation from BCA simulations, where the actual values obtained varied in the range 0.8–0.9 [BCA].

1.2 Threshold displacement energy

The threshold displacement energy E_d has, as is obvious from equations (1) and (2), a crucial role in the calculation of primary damage via the dpa concept. Hence it is also important to understand in detail its nature and limitations. The velocity of a recoil in a lattice is much larger than the conventional thermal velocity (e.g. a 30 eV recoil has a kinetic energy that is 1000 times higher than the average thermal velocity ≈ 0.03 eV), and hence a velocity that is √1000 ≈ 30 times higher. Thus as a rough first approximation, one can imagine that the energy needed to form a defect is obtained by assuming only the recoil atom moves, and determining the potential energy barrier along a straight line in the initial recoil direction, see Figure 1.3. This so called "sudden approximation" has been shown to work well at least in low-index crystal directions in simple crystals [Windl, 1998]. It is very important to understand that this defect production mechanism is very different from the thermally activated formation of Frenkel pairs, because the latter involves typically numerous (billions, trillions, or more) lattice vibrations in the potential well before a defect is formed [Vineyardprefactor] and in metals this can happen only very close to the melting point [Nordlund, 1998a]. Indeed, the threshold displacement energies are typically of the order of 10–50 eV [Lucasson, 1975; Vajda, 1977; Andersen, 1979; Zinkle6], roughly a factor of 5-10 higher than the Frenkel pair formation energies [Ehrhart, 1991].

Figure 1.3. Illustration of the threshold displacement energy concept

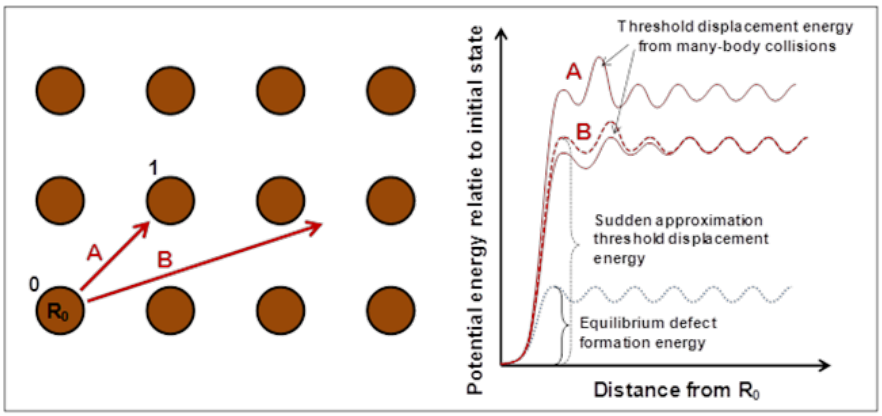

If the bottom left atom 0 at R0 receives a recoil e.g. in directions A or B, it will cause a complex many-body collisional process. In case the atom would move in a straight path along path B and the other atoms would not have time to move at all (which of course in reality will not be the case), the potential energy in the system could be illustrated as on the right side in the "Sudden approximation" curve. At some point there is a maximum in the potential energy curve, before the atom goes into an interstitial position in one of the minima to the right of the original position. This maximum is an estimate of the threshold displacement energy. In reality the atoms respond somewhat to the motion of the recoiling atom 0, which lowers the threshold energy. In equilibrium, the threshold is much lower since all atoms have ample time to relax their position and a defect is formed only when the atom positions and movements happen to be such that a defect can form. Path A illustrates a case where the original atom 0 is directed directly towards another atom 1. In this case the original atom most likely replaces the atom at 1, while atom 1 receives a secondary recoil and becomes an interstitial atom.

It is also important to appreciate that on the atomic level, there is not a single threshold displacement energy, but each crystal direction has its own due to crystal anisotropy [Vajda, 1977, et al.]. In fact at finite temperature the situation is even more complex. Each atom in a lattice has some kinetic energy, distributed according to a Maxwell-Boltzmann distribution. If the thermal velocity vector happens to be in the direction of the recoil energy received, this enhances the damage production probability, and *vice versa*. Moreover, in many cases the production probability of a defect is strongly influenced by recombination, i.e. thermal fluctuations in atom positions and velocities can strongly affect the recombination probability. Molecular dynamics (MD) simulations have shown that even for recoil energies as high as 400 eV, the net amount of defects after all recombinations can sometimes be 0. All these complications mean that even for a single crystal direction, there is an energy range where the defect production probability rises from 0 to 1 [Nordlund, 2005c].

We emphasise that these complications do not, however, prevent the use of the threshold displacement energy concept. It is possible to calculate an average over the threshold displacement functions in different directions for use in the NRT equation. Although usually the threshold energy Ed is considered to be independent of crystal direction, we note that since E_d is a user-defined parameter, the NRT equation can actually be used to calculate dpa for different crystal directions. This calculation would only be strictly relevant for near-threshold displacement events (since multiple directions are involved in energetic displacement cascades), but in principle NRT can incorporate crystal-dependent E_d values. There is some non-uniqueness also in how the average should be calculated, but this does not amount to more than a couple of eV (less than 10% of the total) which is a relatively small uncertainty compared to the other ones related to damage production (described later in this document). We note, however, that to account for the non-uniquenesses, in principle it

should be possible to extend the analytical NRT formalism and higher-level models to include a fluctuation term.

Figure 1.4. Collection of experimental evidence that the defect efficiency ξ between real damage and that predicted by the NRT (modified Kinchin-Pease) equation is much below 1 for recoil energies above ~ 100 eV in Cu

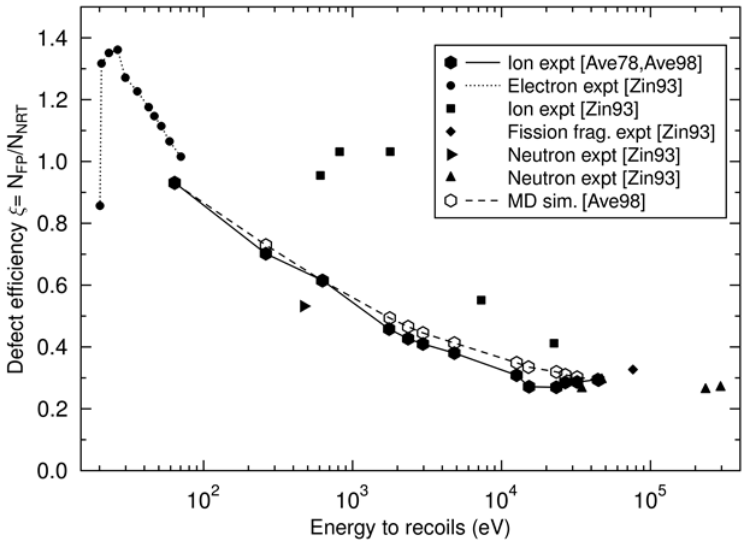

Also shown are early MD results that show the same trend. The data is from earlier review articles collected by co-authors of the current work, [Averback, 1998; Zinkle, 1993]. The electron irradiation data indicates that just above the threshold, the defect efficiency may actually be above 1.

Although the threshold displacement energy has been studied extensively both by experiments and simulations (see e.g. [Lucasson, 1975; Maury, 1975; Vajda, 1977; Jung, 1981; Malerba, 2002; Smith, 2001; Windl, 1998; Caturla, 1994; Miler, l994; Andersen, 1979; Maury, 1976; Urban, 1982; King, 1982; Vitovskii, 1977; Bauer, 1969; Vehse, 1968; Lomer, 1967; Lucasson, 1962; Zinkle6]), there are still uncertainties for several technologically important materials. In particular, for Fe there is no experimental value for the average threshold, and there are big variations in the threshold displacement energies predicted by classical interatomic potentials [Nordlund, 2005c]. Similarly in Si there is a large variation in both experimental and classical molecular dynamics simulations. Very recently, quantum mechanical density-functional theory (DFT) simulations have given more reliable theoretical values for the threshold displacement energies for Fe and Si [Holström, 2008a]. On the other hand, the work in Si also showed that formation of metastable bond-order defects may necessitate the definition of two different threshold displacement energies depending on whether the experimental flux cause the metastable defect to be significant or not. Somewhat surprisingly, one of the materials where the threshold displacement energy is known quite accurately is in carbon nanotubes and graphene [Smith, 2001; Meyer, 2012].

2. Metals

2.1 Review of understanding

2.1.1 Review use of dpa in metals, recommend correct usage and calculations

The procedure to calculate displacements per atoms in a material under neutron irradiation requires the knowledge of: (i) the neutron flux spectrum as a function of neutron energy *E* and time *t*, $\phi(E,t)$, (ii) the atomic displacement cross-section for the particular material, σ_d, which is also a function of the neutron energy *E*, $\sigma_d(E)$. The former is the number of neutrons carrying a certain energy *E* that cross the unit surface per unit time in a location of the nuclear reactor where the material is, and might be varying with time; the latter is the "effective" area which, if crossed by the neutron, leads to atomic displacement. In general terms, the displacement rate at time *t* can be calculated as:

$$\frac{dpa}{s} = \int_0^\infty dE\sigma_d(E)\,\phi(E,t) \quad (1)$$

Correspondingly, the total amount of dpa is obtained by integrating over the exposure time, t_e:

$$dpa = \int_0^{t_e} dt \int_0^\infty dE\sigma_d(E)\,\phi(E,t) \quad (2)$$

For practical purposes, it is convenient to decompose the neutron flux into a factor that carries the time dependence, $\phi_{tot}(t)$ − time dependent flux intensity − and a normalised flux spectrum that, at any time *t*, equals the unit when integrated over energy, $\psi(E,t)$:

$$dpa = \int_0^{t_e} dt\phi_{tot}(t) \int_0^\infty dE\sigma_d(E)\,\psi(E,t) \quad (3)$$

Since one can often consider the flux spectrum to be constant over the exposure time, it can be simplified to

$$dpa = t_e\phi_{tot} \int_0^\infty dE\sigma_d(E)\,\psi(E) \quad (4)$$

In this equation, t_e is known and the decomposed neutron flux spectrum can be calculated, given the main features of the nuclear reactor and the composition of the material. These calculation can be done by using appropriate neutron physics codes, for example MCNP [Malerba; Schultis, 2011]; or it can be measured using dosimeters [Malerba; IAEA, 1970], or generally both.

The atomic displacement cross-section is determined by weighing the result of three different processes:

- nuclear reaction between the incident neutron and the nucleus of the atom and relevant transfer of energy from neutron (*E*) to nucleus (*T*);
- loss of energy acquired by the nucleus via interaction with the electrons of the system ($T \rightarrow T_d$);

- actual production of atomic displacements based on Equation (2), once T_d is known (and assuming E_d is given).

The cross-section relevant for the nuclear reaction comes from nuclear data libraries, which are conveniently available and directly usable from codes such as NJOY [MacFarlane; Kahler, 2010]. The energy loss to electrons can be calculated using Robinson's analytic representation [Malerba; Robinson, 1970] of Lindhard's model of energy partition between atoms and electrons [LSS]. NJOY can directly process nuclear cross sections into dpa usable values that include energy loss to electrons.

In the specific case of Fe and low alloyed steels, because of their practical importance for real applications, an ASTM standard for dpa calculations exists [A]. It provides, together with the tabulated value for $\sigma_d(E)$, also practical indications on how to evaluate cross sections per energy group, in order to calculate numerically in discretised form the integral of the last equation above. While the displacement cross section tabulated there is specific for Fe, the procedure for dpa calculations described is of general validity.

2.1.2 Athermal in-cascade recombination and clustering

In the basic dpa calculation based on the KP or NRT equations, it is assumed that the damage increases linearly with nuclear deposited energy. However, there is strong experimental and simulation evidence that this is not the case in metals. Resisitivity recovery experiments have shown that the damage produced in cascades induced by ions or recoils with energies well above the threshold displacement energy produce substantially less damage than expected from the simple NRT equation [Averback, 1978; Zinle, 1993], see Figure1.4. This is quantified with the damage efficiency parameter ξ which is defined as the ratio of the actual damage to that predicted by the NRT equation. Some data for the damage efficiency is given in Figure 1.4 and Figure 2.10, which show that for recoil energies of the order of 1 keV the damage efficiency has dropped from the value of 1 near the threshold to a value of about 0.5. At recoil energies above about 10 keV the damage efficiency seems to saturate at a value around 0.3.

Classical MD simulations have been crucial in giving insight into the reasons for this behaviour. Although in general MD simulations in materials science suffer from uncertainty of the reliability of the results due to the choice of interatomic potentials, remarkably, MD simulations of cascades in metals very consistently give a qualitatively similar behaviour reproducing the experimental damage recombination [Diaz, 1987; Nordlund, 1998b]. A typical example of the MD simulation results is given in Figure 1.1, which shows how initially (first about 200 fs) a set of ballistic collisions lead to a major production of displaced atoms. It is noteworthy that this number of displaced atoms roughly corresponds to the NRT prediction, or what would be obtained from a BCA simulation. However, after this, the cascade becomes a heat spike (thermal spike), i.e. a dense region of many-body atomic collisions that is underdense in the middle and overdense at the outskirts of the cascade [Brinkman, 1954]. After about 1 ps, the atoms in the spike (if it is dense enough) get a Maxwell-Boltzmann-like distribution of kinetic energies, i.e. behave like a thermodynamic system [Diaz, 1987]. This justifies the use of the word "thermal" or "heat" spike (both terms are used with the same meaning, roughly as commonly). Calculating the average energy of the atoms in the heat spike and converting this into units of Kelvin gives a "temperature" of the order of 10 000 K for the heat spike [Diaz, 1987]. Using the word "temperature" in this context is somewhat controversial, as the high-kinetic-energy phase only lasts some tens of picoseconds, and

hence this is naturally not a normal equilibrium temperature. However, the textbook definitions of temperature [Mandl] state that local thermodynamic equilibrium can be used if the time scale of the system is much larger than the relaxation time in the same system. As the heat spike relaxation time is about 3 lattice vibrations [Diaz, 1987], roughly 1 ps, a heat spike lasting about 10 ps can be considered a thermodynamic system.

The cooling down of the heat spike can be considered a very rapid (ps time scales) recrystallisation process of the hot liquid. Since a recrystallisation process tends to produce perfect crystal, it is natural that much of the displaced atoms generated in the thermodynamic phase of the cascade regenerate (in other words, interstitials and vacancies recombine) and the produced damage is less than the initial number of displaced atoms (the NRT prediction). This explains the damage efficiencies clearly below 1. Since this recombination process does not require any thermally activated defect migration (atom motion is caused primarily by the high kinetic energy introduced by the recoil atom), this recombination is called "**athermal**" (i.e. it would also happen if the ambient temperature of the sample would be 0 K).

A recent systematic comparison of MD cascade results in Fe [Malerba, 2005a] showed that all potentials used to simulate this material gave a similar trend of ξ as a function of energy and always saturation values between 0.2 – 0.5, with the dominant values being about 0.3, in agreement with experiments (see Figure 2.1).

By the argumentation given above, one could argue that *all* damage in metals would recombine, and the resulting ξ = 0. This is, however, not observed either experimentally or in simulations. Instead, what typically happens is that a few isolated interstitials and interstitial clusters remain at the outskirts of a heat spike region, some vacancies are randomly distributed, and the center of the heat spike usually contains a vacancy cluster. Most of this behaviour is well understood. Isolated interstitials can be created by ballistic displacements of high-energy recoils and replacement collision sequences [Gibson, 1960]. If these create the interstitial well outside the heat spike region, it is not likely to re-enter it and be recombined. Isolated vacancies can be created if the recrystallisation front moves so rapidly that there is not enough time to create perfect lattice (there is always a finite probability of vacancy creation given be $exp(E^f/k_Bt)$, where E^f is the vacancy formation energy and T the temperature at the recrystallisation front, which is about the melting temperature). The formation of vacancy clusters in the middle can be understood as follows: since a few interstitials are formed at the outskirts of the cascades, vacancies are left in the heat spike. These are pushed towards the center by the recrystallisation front, and hence form a cluster there when recrystallisation is complete (this mechanism can be proven explicitly by MD simulations of a bilayer material with different melting points [Nordlund, 1999b].

The formation mechanisms of interstitial clusters are somewhat less well established, and it seems several mechanisms can be active. The reported mechanisms include having an asymmetric recrystallisation front that isolates a liquid pocket with an excess of atoms, leaving it behind as an interstitial cluster [Nordlund, 1998b]. It has also been shown that the interaction of two supersonic shock fronts from nearby centres of heat spikes can lead to the stronger front injecting atoms into the underdense core of the weaker one, thus leading to the formation of an interstitial-rich region [Calder, 2010b]. These two mechanisms are likely related to each other, i.e. the latter may explain why the liquid pocket that becomes isolated forms initially. Also dislocation loop punching [Brown, 1970; Trinkaus, 1984] has been

suggested to be possible in cascades [Diaz, 1991], but the same lead author later found that this observation was due to an insufficiently short simulation time [Diaz, 1996]. It seems that direct interstitial loop punching is not possible except near to surfaces [Nordlund, 1999a].

The formation mechanisms of defects and defect clusters in cascades are thus reasonably well understood, and the total number of defects has been measured with resistivity recovery experiments and agrees well with MD simulation using modern interatomic potentials at least in Fe [Björkas, 2007a; Malerba, 2010a]. However, what fraction of defects is in clusters cannot be fully reliably predicted by MD or easily measured experimentally. Even the most modern MD potentials give significant variation in what fraction of damage is in clusters [Björkas, 2007a], and this fraction is also affected by uncertainties in how to treat the low-energy limit of electronic stopping power and the electron-phonon coupling [Björkas, 2009a; Zarkadoula, 2013]. Traditional transmission electron microscopy experiments can readily observe large (> 2 nm in diameter) defect clusters [Suzudo; Lucasson, 2008]. Modern microscopes can also detect smaller clusters, but there is limited work currently on the topic. Moreover, a recent combined MD-Kinetic Monte Carlo (KMC) simulation work indicates the fraction of primary damage in large clusters may have a significant effect on the long-term damage evolution [Björkas, 2011]. Hence clearly more work is needed to establish what fraction of damage is in clusters, the structure of the clusters and their effect on the macroscopic damage evolution. Modern aberration-corrected TEM's could give significant advances on the topic.

Figure 2.1. Comparison of surviving defect fraction obtained from MD simulations with different potentials and groups based on the data available in 2005 [Malerba, 2005]

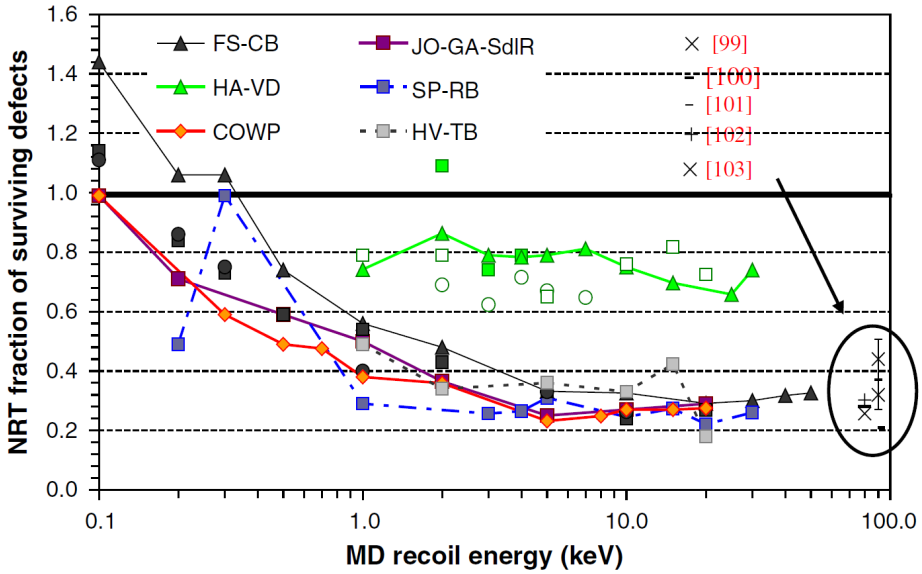

It is important to emphasise that this microscopic damage distribution is a significant factor for the durability of metals in high-radiation environments. Caro and Caro showed in 1999 that the damage efficiency ξ can give macroscopically significant results, such as shifts of the brittle-to-ductile transition temperature in reactor pressure vessel steels of tens of degrees C, which in turn could affect the lifetime of the reactor by (in their estimate) five years [Caro, 2000b]. While this estimate is specific to one analysis for one pressurised heavy

water nuclear reactor, and could have to be revised as better understanding of damage clustering and long-term evolution becomes available, it demonstrates well that the issue of athermal damage recombination is, in addition to being scientifically interesting, of major practical importance.

2.1.3 Ion beam mixing

Ion beam mixing broadly refers to the relocation of atoms in energetic displacement cascades and thus represents a basic component in describing the primary state of damage. For pure elements, of course, such mixing has little consequence for the evolution of the materials under prolonged irradiation, but most materials of interest for applications are composed of two- or more- phase alloys in metals, and compounds in semiconductors and insulators. A few examples that illustrate the critical importance of ion beam mixing to understanding radiation damage are dissolution of precipitates in two-phase alloys, resolution of fission gas in nuclear fuels, and chemical disordering and amorphisation of intermetallic or ionic compounds. One of the early recognitions of ion beam mixing in fact derives from measurements of disorder in Cu_3Au during low temperature, fast-neutron irradiation [Ave0]. In order to explain the large changes in the electrical resistivity that occurred, Siegel estimated already in 1949 that many Cu and Au atoms must exchange locations for each Frenkel pair that was created [Siegel, 1949].

Figure 2.2. Recoil implantation of Cu into Al during 500 keV Xe bombardment

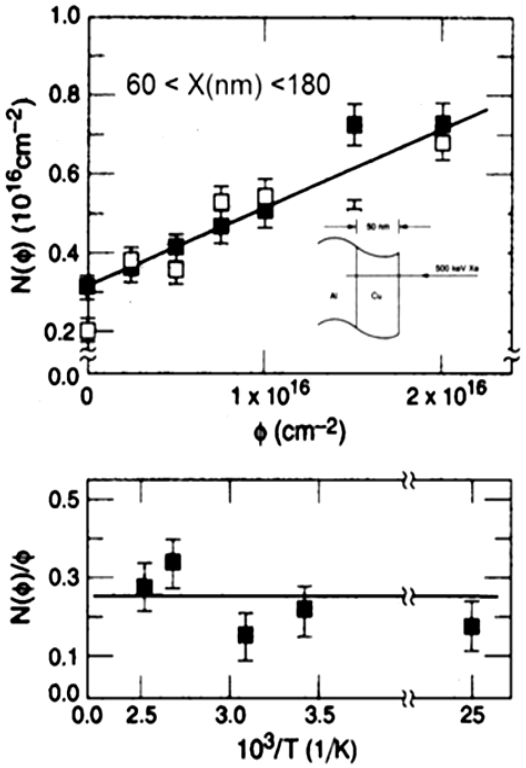

Three mechanisms of ion beam mixing have now been identified, each operating in a different phase in the evolution of the cascade.

Recoil implantation: As energetic ions slowdown in solids targets they undergo a series of collisions with target atoms via a screened Coulomb interaction. Two consequences of the screened Coulomb interaction is: (i) the initial ion only slowly changes its incident direction, and (ii) it transfers large energies to only few atoms. This results in a few target atoms receiving high energies, with their motion close to the direction of the initial ion. For ion irradiations this results in the forward recoiling of atoms into the sample. For neutron or fast fission fragments, the directions are random, but nevertheless a few atoms recoil very large distances. Recoil implantation can thus play an important role, for example in the resolution of fission gas bubbles in reactor fuels or destabilising nano-ODS (oxide dispersion strengthened) steel alloys, materials presently under consideration for advanced reactors components.

An example of recoil implantation is shown in Figure 2.2, where the number of Cu atoms recoiling more than 60 nm into Al is shown as a function dose for 500 keV Xe irradiation. Notice that the number of recoil atoms scales linearly with dose and is independent of temperature, as recoil atoms derive from primary recoils. Boltzmann transport theory [Ave1] provide reasonable accuracy for recoil implantation since the binary collision model is appropriate for high energy collisions. BCA simulation models like TRIM, however, are generally more accurate and easier to employ. Recent calculations for dissolution of He and Xe bubbles in UO_2 using either TRIM-like codes or MD are found in [Ave2; Ave3].

Ballistic mixing: The momentum of displaced atoms in energetic displacement cascades resulting from higher order displacement events is nearly isotropic. Ballistic mixing, therefore, operates similarly to diffusion processes. The mixing is considered “ballistic” in the sense that alloy components flow down gradients in their concentrations during prolonged irradiation, and not gradients in their chemical potential. Various models have been developed to calculate ballistic mixing. The result derived by Sigmund and Gras-Marti using Boltzmann transport theory [Ave1] is widely used for the magnitude of mixing. They find for the mean square displacement of a target atom, normalised by the deposited damage energy density, is given by:

$$\xi_{BM} = \frac{\langle R_a \rangle^2}{\Phi F_D} = \frac{\Gamma_0 \zeta_{21} \lambda_c^2}{3 N_0 E_c} \tag{5}$$

where Γ_0 is a dimensionless constant (=0.608), $\zeta_{21} = 4\left(m_1 m_2\right)\Big/\left(m_1 + m_2\right)^2$ E_c is the minimum energy for atomic displacements and λ_c is the mean range of a recoil distance of energy E_c. Typical values for ξ_{BM} are ≈ 10 A^5/eV or ≈ 50 A^2/dpa. The assumption employed in eq.(y) is the validity of the binary collision approximation. Ballistic mixing thus corresponds to the NRT model of defect production, and similar to NRT, ballistic mixing scales reasonably well with damage energy, as indicated by the equation above.

More quantitative calculations of ballistic mixing can be made using computer simulations, such as TRIM. A few examples are provided in Table 2.1. Notice that the mixing, which is normalised by dpa, is nearly independent of energy and target mass. For lighter targets, such as Si, low-order recoils (i.e. secondaries, tertiaries, etc.) appear to increase significantly the cascade mixing, but are more a part of recoil implantation. For this reason the mixing parameter is high for light elements.

Table 2.1. Values of ion mixing parameter, (in A2/dpa) for self-ion irradiation determined by a modified version of SRIM. The displacement energy was assumed to be 25 eV. Displacements from primary recoils were excluded

	10 keV	100 keV
Si	197	372
Cu	8.7	13.5
Au	15.5	21

Thermal spike mixing: Koehler and Seitz [Ave4] and later Vineyard [Ave5] considered whether atomic jumps could take place during the thermal spike phase of the cascade. The number of jumps is simply calculated by the integral:

$$\eta = \int d^3r \int A \exp\left[\frac{-Q}{kT(r,t)}\right] dt \tag{6}$$

where the jump rate per unit volume of material is $R = A\exp\left[-Q/kT\right]$. Q is the activation barrier for atomic jumping. For a spherical geometry, assuming the initial cascade energy is deposited as a delta function, Vineyard finds,

$$\eta = \frac{0.02226 A \varepsilon_0^{5/3}}{C^{2/3} \kappa Q^{5/3}} \tag{7}$$

where $\varepsilon = \varepsilon_0 \delta(r)$ is the initial energy of the cascade, C is the specific heat, κ is the thermal conductivity and Q is the activation energy for diffusion.

Different models include different assumptions about Q, however, MD simulations have shown that unless the local temperature exceeds the melting temperature, diffusion is negligible on the time scale of thermal spikes. As a consequence, thermal spike mixing becomes increasingly important as the atomic mass of the material increases and the melting temperature decreases.

While dividing the cascade into different stages is conceptually attractive, accurate calculations require MD computer simulations. Figure 2.3 illustrates the time evolution of mixing in Si (Figure 2.3 left) and in several metals (Figure 2.3 right) for cascade energies up to 10 keV. Clearly noticeable is that in Si the mixing is complete within a few tenths of picoseconds, but it continues up to a few picoseconds in heavier metals. For higher energy cascades the time required for complete mixing extends even longer. This shows that in Si, which has low atomic number and fairly high melting temperature, the mixing is mostly ballistic, but in metals, it is resulting mostly from the thermal spike.

Figure 2.3. Time development of the ion beam mixing in crystalline and amorphous Si as well as several metals. From reference [Nordlund, 1997c]

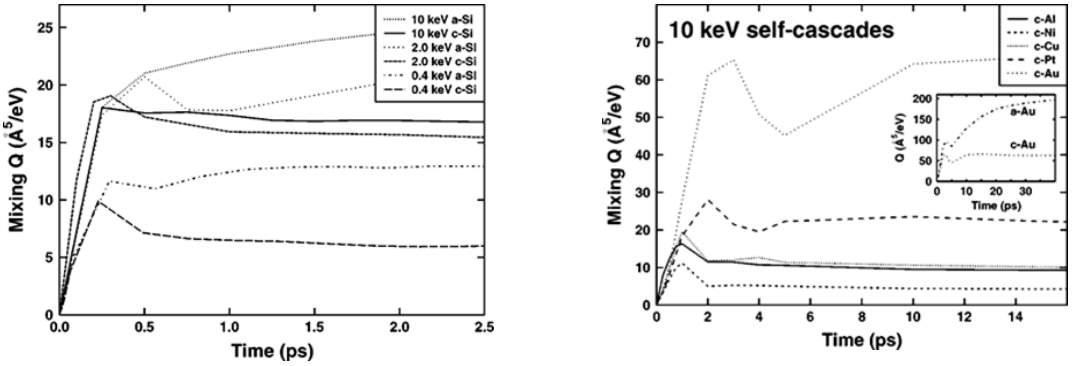

Only few MD simulations have been performed at energies typical of recoil events from fast neutrons, E > 50 keV. The results from one such study on Ni, Pd, and Pt for energies up to 200 keV is shown in Table 2.2 and Figure 2.4. The mean square displacement of atoms was well described by the expression,

$$\left\langle R^2 \right\rangle = a \frac{E^{3/2}}{b^{1/2} + E^{1/2}} \tag{8}$$

where a and b are constants. At high energy, $\left\langle R^2 \right\rangle$ scales linear with energy. Values for a and b, as well as values of the mixing parameter are listed in Table 2.2.

Table 2.2 Comparison of ion beam mixing of MD simulation with experiments [Nordlund, 1998c]

	a	b	Q(MD)	Ion/energy	Q(exp)
Ni	5.638	44400	5.1 ± 0.4	600 keV Kr	4.8 ± 0.5
Pd	16.60	5412000	9.5 ± 0.8	400 keV Kr	9 ± 1
Pt	4506	7.077×10^{10}	14 ± 1	1 MeV Kr	14 ± 2

Ion beam mixing has been measured on several metals at low temperatures in many systems using tracer impurities. A few results for high energy heavy ion irradiation taken from [Ave6] are listed in Table 2.3. More complete results can be found in [Ave7]. The results illustrated that mixing increases with decreasing melting temperature and increasing atomic number. It is noteworthy that the small mixing parameters for metals like Fe and Ni are comparable to values obtained for ballistic mixing, alone, indicating that thermal spikes in these metal have only small effect on mixing.

Table 2.3 Values for the ion beam mixing for several metals

Element	C	Al	Ti	Fe	Ni	Cu	Mo	Ru	Ag	Hf	Ta	W	Pt	Au
$\langle R^2 \rangle / \phi F_D \left(A^5 / eV \right)$	14	112	36	27	39	150	28	44	450	90	54	72	115	730

2.1.4 Clustering, migration (long-time scale)

If a material is irradiated under extremely low temperature condition such as less than 10 K, almost all defects created by radiation are immobile. In this case the long-term damage may be estimated only by the superposition of many primary radiation damage events (buildup of the athermal damage production). In most practical situations such as in materials applied in nuclear power plants, however, the exposure temperatures are sufficiently high for thermally activated motion of defects, leading to clustering, precipitating, and segregating at dislocations and grain boundaries. Such micro- and often nano structural evolutions may lead in the long run to significant change of thermo-mechanical properties of materials: typically hardening and embrittlement, as well as swelling, irradiation creep, and other degradation processes.

Figure 2.4. Simulated R^2 values (circles) fit of the function $R^2(E)$ to the simulated data, and mixing Q'(E) (dashed line) for Ni

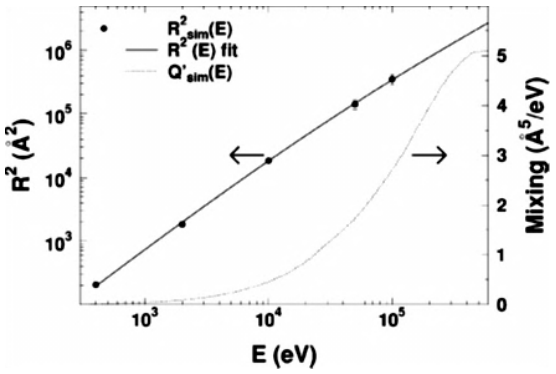

An excellent fit to the simulated data is obtained over about three orders of magnitude in both energy and mixing. From [Nordlund, 1998c].

These effects cannot be predicted solely by atomistic modelling methods like MD, because the current computer technology allows only the temporal development of MD of ~10^{-10}s, while the time scale of the thermo-mechanical properties' change may become more than years. For this reason, in addition to atomistic modelling, it is necessary to resort to mesoscopic/macroscopic modelling methods. These include Kinetic Monte Carlo methods (KMC) and rate equation (RE) modelling [RE1, RE2]. Both of these require as input the rates of all processes that occur in the system, such as the defect or impurity migration jump rate or the rate at which new radiation events occur in a system by e.g. collisions with ions. Once these are known, KMC can be used to simulate the time evolution of a discrete set of atoms (atomic KMC, AKMC) or defect objects (object KMC, OKMC). KMC methods, although dating back to the 1960's (and curiously having been invented independently by at least three different groups under different names working in different fields of natural sciences, have been under intense development in recent years. Promising developments include speedup

schemes like first-passage KMC (FPKMC) in which long sequences of jumps of an isolated defect are treated in a single summed-up step for efficiency [FPKMC].

Rate equations, on the other hand, form a set of differential equations of the time evolution of the spatial distribution function of defects and impurities. In the following, we discuss in greater detail these methods and in particular a recent use of mean-field modelling method using a set of rate equations, sometime called mean-field rate theory (MFRT).

By using multiscale modelling method with the combination of MD and MFRT, a wide range of time scales can be investigated. However, the usefulness of this combination is limited, especially when the radiation causes cascade displacements. Vacancies and self-interstitial atoms (SIAs) created by a cascade displacement event are still spatially correlated even when the thermal equilibrium is regained, but once the information on defects is transferred to MFRT we lose all the positional information of defects. Therefore in-cascade recombination events cannot be properly modelled by the combination of MD and MFRT; this is suggested by [Suzudo; Souidi, 2006] which compares two KMC simulations with different input data, that is, random point defect distributions and point defects directly given by MD. Note that the former case is equivalent to the mean field approximation. These two KMC time developments lead to significantly different results to each other and strongly suggest that thermal in-cascade reactions after the cascade displacement events largely influences the microstructural evolution. This is also confirmed simply by the comparison between KMC and MFRT [Suzudo; Ortiz, 2007]. A systematic investigation of the effect of differences in the nanostructural evolution depending on the cascade source term was done in [Malerba; Souidi, 2005]. Thus it is essential to model further time-development of cascade displacements while keeping the positional information of defects. A suitable modelling methodology for this purpose is given by the KMC simulation that takes the last atomic configuration of cascade displacement simulation from MD and lets the system develop until the spatial correlation between defects disappears, so that the results can be used in the mean field modelling. This kind of KMC simulations are sometimes referred to *as cascade annealing*. A cascade annealing simulation can be thus used to provide the damage source term in MFRT, using MD results as input.

There are a several previous studies on cascade annealing, some of which are a study of Cu [Suzudo; Heinisch, 1996] and others are of α-Fe [Suzudo; Doran, 1970] [Suzudo; Soneda, 1998] [Suzudo; Gao, 1999], although they do not necessarily target the MD-KMC-MFRT multiscale modelling approach. In the following, we introduce a typical method of cascade annealing based on a recent study of α-Fe by [Suzudo; Suzudo, 2012].

First of all, it is necessary to conduct an MD cascade displacement simulation (see for example [Suzudo; Phythian, 1995]) under the targeting temperature and recoil energy. As previously discussed, the electronic excitation is ignored in the simulation. The simulation ends when the thermal equilibrium is reached; a typical time length of the simulation is ~10ps. The atomic configuration given by the MD results is analysed for identification of the locations of created vacancy and SIA, and for finding defect clusters (Suzudo; Lucasson, 2008). A defect configuration determined through this data processing will become an initial condition of the cascade annealing simulation.

A cascade annealing simulation is conducted as follows: putting the above results at the center of KMC simulation box whose size is much larger than that of the displaced region (Figure 2.6); running a KMC simulation under the targeting temperature condition; counting

all kinds of defects when they escape from the simulation box during the time development. The calculation ends when all the mobile defects have escaped from the box, i.e. the time when the spatial correlation between mobile defects disappear. The count of escaped and remained defects will become part of database for conducting MFRT calculation for microstructural evolution caused by radiation damage.

Figure 2.7 shows a typical result of cascade annealing applied to α-Fe, that is, time development of surviving and escaped defects in logarithmic time scale. This result was obtained for the damage energy of 20 keV with an annealing temperature of 343 K, where the damage energy means part of primary knock-on atom's energy that is not used for electronic excitation. The detailed shape of these curves depends on the migration parameters, but generally speaking events occur in the following order:

1. single SIAs and their clusters start migrating; some of them escape from the box, others cause clustering and recombination;
2. single vacancies and their clusters start migrating; some of them escape from the box, others cause clustering and recombination;
3. all SIAs and SIA clusters escape from the box;
4. all vacancies and mobile vacancy clusters escape from the box.

Note that the order of phases 2 and 3 may be inverse depending on the annealing temperature [Suzudo; Suzudo, 2012].

Figure 2.5 shows the ratios of total escaped SIAs after the annealing to the NRT standard value over the wide range of recoil energy. For comparison, the ratios of surviving SIAs before the annealing to the NRT standard value are also shown. The figure indicates that the number of SIAs decrease by about 30% by long-time evolution of cascade displacement. A size distribution of SIA clusters before and after the cascade annealing is shown in Figure 2.8 and this can be used for defect generation terms in MFRT models. As seen in these graphs, the number of single SIAs significantly decreases during the annealing. The absence of cascade annealing simulations underestimates in-cascade recombination event and overestimates the number of surviving single SIAs.

Figure 2.5. Ratios of total escaped SIAs after annealing to NRT standard value over the wide range of recoil energy

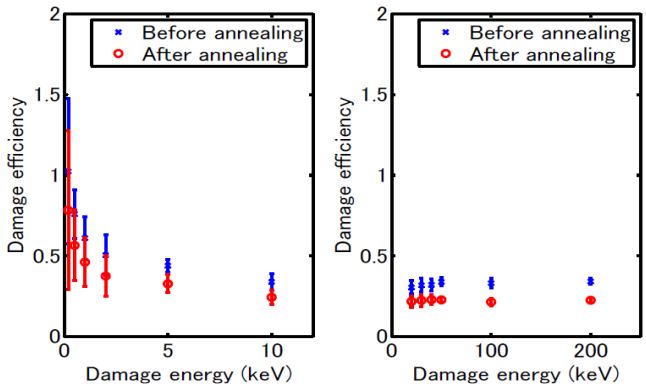

If one uses a simpler MD-MFRT multi-scale modelling instead of MD-KMC-MFRT, the overestimation of single SIAs propagates to the evaluation of, for example, the grain boundary segregation of solute atoms. This is because single SIAs in alloys strongly promote the mobility of solute atoms, which is a typical error expected by MD-MFRT multiscale modelling. It is known that the grain boundary segregation of some elements, for instance P, lead to a decrease in the grain boundary cohesion and consequently to an increase in the ductile-to-brittle transition temperature [Suzudo; English, 2001]. Consequently long-time migration and clustering of displacement cascade using the cascade annealing simulation is critical. As an alternative to the combination of KMC and MFRT, KMC models can be used to simulate a whole irradiation process, spontaneously including any kind of existing spatial correlations [Malerba; Jansson, 2013].

Figure 2.6. Schematic picture explaining cascade annealing simulation using the KMC method

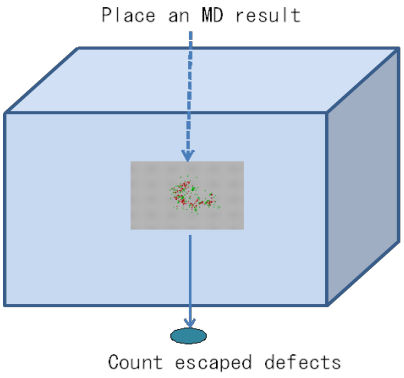

The accuracy of cascade annealing simulations is strongly dependent on the defect migration parameters, and such parameters cannot be uniquely determined at this time. For example, in the case of α-Fe the dimensionality of small SIA clusters motion is still unresolved. In addition, uncommon immobile SIA clusters are also formed [Suzudo; Terentyev, 2008], and we have little information on the relative fraction of mobile and immobile SIA clusters produced by cascade events. The evaluation of how these uncertainties influence cascade annealing is also an important task for the further development of radiation damage modelling.

Figure 2.7. Surviving defects (a) and escaped defects (b) during the annealing after a cascade event with the damage energy of 20 keV

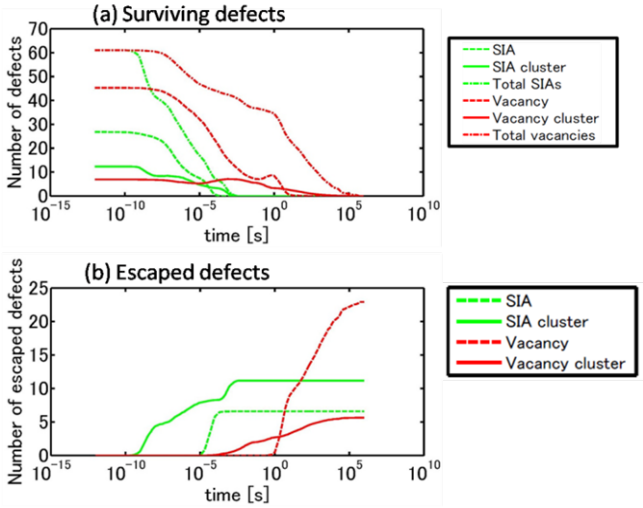

Each value is averaged over many cascade events simulated by MD [Suzudo; Stoller, 2000], see more detail at [Suzudo; Suzudo, 2012].

Finally, it should be mentioned that the kMC approach used to conduct cascade annealing can also have a significant impact on the predicted fraction of point defects that survive [Xu, 2013].

Figure 2.8. SIA cluster size-distribution before and after annealing at *T*=343K

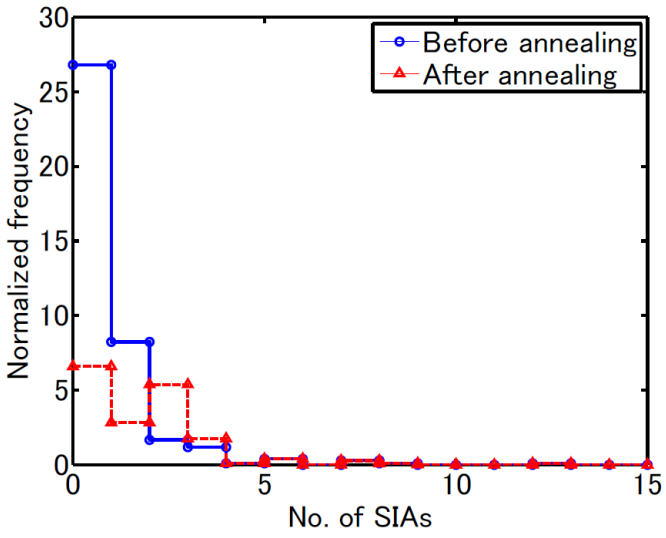

2.1.5 High-fluence effects

Most of the discussion above has been centered on the damage production mechanisms in individual cascades. When the radiation fluence/dose increases, the damage produced by cascades will start overlapping, and several nontrivial effects may result. In fact there is a major difference between metals and semiconductors in this respect. Elemental pure bulk

metals have never been made amorphous by any method, and irradiation is no exception. When a pure metal like Cu is irradiated to high fluences, the damage production efficiency decreases and the damage level eventually saturates. In Cu this saturation level has been experimentally found to be about 1% displaced atoms [Averback, 1977]. This, of course, means that on higher fluences a "dpa" value becomes completely disconnected from the actual number of defects, i.e. at a nominal dpa value of, say, 10 or 100, the defect concentration still remains at (roughly) 0.01.

The origin of the saturation can be fairly well understood from MD simulations. Simulations of collision cascades made on simulation cells with pre-existing point defects showed that for concentrations of pre-existing defects exceeding about 1%, the defect concentration actually decreased [Nordlund, 1997b]. A similar study on cascades overlapping the damage created by previous cascades, and similarly found that the damage level may reduce [Gao, 1996]. Taken together, these observations explain the saturation of point defect damage. The fundamental physical phenomenon underlying this is the same as to why bulk amorphous elemental metals cannot be made: the high packing fraction of the material [Ashcroft-Mermin, 1976] leads to a very strong tendency of the metal to recrystallize, such that even the heat spike recrystallisation front is not fast enough to retain the material in an amorphous state.

However, the saturation of the point defect level does not necessarily mean that other kinds of material damage may not grow indiscriminately: for instance, the vacancies may agglomerate to voids, which can lead to swelling of the material (even though the material between the voids may remain in an almost perfect crystalline state) [Garner, 2005; Chung, 2006]. In some cases this swelling may be in principle limitless, such as in the case of plasma-irradiated tungsten where the swelling leads to the growth of a porous "fuzz" layer with a square root dependence on fluence.

2.1.6 Metal alloys

The scope of radiation effects phenomena in multicomponent alloys (i.e. containing more than one element) introduces several new displacement damage aspects compared to pure elements. The main additional features that are of potential importance in alloys include:

- More complex defect production, particularly for near-threshold displacements;
- Chemical mixing (including order-disorder transitions);
- Solid state crystalline-amorphous phase transitions (e.g. intermetallics, bulk metallic glasses);
- Radiation-modified solute segregation and precipitation;
- Precipitate dissolution or coarsening for multi-phase systems.

The presence of multiple elements (each of which may have a different displacement energy) creates the possibility of several new defect production scenarios compared to pure elements. These effects are particularly pronounced for low primary knock-on atom (PKA) energy events, which would lead to preferential displacement of the lower mass (or lower E_d) element. In addition, enhanced near-threshold displacement of heavy atoms by a two-step process (initial displacement of a low-mass element, followed by displacement of a high-mass

element by the light ion) can strongly affect measurements of displacement energies in multi-component materials [Zinkle, 1997].

Experimental studies of radiation-induced ordering or disordering in alloys date back to some of the earliest studies of bulk radiation effects in materials [Siegel, 1949; Rosenblatt, 1955]. Chemical mixing that ranges from 1 to ~100 times larger than the calculated defect production value has been observed in irradiated alloys [Kirk, 1978; Paine, 1985; Zinkle, 1993; Averback, 1998]. Depending on the irradiation temperature, PKA spectrum, and initial amount of short- and long-range order, irradiation can lead to either enhanced ordering [Averback, 1998; Ravelosona, 2000] (via radiation enhanced diffusion [Dienes, 1958; Sizmann1978] processes) or increased disorder (due to Frenkel pair production, replacement collision events, and ballistic mixing in energetic displacement cascades) [Averback, 1998].

Whereas solid state crystalline to amorphous phase transitions generally do not occur in pure metals, amorphisation is frequently observed during irradiation of ordered intermetallic alloys [Thomas, 1982; Nastasi, 1991; Motta, 1997; Lam, 1997; Nagase, 2012], in part due to higher point defect migration enthalpies and crystalline free energies that are closer to the amorphous free energies. The role of radiation-induced disorder has been identified as a key factor in several evaluations [Nastasi, 1991; Motta, 1997; Lam, 1997]. Irradiation-induced amorphisation is most easily induced in alloys with limited phase stability such as intermetallic compounds, irradiated at low temperatures at high damage rates using irradiation sources that have high average PKA energies [Koike, 1989; Motta, 1997]. Amorphisation can also be induced in metallic multilayers irradiated under energetic cascade damage conditions [Liu, 2000]. Irradiation of amorphous metallic materials at elevated temperatures can stimulate the inverse solid-state reaction, i.e. radiation-induced crystallisation, due to radiation-enhanced diffusion [Nagase, 2012].

The preferential coupling of solute atoms and radiation defects can cause a variety of radiation-modified solute segregation processes [Johnson, 1976; Okamoto, 1979; Marwick, 1981; Russell, 1984; Nastar, 2012], which in turn can lead to dramatic differences in solute profiles near grain boundaries and other microstructural features compared to thermal equilibrium solute profiles [Lee, 1981; Maziasz, 1989; Wakai, 1995; Faulkner, 1996]. For example, chromium depletion occurs at grain boundaries in irradiated austenitic steels, and is an important contributor to the degraded stress corrosion cracking behaviour of these steels in nuclear reactors [Kenik, 2012]. In general, the radiation-modified solute segregation behaviour during irradiation can lead to radiation-enhanced, -modified, or -induced precipitation in alloys [Lee, 1981]. Radiation-enhanced precipitation is chemically and structurally similar to that observed after thermal aging processes, but the formation and growth kinetics are accelerated due to radiation-enhanced diffusion. Radiation-modified precipitates may contain different chemical compositions due to radiation-induced segregation of certain solute elements. Radiation-induced precipitates form only under irradiation conditions due to pronounced radiation-induced segregation behaviour, and are thermally unstable (dissolve) if subsequently annealed at the irradiation temperature.

A related phase stability phenomenon in alloys containing one or more dispersed phases is precipitate dissolution and coarsening [Hudson, 1975; Russell, 1984]. Under energetic displacement cascade conditions, ballistic dissolution of nanoscale precipitates can occur. Depending on the thermodynamic driving force for precipitate re-nucleation and the temperature (kinetics), possible outcomes include complete particle dissolution, particle

growth (via Ostwald ripening or other mechanisms), or quasi-equilibrium stability in particle size. Knowledge of the competing dissolution and growth mechanisms can be used to synthesis nanoscale precipitate arrays with controlled size and density for electronic applications [Rizza, 2007; Rizza, 2007b], and is also important for developing next-generation radiation-resistant materials for nuclear reactor structural applications [Certain, 2013].

2.2 Athermal recombination-corrected dpa (arc-dpa)

2.2.1 Review of defect production efficiency

Building upon the defect production models originally proposed by Kinchin and Pease [Kinchin, 1955] and later modified by Norgett, Robinson and Torrens [NRT], numerous experimental and modelling studies have been performed to obtain improved understanding of defect production in irradiated materials. Some of these results are summarised in a series of review articles that provide a perspective on the evolution of knowledge of defect production processes in pure metals and more complex materials [Wollenberger, 1970; Lucasson, 1975; Merkle, 1976; Vajda 1977; Zinkle, 1993; Averback, 1994; Schilling, 1994; Rubia, 1995; Zinkle, 1997; Averback, 1998; Stoller, 2012].

One important aspect has been the synergistic use of MD simulations and experimental monoenergetic particle irradiation studies to investigate the crystallographic and temperature dependence of threshold displacement energies in materials. For example, although experimental measurements of displacement energies have been reported since the early 1950s, the first investigations of the crystallographic dependence of displacement energies utilised MD modelling [Gibson, 1960; Erginsoy, 1964], and these results stimulated a large number of subsequent experimental and modelling studies. Most experimental studies have used electrical resistivity to monitor defect production, where the atomic concentration can be directly obtained if the specific resistivity per Frenkel pair is known; compilations of recommended values are available [Jung, 1991; Broeders, 2004]. Several other experimental methods have also been utilised, including direct observation of defect cluster formation during electron irradiation in a transmission electron microscope. Table 2.4 summarises some of the experimental results for the threshold and recommended volume-averaged displacement energies for 29 different pure elements that are important for physics and nuclear science studies. Experimental data on threshold displacement energies for another 19 elements have been compiled by Jung [Jung, 1991].

Table 2.4. Values of threshold and average displacement energies

Element	Crystal structure	Threshold E_d (eV)	Average E_d (eV)
Al	FCC	16 [Jung, 1981]	27 [Lucasson, 1975] 25 [ASTME521]
Cu	FCC	19 <110> [Vajda, 1977] 19 <100> [Vajda, 1977] 45 <111> [Vajda, 1977] 19 [Jung, 1981]	29 [Lucasson, 1975] 30 [ASTME521]
Ni	FCC	22 <110> [Vajda, 1977] 35 <100> [Vajda, 1977] 60 <111> [Vajda, 1977] 23 [Jung, 1981]	33 [Lucasson, 1975] 40 [ASTME521]
Ag	FCC	23 <110> [Vajda, 1977] 24 [Jung, 1981]	39 [Lucasson, 1975]
Au	FCC	36 <110> [Vajda, 1977] 36 <100> [Vajda, 1977] 36 <111> [Vajda, 1977] 34 [Jung, 1981]	43 [Lucasson, 1975] 40 [Vajda, 1977]
Pb	FCC	12.5-15 [Jung, 1991]	19 [Lucasson, 1975] 25 [ASTME521]
Co	FCC	23 <110> [Vajda, 1977] 30 <100> [Vajda, 1977]	
Pt	FCC	39 <110> [Vajda, 1977] 37 <100> [Vajda, 1977] 34 [Jung, 1981]	44 [Lucasson, 1975]
Pd	FCC	34 [Jung, 1981]	41 [Lucasson, 1975]
Th	FCC	35 [Jung, 1991]	44 [Lucasson, 1975]
Ge	Diamond cubic	14 [Corbett, 1966]	18 [Loferski, 1958] 20 [Poulin, 1980] 30 [Vitovskii, 1977]
Si	Diamond cubic	13 [Corbett, 1966] 13 <111> [Loferski, 1958]	
C (diamond)	Diamond cubic	32 <110> [Steeds, 2011] 27 <100> [Steeds, 2011] 34 <111> [Steeds, 2011]	40 [Zinkle, 1997]
C (graphite)	HCP	25 [Corbett, 1966]	30 [Zinkle, 1997]
V	BCC	39 <110> [Vaj, 77] 30 <100> [Vaj, 77] 35 <111> [Vaj, 77] 25 [Jung, 1981]	40 [ASTME521]

Table 2.4. Values of threshold and average displacement energies (continued)

Element	Crystal structure	Threshold E_d (eV)	Average E_d (eV)
Cr	BCC	34 <110> [Vajda, 1977] 21 <100> [Vajda, 1977] 24 <111> [Vajda, 1977] 28 [Vajda, 1977]	40 [ASTME521]
Mn	BCC		40 [ASTME521]
α-Fe	BCC	30 <110> [Vajda, 1977] 20 <100> [Vajda, 1977] 25 <111> [Vajda, 1977] 17 [Jung, 1981]	44 MD - [Lucasson,1975] 40 [ASTME521] 40 (Average of MD sims with 10 potentials in [Nordlund, 2005c]
Nb	BCC	28 [Jung, 1981]	78 [Lucasson,1975] 60 [ASTME521]
Mo	BCC	35 <100> [Vajda, 1977] 45 <111> [Vajda, 1977] 34 [Jung, 1981]	65 [Lucasson,1975] 60 [ASTME521]
Ta	BCC	33 <100> [Vajda, 1977] >55 <111> [Vajda, 1977] 32 [Jung, 1981]	85 [Lucasson,1975] 90 [ASTME521]
W	BCC	>58 <110> [Maury, 1978] 42 <100> [Maury, 1978] 44 <111> [Maury, 1978]	100 [Lucasson,1975] 90 [ASTME521]
Ti	HCP	23 <0001> [Karim, 1978]	30 [Lucasson,1975] 30 [ASTME521]
Mg	HCP	10 [Jung, 1991]	20 [Lucasson,1975]
Co	HCP	25 <1120> [Vajda, 1977] 30 <1010> [Vajda, 1977] 36 <0001> [Vajda, 1977]	36 [Lucasson,1975] 40 [ASTME521]
Zn	HCP	14 <1120> [Vajda, 1977] 19 <0001> [Vajda, 1977]	29 [Lucasson,1975]
Zr	HCP	21 [Jung, 1991]	40 [Lucasson,1975] 40 [ASTME521]
Cd	HCP	21 <1120> [Vajda, 1977] 40 <0001> [Vajda, 1977] 19 [Jung, 1991]	30 [Lucasson,1975]
Re	HCP	44 [Jung, 1991]	60 [Lucasson,1975]

Note that some values are not experimental; for instance the value of 44 eV for Fe cited in [Lucasson, 1975] comes from MD simulations done with pair potentials in 1963 by Erginsoy et al. [Erginsoy, 1964].

The effect of temperature on the displacement energy has been experimentally studied for a few materials, in particular Cu. Even though the energy associated with room temperature thermal vibrations of lattice atoms is only ~0.025 eV, thermal effects can affect the displacement energy due to atomic momentum effects [Sosin, 1969; Jung, 1981a] as well as reducing correlated recombination of close Frenkel pairs [Roth, 1975; Drosd, 1978;

Lennartz, 1977; Urban, 1981] and lattice softening effects [Jung, 1981a]. Early molecular dynamics calculations on alpha-Fe [Agranovitch, 1971] found that the crystallographic anisotropy became less pronounced at high temperatures. Experimental studies on Cu, Ag, Au and Mo have found that the magnitude of the displacement energy may be reduced by up to a factor of two at elevated temperatures near 0.5 T_M compared to low-temperature results [Drosd, 1978; Jung, 1981a; Urban, 1981; Hohenstein, 1989; Sigle, 1994; Zag, 1983]. This big drop may in part be due to athermal effects such as the atomic momentum and lattice softening effects, in part thermally activated recombination of close Frenkel pairs.

There are several lingering shortcomings in the NRT displacement model. As noted in several previous reviews [Lucasson, 1975; Merkle, 1976; Vajda, 1977; Lucasson, 1978; Merkle, 1983], defect production behaviour near threshold energies for displacement damage is significantly more complex than the step function plus linear behaviour assumed in the NRT model. This is due in part to the simplifying assumption of a constant scalar displacement energy (usually taken to be the crystallographic-averaged value), whereas the actual threshold displacement energy varies strongly with crystallographic direction. For example, as noted in [Lucasson, 1975], the ratio of the average displacement energy to the lowest threshold displacement energy (cf. columns 3 and 4 in Table2.4) is typically ~1.5 for FCC metals and ~2 for BCC metals.

A second issue with the NRT displacement model is that the retained defect concentration is generally not equal to the calculated dpa value. The discrepancy is particularly pronounced for PKA energies that are greater than a few times the threshold displacement energy (even at low temperatures where random walk defect migration and recovery does not occur), and the discrepancy becomes increasingly larger with increasing PKA energy. This discrepancy in retained defects compared to the NRT calculated value is largely due to two simplifications in the NRT model: isotropic displacement energy (briefly mentioned in the previous paragraph) and neglect of ballistic in-cascade recombination effects. At low energies, the fact that the threshold displacement energies exhibit local minima near low-index crystal directions, see Figure 2.13, has the consequence that a single defect displacement can be achieved at the (orientation-specific) threshold displacement energy along a low index direction, whereas production of two defects can require up to ~6 E_d [Lucasson, 1978]. As a direct consequence, the defect production efficiency for PKA events near the displacement threshold energy will be >1 if the PKA collision is along a low-index direction such as <111> in FCC metals and the crystallographic-averaged E_d is used in the NRT displacement equation, and it could be <1 if the PKA collision is along a high-index direction and/or if the minimum threshold displacement energy is used in the NRT displacement equation. For PKA energies up to ~4-6 E_d, focused replacement collisions along low index directions can efficiently dissipate the initial PKA energy while creating only one defect, whereas high-index collisions can require significantly higher energy than the low-index threshold displacement energy to create a Frenkel pair. As a consequence, the calculated and measured values of retained defects for PKA energies near 100-400 eV are about a factor of 1.5 to two smaller than the NRT prediction [Lucasson, 1975; Lucasson, 1978; Stoller, 2012] – e.g. based on [Lucasson, 1975] analysis of thermal neutron and electron irradiation data published by [Coltman, 1967] and [Wurm, 1970]. For higher PKA energies, an additional important factor is enhanced defect recombination within the energetic displacement cascade due to the high kinetic energy imparted to multiple atoms [Merkle, 1977; Averback, 1978]. Since the kinetic energy transferred to the host atoms in an energetic displacement

cascade can be many times higher than the defect migration enthalpies, pronounced defect recombination can occur during the cascade quench phase, resulting in defect production efficiencies that are 20-40% of the calculated NRT values.

Figure 2.9. Anisotropy of the threshold displacement energy in FCC crystals

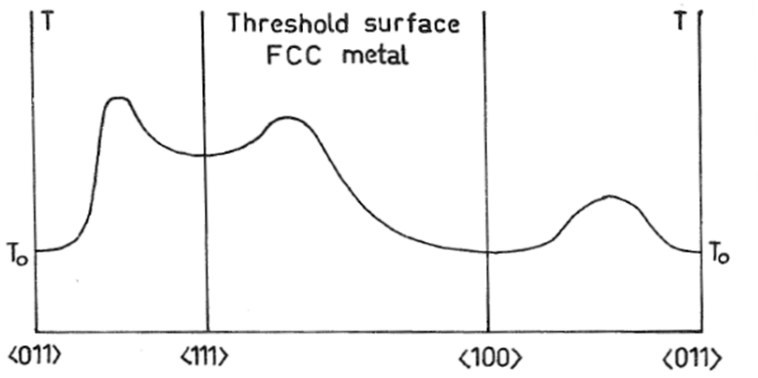

Note how the threshold energy has minima near the low-index crystal directions. From [Lucasson, 1978].

For the most precise quantitative measurements of defect production efficiencies, near-monoenergetic PKA energies with well-defined crystal orientations (particularly for near-threshold displacements) are preferred; however, most experimental studies have used polycrystalline specimens and thereby measure the crystallographic-averaged defect production. The residual defect concentration in irradiated metals is often monitored using electrical resistivity measurements. This technique produces accurate measurements of defect concentrations if defect clustering does not occur. The electrical resistivity per unit concentration of defects can change significantly if pronounced clustering occurs, although it is fortuitous that the resistivity per defect for nanometer-sized SFTs and dislocation loops in metals such as Cu is comparable to the isolated Frenkel pair value [Thompson, 1973; Zinkle, 1988].

The results of a systematic investigation of the effect of average recoil energy on the surviving defect fraction for ion irradiated copper [Averback, 1978] is plotted in Figure 1.4. The interpretation of the ion irradiation results is somewhat complicated due to the relatively wide range of PKA energies associated with the long-range Coulombic interactions between the incident ions and target atoms. Nevertheless, a clear trend of decreasing defect production efficiency (relative to the NRT equation) is observed with increasing PKA energy up to at least 10 keV. Some evidence for saturation of the defect production efficiency in irradiated copper is evident for PKA energies >10 keV.

Numerous experimental investigations have examined the effect of PKA energy on defect production efficiency for more than a dozen pure metals, primarily using electrical resistivity techniques during irradiation near 4 K with electrons [Lucasson, 1962; Iseler, 1966; Wurm, 1969; Jung, 1973; Jung, 1975; Maury, 1975; Maury, 1976; Vajda, 1977], thermal neutrons [Coltman, 1967; Klabunde, 1974; Coltman, 1975; Horak, 1975; Coltman, 1978], ions [Averback, 1978; Averback, 1983], fission neutrons [Horak, 1975; Kirk, 1979; Coltman, 1981; Klabunde, 1982; Wallner, 1988], fission fragments [Birtcher, 1978], 14 MeV neutrons [Guinan, 1982,

Guinan1985], and D-Be stripping neutrons [Roberto, 1977]. Many of the neutron irradiation data have been reviewed by Broeders and Konobeyev [Broeders, 2004].

Figure 2.10 summarises experimental measurements of defect production efficiency for iron, nickel and copper irradiated with near-monotonic-energy PKA sources (electrons, thermal neutrons, fission neutrons, D-T fusion neutrons, and d-Be neutrons). For this evaluation, the original data were reanalysed using the Frenkel pair resistivity values recommended by Jung [Jung, 1991]. The electron displacement damage values were calculated using the tables by Oen [Oen, 1973] and converted to the NRT damage function using the ASTM recommended average displacement energies listed in Table 2.4 [ASTM E521]. The measured defect production efficiencies are plotted as a function of damage energy, where the ionisation losses have been subtracted from the PKA energy. The general dependence of the defect production efficiency on damage energy is similar for all three of these materials. There are three key features evident from this plot: 1) damage efficiencies >1 occur at very low damage energies; this is a consequence of well-known shortcomings of the NRT damage equation near threshold displacement energies [Lucasson, 1978; Merkle, 1983; King, 1983] and is also due to the use of the average E_d rather than the threshold E_d value in the NRT damage calculation. This results in an artificially suppressed calculated displacement value for damage energies near the threshold. 2) The defect production efficiency decreases rapidly with increasing damage energy at intermediate energies of ~100 eV to ~5 keV. 3) The defect production efficiency approaches an apparent saturation value of ~0.3 for all three metals for damage energies above ~5 keV. Prior work has related the lower bound energy for saturation of the defect production efficiency with the onset of defect subcascade formation [Merkle, 1976; Lucasson, 1978; Muroga, 1985]. Qualitatively similar results are observed for several other elements, including Al, Ag, Pt and Mo.

Figure 2.10. Experimental (electrical resistivity) measurements of the effect of damage energy on defect production efficiency for near-monotonic PKA irradiations in Cu, Ni, and Fe

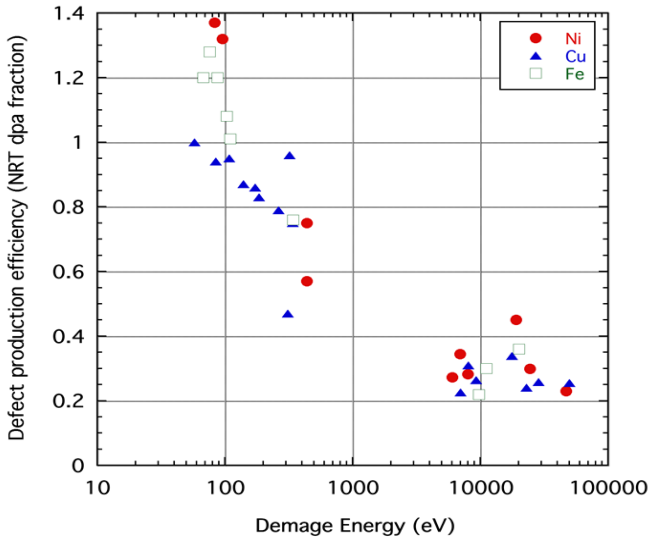

2.2.2 Derivation and motivation for new functional form

As discussed in detail in the previous section, it is well established that the number of stable point defects produced in elemental metals is much smaller than the value predicted by the NRT equation that forms the basis for standard dpa calculations. To summarise, the experimental and simulation studies discussed above have shown that in most metals studied, the damage level for low-energy recoils is fairly close to the NRT value, but with increasing nuclear damage energy, the relative damage efficiency decreases from ξ ≈ 1 near the threshold to a value that saturates around roughly 0.2-0.4.

$$\xi(E) = \frac{N_{True-number-of-FP's}}{N_{NRT-prediction}}$$

Note that in this discussion, E signifies specifically the nuclear deposited (damage) energy by a single recoil $F_{D,n}$. Part of the total recoil energy E_{rec} also goes into electronic deposited energy $F_{D,e}$ and for very high recoil energies (MeV or more) some may also go into nuclear reactions $F_{D,nr}$ such that $E_{rec} = F_{D,n} + F_{D,e} + F_{D,nr}$.

At intermediate energies, several groups have found that the data increases following a power law E^x where the exponent gets a value of about 0.8, see Figure 2.11. On the other hand, it is clear from binary collision approximation simulations and high-energy MD simulations [Nordlund, 1998c; Zinkle; Stoller, 2012] that at very high energies (of the order of 10-100 keV depending on material) the cascades tend to split into separated subcascades (although very recent MD simulations in Fe indicate the split may not be complete [Zarkadoula, 2013]). Hence the scaling with energy must eventually turn to be linear with damage energy.

Figure 2.11. Number of Frenkel pairs produced in self-recoil induced collision cascades in Fe

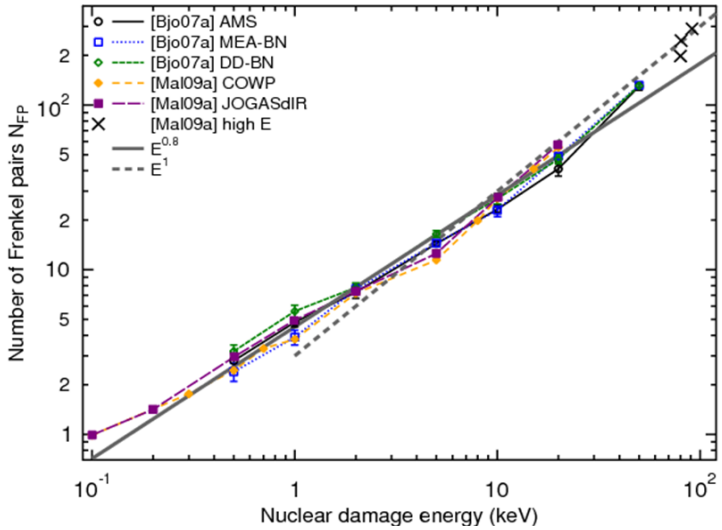

Also shown is fits of a power law $E^{0.8}$ to the data up to 20 keV and a linear power law E^1 for the high-energy data. The data sets and their notations are from [Björkas, 2007a; Malerba, 2010].

As part of this work, we developed a new damage function formalism.

To be able to describe the two regimes of energy dependence described above, the function $N_{FP}(E)$ to be fit has to fulfil at least the limit $N_{FP}(E) \rightarrow aE^1$ when $E \rightarrow \infty$ but cannot be just linear at intermediate energies based on the previous results of $E^{0.8}$ at low E. A simple function that fulfils these requirements is:

$$N_{FP} = a' E^{b+1} + c' E^1$$

where a, b and c are parameters to be fitted. The corresponding damage efficiency function becomes:

$$\xi(E) = \frac{N_{FP}}{N_{NRT}} = \frac{a' E^{b+1} + c' E^1}{0.8E/(2E_d)} = \frac{a' E^b + c'}{0.8/(2E_d)} = aE^b + c$$

From this form one sees that the constant c corresponds to the saturation level at high E, and hence $c \approx 0.3$.

Although this form could be used as it is (and was found to provide quite good fits to the data in Fe), it has the disadvantage that the fit can easily give values for $\xi > 1$, which leads to a discontinuity when combined with the NRT equation. Hence we impose the further constraint that exactly at the beginning of the linear term, $2E_d/0.8$, the function ξ should be exactly 1. This can be easily achieved by solving:

$$\xi(2E_d/0.8) = a(2E_d/0.8)^b + c = 1$$

for one of the adjustable parameters. We recognise that this is a simplification, as it is known that ξ can sometimes be larger than 1 [Zinkle, 1993], and moreover the step function is also well known to be a simplification [Nordlund, 2005c]. However, doing this has the major advantage that it allows to reduce the number of fitting parameters by one. Solving for the a parameter, we obtain:

$$\xi(E) = \frac{1-c}{(2E_d/0.8)^b} E^b + c$$

One could of course replace the numerical values 2/0.8 with 2.5, but for consistency with previous literature, we maintain the factor 2/0.8 explicitly.

The functional form for mixing also has the advantage that the b fitting parameter has a physical interpretation: it gives the point where the transition from a power law behaviour E^c starts to transform into a linear behaviour corresponding to cascades being split into subcascades. The c parameter can be also given a qualitative physical interpretation. It is partly related to how efficiently interstitials are transported to the outer periphery of the displacement cascade: if they are efficiently transported, recombination is less likely resulting in a higher c value. On the other hand, it is also related to cascade density and melting point of the material: if the density is low, and melting point is high, the heat spike is small or absent, which reduced the recombination probability. As a case in point, in Si the damage production follows well the NRT prediction even at high energies, because the open crystal structure and relatively low atomic density leads to efficient ballistic transport of interstitials far from the cascade center, and the low density and high melting points leads to an absence of heat spikes [Nordlund, 1998b] (cf. Section 3).

Figure 2.12 illustrates that this damage function fits very well the data for fraction of surviving defects in Fe. Considering that there is fairly large variation between data obtained with different potentials, it does not make sense to aim for a better fit until the data itself becomes more reliable.

Figure 2.12. Fit of the new damage function ξ (E) to data in Fe for the arc-dpa

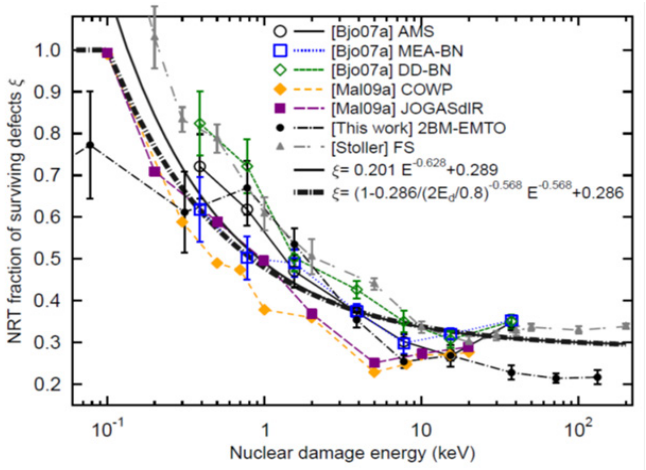

The data sets and their notation are from [Björkas, 2007a; Malerba, 2010]. The data set "[This work]" is new data simulated for the current work using the Fe part of the 2BM-EMTO potential from [Wal04], which is the AMS potential. The data marked [Stoller] is a collection of MD cascade data by one of the co-authors, Roger Stoller.

Our proposal is thus that in dense metals, where it is well established that athermal recombination of damage within energetic displacement cascades reduces the residual damage levels from the NRT equation prediction, calculations and computer codes that currently use the NRT equation to calculate displacement damage exposure values (old NRT-dpa):

$$N_d(E) = \begin{bmatrix} 0 & E < E_d \\ 1 & E_d < E < 2E_d/0.8 \\ \dfrac{0.8E}{2E_d} & 2E_d/0.8 < E < \infty \end{bmatrix}$$

should provide as an alternative to calculate the athermal recombination corrected displacement damage (arc-dpa)

$$N_{d,arcdpa}(E) = \begin{bmatrix} 0 & \text{when} & E < E_d \\ 1 & \text{when} & E_d < E < 2E_d/0.8 \\ \dfrac{0.8E}{2E_d}\xi(E) & \text{when} & 2E_d/0.8 < E < \infty \end{bmatrix}$$

Figure 2.13. Illustration of the original NRT damage function for dpa calculations and the new function that accounts for athermal recombination (arc-dpa)

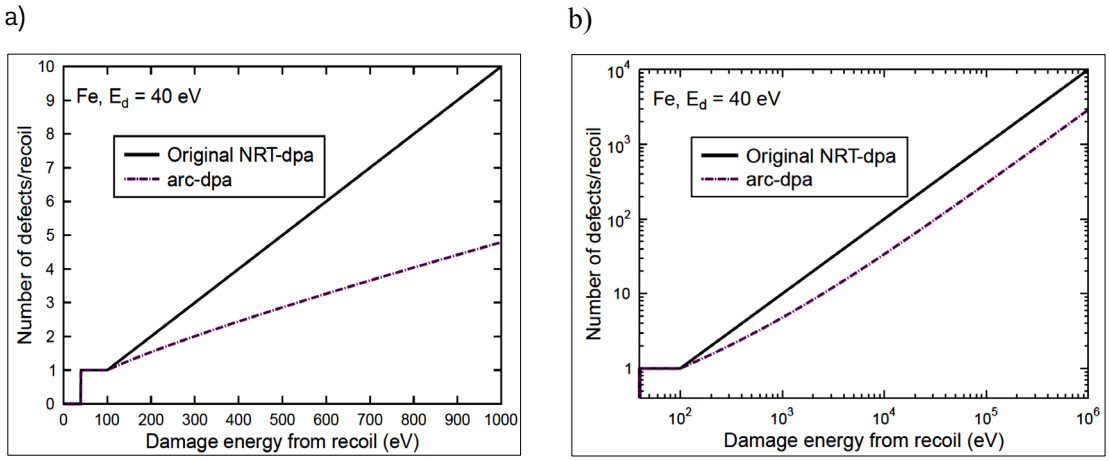

The functions are shown both on a linear and a log-log plot. The parameters used are for Fe with E_d = 40 eV (following the ASTM standard), b = *-0.568* and c = *0.286*. Note from the log-log plot that due to the chosen functional form, at high energies the arc-dpa becomes linear with the energy.

with the efficiency function $\xi(E)$ given by:

$$\xi(E) = \frac{1 - c_{arcdpa}}{(2E_d/0.8)^{b_{arcdpa}}} E^{b_{arcdpa}} + c_{arcdpa}$$

where E is the damage energy. Here the subscript "*arcdpa*" was added for the constants to avoid possible confusion with other quantities using the same letter and the "*rpa*" constants introduced later. However, any use should keep in mind that either form is still only a damage exposure parameter that allows comparing different irradiations in a physically motivated way, but cannot predict the exact nature of the microscopic damage which involves many complicated issues such as damage cluster size, thermal mobility and recombination, nonlinear damage buildup at high doses, etc.

Instead of the previous single material-specific parameter (the threshold displacement energy E_d), the arc-dpa displacement parameter is based on 3 tabulated parameters: E_d, b_{arcdpa} and c_{arcdpa}. The parameter b_{arcdpa} gives a measure of how fast with increasing energy the residual displacement damage reduces by athermal recombination towards the saturation value for PKA energies above the onset for subcascade formation. The saturation value is given by the parameter c_{arcdpa}. Both b_{arcdpa} and c_{arcdpa} are unitless.

The old NRT-dpa and new arc-dpa function are illustrated in Figure 2.13.

Usage of the new form implies that the materials-specific parameters to be used increase in number from 1 to 3. This is illustrated with current best-fit values for the MD data shown in Figure 2.12 in Table 2.5.

Table 2.5. Materials parameters for Fe for the NRT-dpa and arc-dpa equations

Material	Model	E_d (eV)	b_{arcdpa}	c_{arcdpa}	Source of data
Fe	NRT-dpa	40	-	-	ASTM standard
Fe	arc-dpa	40	-0.568±0.020	0.286±0.005	E_d: ASTM standard *b*, *c*: fit to composite MD data

The fitted parameters and their uncertainties are obtained from a Levenberg-Marquardt least squares fit to the data [Bevington, 1992; Numerical Recipes].

The parameter values E_d, *b* and *c* can be obtained from experimental studies or MD simulations. Comprehensive experimental data obtained systematically as a function of energy is available only for a few elements such as Al, Cu, and Mo, whereas partial experimental information under electron [Wollenberger, 1970; Vajda, 1977], thermal neutron [Coltman, 1967], fast fission neutron [Coltman, 1981; Klabunde, 1982; Wallner, 1988] and 14 MeV fusion neutron [Guinan, 1982; Guinan, 1985] conditions is available for about a dozen elements. Naturally the fits can be redone when improved MD or experimental data becomes available.

2.2.3 Obtaining additional data by molecular dynamics

Additional data for fitting the two new constants can be obtained by MD simulations using well established techniques, which we briefly summarise here. In molecular dynamics simulations the Newton equations of motion are solved iteratively over a finite-sized time step to obtain the dynamical motion of atoms. The basic approach for equilibrium molecular dynamics is very well established [Allen-Tildesley, 1989], and we concentrate here on the specific aspects needed to simulate radiation effects.

Bulk collision cascades can be simulated using the standard molecular dynamics technique of periodic boundary conditions [Allen-Tildesley, 1989], i.e. making atoms at one side of a simulation cell "see" and interact with atoms on the opposite side as if the simulation cell boundary does not exist. In this way a finite system can be simulated without any free surfaces. Atom coordinates for the simulation cell can be constructed to correspond to any known crystal, polycrystalline or amorphous sample structure. After generating the coordinates, it is important to simulate the cell for some time (at least a few picoseconds) at the desired temperature to get a realistic Maxwell-Boltzmann distribution of the atom velocities and corresponding displacements of atoms from the equilibrium positions. In the same initial simulation, the pressure should be relaxed by using pressure control techniques [Allen-Tildesley, 1989; Berendsen, 1984] to make sure the cell is at zero (or some other desired) pressure.

After the cell is properly equilibrated, a recoil can be initiated by giving a randomly chosen atom a velocity corresponding to the desired kinetic energy in a random direction. After the recoil is initiated, the volume where the collision cascade develops should be simulated in the NVE thermodynamic ensemble, i.e. not using any pressure or temperature control. On the other hand, since the recoil introduces extra kinetic energy (heating) to the system, and a pressure/heat wave, the extra temperature introduced should be removed and the wave damped. This can be achieved by using some temperature control or velocity scaling scheme at the simulation cell boundaries (see [Samela, 2005] and references therein). Frequently used schemes include random Langevin forces [Postawa, 2003] or locally applied

Berendsen temperature control [Berendsen, 1984]. Naturally one should ensure that any atom with high kinetic energies does not enter the temperature damping region. The evolution of the system should be followed until all parts of the collision cascade have cooled down to the ambient temperature, which typically takes 5-50 ps depending on the mass of the atoms in the system.

Since a collision cascade involves high kinetic energies, the interatomic potential used should also have a realistic high-energy part. The most common approach to achieve this is to spline (smoothly join) the equilibrium interatomic potential to the Ziegler-Biersack-Littmark universal repulsive potential [ZBL] or a pair-specific repulsive potential calculated with quantum mechanical methods [Nordlund, 1997a]. Because the atom velocities are very high, also the time step should be much shorter than the equilibrium one. A time step that is inversely proportional to the maximum velocity and to the product of maximum velocity and maximum forces (choosing the smaller value of the two) has been found to give accurate solution of the equations of motion up to MeV energies [Nordlund, 1995; Nordlund, 2007b].

Energetic ions, at least when their kinetic energies are higher than ~ 100 eV, always lose energy also via electronic stopping (ionisation) [LSS; ZBL]. The fraction of energy lost via this mechanism is almost always about 20%, and protons lose most of their energy via electronic mechanisms in almost all materials [SRIMbook]. Decades of BCA simulations [Robinson, 1967; NRT; Robinson, 1992; Hou, 1994; Gãrtner, 1995], and more recently MD ion range calculations [Nordlund, 1995; Hobler, 2000; Posselt, 2000b], have established that the electronic energy loss can well be treated as a frictional force with the magnitude of the electronic stopping slowing down the motion of energetic ions. This approach has been implemented by many groups using MD simulations [Caro, 1989; Pronnecke, 1991; Caro, 1994; Torri, 1994; Nordlund, 1998b; Cai, 1998; Ji, 2004; Duvenbeck, 2007b; Rutherford, 2007; Sandoval, 2009; Page, 2009; Nakagawa, 2010], while especially groups simulating cascades in Fe have usually not included the electronic stopping [Phythian, 1995; Malerba, 2007]. In the latter case, the MD recoil energy is interpreted to correspond to the original primary-knock-on atom energy after the electronic energy loss has been subtracted out from it.

We note that although the treatment of the electronic stopping at keV energies is quite accurate (this can be demonstrated by comparison of ion depth distributions with experiments [Beadmore, 1998; Sillanpää, 2000; Peltola, 2003a]), there is some uncertainty of how the low-energy limit of the stopping power should be treated [Page, 2009; Björkas, 2009a; Draxler, 2005; Pruneda, 2007; Zeb, 2012]. The simplistic approach of using a conventional electronic stopping, which is linearly proportional to ion velocity, at all atom velocities is clearly not reasonable as this would quench out all energy from the system very rapidly.

A partly related issue is how the so called electron-phonon coupling (EPC) should be treated in collision cascades. Generally the electron-phonon coupling means transfer of energy from an initially hot electronic subsystem (heated e.g. by a laser) to lattice atoms [Ivanov, 2003], but in collision cascades the initially hot atomic subsystem will heat the electronic one [Flynn, 1988; Koponen, 1993; Hou, 2000]. Since the hot atoms are in a disordered state, the two directions of energy transfer are not symmetric. How to treat the EPC precisely remains unclear [Page, 2009; Björkas, 2009a], but the experimental measurement of a heat spike lifetime of 6 ps [Stuchbery, 1999] and the observation that

experimental ion beam mixing coefficients can be well reproduced without any EPC [Nordlund, 1998c] indicate it is not overly significant for cascade cooling.

The damage obtained from collision cascades can be analysed in many different ways, including potential energy of atoms, Wigner-Seitz cells and spheres centered on lattice sites [Nordlund, 1998b], detection of under- or over-coordinated atoms by bond counting, angular structure factor analysis [Zhu, 1995] and ring analysis [Xiaglong, 2002]. In many cases (when recombination is not important) Wigner-Seitz analysis gives results which correspond fairly closely to defect numbers obtained from e.g. BCA calculations.

Figure 2.14. Sputtering yields of Au(111) surfaces from experiments (solid line) compared with two different MD interatomic potentials

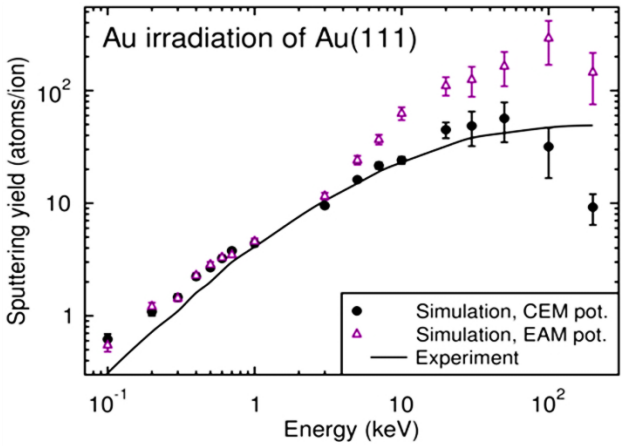

Note: The two MD potentials agree well with each other at low energies (linear collision cascade regime) but disagree significantly at high energies (heat spike regime). The simulation data is from [Samela, 2005] and the experimental from [Szymczak, 1993].

A key question for the simulations is naturally how reliable they are. The basic MD algorithms such as the solution of the Newton equations of motion and handling neighbour lists can be made very accurate. Hence the three reliability issues that remain are (i) accuracy of interatomic potentials, (ii) accuracy of electronic stopping, and (iii) how to handle the electron-phonon coupling. As discussed above, issues (ii) and (iii) remain somewhat uncertain but these seem to still be less than a factor of roughly 2 in the damage production.

The interatomic potential reliability issue, which will always be present in classical MD, is still a major problem for obtaining predictive MD simulations. Ideally the reliability of interatomic potentials should be assessed with comparisons with experiments, but it is very difficult to carry out experiments on the primary damage state. On the other hand, comparisons with other quantities that depend directly on the initial collision cascades, such as sputtering yields and ion beam mixing, can be instructive. Recent comparisons of simulated and experimental sputtering yields have shown that even with modern many-body interatomic potentials, there are major (up to factor of ~5) differences between the sputtering yields obtained with different potentials and experiments [Samela, 2005; Samela, 2006]. Moreover, the study of sputtering yields of Au showed that the same potential may agree excellently with experiments in one energy range and disagree badly in another [Samela, 2005], see Figure 2.14. This shows that even if good agreement is demonstrated

with experiments for one or a few data points under one irradiation condition, it may not agree with experiments under other conditions.

Major efforts have been recently done to understand primary damage production in Fe. An overview of historical MD simulation results showed a major variation of damage production results predicted by different potentials [Malerba, 2006]. Later analyses showed that these differences can at least to a fairly large extent be associated with variations in how the potentials describe the interstitial, in particular its ground state structure and mobility. This was because the structure and mobility affect how likely it is that the interstitial finds a vacancy to recombine with in the heat spike phase of a cascade. When the potential comparison was limited to modern interatomic potentials which describe at least the ground state structure of the interstitial and the melting point of Fe well, very good agreement was found in the total damage production [Björkas, 2007a]. However, even this is not the end of the story: an even more recent study showed that even when the total damage production remains the same, the fraction of very large vacancy clusters produced by different potentials may have a huge influence on the long-term damage evolution [Björkas, 2011]. This shows that even in the most studied material (Fe), interatomic potential reliability remains an issue.

A possible emerging solution to this conundrum is that it has very recently become possible to carry out quantum mechanical DFT MD simulations of radiation effects. As DFT is a more fundamental method than classical potentials, and shown to describe a wide range of defect properties well with relatively little variation of the numbers predicted by different DFT approaches [Puska, 1998; Wil, 2001; Fu, 2004; Olsson, 2003; Derlet, 2007; Terentyev, 2008b; Rieth, 2012], it can reasonably be expected to provide a more reliable description of radiation effects than classical potentials. Although this approach is strongly limited by computer capacity, it has by now allowed simulation of the threshold displacement energy in graphene [Meyer, 2012], Si [Holström, 2008a] and Fe with very good agreement with the available experiments. When computer capacity increases further, it should become possible to carry out DFT MD calculations of at least low-energy cascades and use these to assess the reliability of, or to calibrate, classical MD potentials.

2.3 Replacements-per-atom (rpa) function

As discussed in Section 2.1.3, ion beam mixing is an experimentally measurable quantity that (in the absence of diffusion) directly depends on the atom replacements in a collision cascade. Analyses of the experimental ion beam mixing values have shown that in dense materials, the amount of atom mixing has a major component from heat spikes [Gades, 1995; Nordlund, 1998d; Nordlund, 1998c]. Hence the actual number of atoms that are displaced from their initial lattice site in a cascade and end up in another site (replaced atom) can strongly exceed that predicted by a BCA model and a dpa value.

Here we present a **"replacements-per-atom" (rpa)** equation that accounts in a relatively simple functional for a number of replaced atoms obtained from MD simulations. Similarly to the arc-dpa value, the rpa equation is based on a mixing damage efficiency correction function:

$$\xi_{rpa}(E) = \frac{N_{True-number-of-replaced-atoms}}{N_{NRT-prediction}}$$

This function should start at $\xi_{rpa} = 1$ and converge to a constant value for energies higher than the subcascade breakdown threshold. However, since $\xi_{rpa} > 1$ we found that a similar functional form as that used for the arc-dpa value does not work. Instead, we choose a similar form as that used in [Nordlund, 1998c] for the related quantity of the square of the total atom displacements. The basic form is:

$$\xi_{rpa}(E) = a_{rpa}\frac{E^{c_{rpa}}}{b_{rpa}{}^{c_{rpa}} + E^{c_{rpa}}}$$

which has the correct limit of becoming constant for large E. Again we use the criterion:

$$\xi_{rpa}(2E_d/0.8) = 1$$

which allows to fix the *a* fitting constant. Thus one arrives at:

$$\xi_{\mathrm{rpa}}(E) = \left(\frac{b_{rpa}{}^{c_{rpa}}}{(2E_d/0.8)^{c_{rpa}}} + 1\right)\frac{E^{c_{rpa}}}{b_{rpa}{}^{c_{rpa}} + E^{c_{rpa}}}$$

for the rpa correction function. The b_{rpa} constant has units of energy while c_{rpa} is unitless. The total function becomes, fully analogously to the arc-dpa form:

$$N_{replaced-atoms}(E) = \begin{bmatrix} 0 & E < E_d \\ 1 & E_d < E < 2E_d/0.8 \\ \frac{0.8E}{2E_d}\xi_{rpa}(E) & 2E_d/0.8 < E < \infty \end{bmatrix}$$

A fit of the ξrpa function to data in Ni, Pd and Pt is shown in Figure 2.15. The total xinmig coefficient obtained with this fit is given in Table 2.6 together with experimental values. Note that the rpa values are ~15-25 times larger than the NRT-dpa value.

The data in the figure shows that at low energies, the mixing efficiency is already above 1, something which the current functional form does not capture as it is forced to equal to 1 at $2E_d/0.8$. As for the arc-dpa form, this choice was made to force the function to be continuous and consistent with previous calculations near the threshold. Although the data for Ni, Pd and Pt would indicate an extension of the functional form is needed, using a single data set without experimental verification to complicate the functional form and introduce additional fitting parameters is not justified. If it turns out from a wider range of simulations and experiments the high mixing efficiencies just above the threshold are a common feature, an extension of the functional form would be well motivated in the future.

Table 2.6. Simulated (present work) and experimental ion beam mixing coefficients in Ni, Pd and Pt

Material	Beam	Q_{sim} (Å^5/eV)	Q_{exp}(Å^5/eV)
Ni	600 keV Kr	4.7	4.8 ± 0.5[a]
Ni	650 keV Kr	5.0	5.0 ± 0.7[b]
Pd	600 keV Kr	12.6	8.4 ± 0.8[a]
Pd	400 keV Kr	13.2	9 ± 1[c]
Pt	1000 keV Kr	16.9	14 ± 2[b]

[a][Nordlund, 1998c]; [b][Kim, 1988]; [Fenn-Tye, 1987]. These values differ somewhat from those presented in Section 2.1.3 since in the current work new data was collected to provide much higher statistics.

Figure 2.15. Fits of rpa correction factor ξ_{rpa} to ion beam mixing data in Ni, Pd and Pt

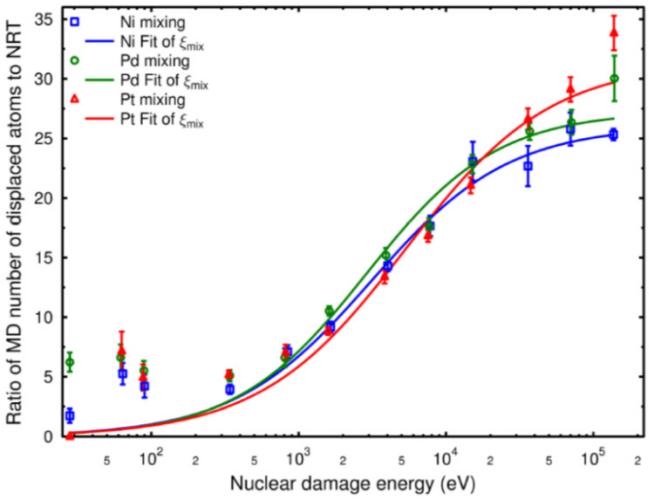

For this calculation the average threshold displacement energies of 39, 41 and 44 eV [Jung, 1991] were used for Ni, Pd and Pt, respectively. The electronic stopping was subtracted out from the initial PKA energy to give the nuclear deposited (damage) energy.

The constants obtained are given in Table 2.7:

Table 2.7. Materials parameters for Ni, Pd and Pt for the RPA equations

Material	Model	E_d (eV)	b_{arcdpa} (eV)	c_{arcdpa}	Source of data
Ni	rpa	39	3107	0.930	Fit to MD data of current work
Pd	rpa	41	2877	0.980	Fit to MD data of current work
Pt	rpa	44	5500	0.881	Fit to MD data of current work

The fitted parameters and their uncertainties are obtained from a Levenberg-Marquardt least squares fit to the data [Bevington, 1992; NumericalRecipes].

3. Semiconductors

Radiation damage production mechanisms in semiconductors differ clearly from those in metals [Averback, 1998]. For the primary damage production, this has been attributed to the open crystal structure [Nordlund, 1998b] and the much slower recrystallisation [Marques, 1994] which leads to the possibility to form amorphous pockets [Ruault, 1984; Rubia, 1995; Jenčič, 1996]. These are also stable at room temperature over macroscopic times in most tetrahedral semiconductor materials [Ruault, 1984; Caturla, 1995b; Jenčič, 1996; Hensel, 1997], although in for instance GaAs they can recrystallize already at room temperature [Bench, 2000].

On prolonged irradiation at low temperatures, the semiconductors become completely amorphised [Morita, 1991; Holland, 1985; Glover, 2000c; Wen, 2002; Williams, 1998]. In other words, the damage saturation effect described in Section 2 for metals does not necessarily exist in semiconductors. At elevated temperatures, however, also semiconductors do not amorphise at any fluence [Linnros, 1987; Goldberg, 1993; Caturla 1996; Pelaz 2004]. In other words, there is a critical temperature for amorphisation which is typically a few hundred degrees C above room temperature. For instance, for Si it is about 300 ^{o}C and for SiC about 200 ^{o}C (the precise value depends on ion species, energy and flux). The reason to this is attributed to defect migration that allows defects to recombine at elevated temperatures as well as thermal recrystallisation of amorphous pockets that prevents amorphisation [Goldberg, 1993; Caturla 1996; Pelaz 2004]. However, this mechanism is different from the one in metals, where (as discussed in section 2) the recombination can occur without any thermal activation by overlapping cascades.

The formation of amorphous pockets (disordered zones) complicates damage analysis in that it is not obvious how many atoms to define as a “defect” in such a zone, and in fact analyses of atom coordinates obtained from MD have shown that the “defect number” can vary as much as an order of magnitude for the exact same configuration depending on criterion used [Nordlund, 1998b]. However, the different numbers are fairly well proportional to each other, which means that this is not necessarily a big problem.

In this section, we briefly summarise some of the main complications that arise in damage production in semiconductors.

3.1 Threshold displacement energy experiments and modelling

The threshold displacement energies have been measured in several semiconductors; however, the data is often scattered since in many cases there is significant damage recombination going on already at room temperature. As an extreme example, for ZnO some experiments reported a threshold of 563 eV for O [Look, 1999] at room temperature, whereas others, done at 15 K, reported an upper limit of 65 eV. Since defects in ZnO are

mobile at 110 K, it seems clear the discrepancy is explained by defect recombination at temperatures above this.

Focusing on low-temperature experiments, several studies have given a minimum threshold displacement energy of 13 eV for Si in the 111 crystal direction [Loferski, 1958; Corbett, 1966], a value that is well reproduced by recent DFT MD simulations [Holström, 2008a]. Regarding the average threshold, there is to no direct low-temperature experiment measured over all crystal directions (the value of the "effective" threshold of 21 eV by Corbett and Watkings [Corbett, 1965] is an indirect determination and based on measurements for only the 3 principal directions). Recent DFT calculations indicate that even the definition of a threshold in Si may not be unique: in case the bond order defect (IV pair [Tan, 96; Car, 97b; Goe, 02]) is counted as a defect, the average threshold was 24 eV, and in case only Frenkel pairs are counted, the threshold was 36 eV in the DFT calculations in [Holström, 2008a]. Since the IV pair is metastable with a recombination barrier of about 1 eV [Tan, 96; Car, 97b], this indicates that at low fluxes or high temperatures where IV pairs recombine, one should use a different threshold from conditions where they do not.

Figure 3.1. MD simulation of the damage evolution in a cascade induced by a 5 keV recoil in Si

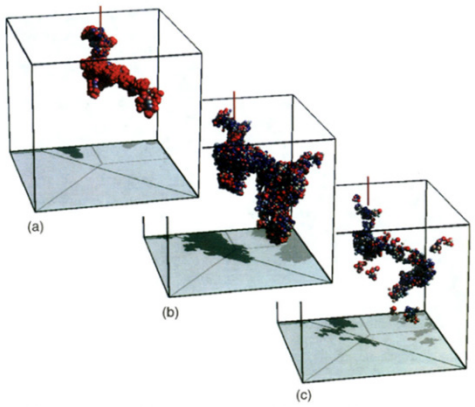

The spheres show atoms with a potential energy more than 0.2 eV higher than the ground state, and the colours and atom sizes indicate how much above the ground state it is (red being >= 1 eV above). a) 0.1 ps, b) 1 ps and c) 8 ps after the cascade starts. The final state at 8 ps is stable over MD time scales at room temperature. From [Rubia, 1995]. Copyright (1995) The American Physical Society, Reprinted with permission from the authors.

In Ge the minimum threshold seems to be similar to that in Si, 14 eV [Corbett, 1966]. For the average threshold, values of 18 eV [Loferski, 1958], 20 ± 5 eV [Poulin, 1980] and 30 eV [Vitovskii, 1977] have been reported. DFT MD simulations gave average values of 21 eV considering the IV pair and Frenkel pairs, and 23 eV considering only Frenkel pairs, i.e. it seems like the IV pair affects the results clear less than in Si [Holmström, 2008a].

Threshold displacement energies have also been measured in several compound semiconductors. Here we discuss only, as examples, GaAs and GaN. In GaAs experiments indicated that the minimum threshold energy is about 10 eV on both the Ga and As sublattices [Lehmann, 1993; Hausmann, 1996]. Classical MD simulations gave exactly the same result, and also indicated that single recoils of 15 eV can produce directly antisite defects in the material [Mattila, 1995]. In GaN, where there is a large difference between the masses of the elements, there appears to be an elemental asymmetry in the damage production. Experiments have reported an average threshold of 41 eV for the Ga sublattice

[Wendler, 2003]. MD simulations with classical potentials gave average thresholds of 45 and 110 eV for Ga and N, respectively [Nordlund, 2002a], while DFT MD simulations gave the opposite behaviour with an average of 73 eV for Ga and 32 eV for N [Gao, 2011]. Although the latter value seems to agree less well with experiments, the DFT method should in principle be more reliable than classical MD. Thus, the situation regarding the correct values of the threshold energies in GaN remains unclear.

3.2 Defect production efficiency

In the elemental semiconductors Si and Ge, MD simulations consistently show a linear increase of damage production with ion energy, i.e. there is no athermal damage recombination effect similar to that in metals [Rubia, 1995; Nordlund, 1998b]. This is consistent with experiments which show, to a first order approximation, that damage production scales fairly well with energy deposition; a dose of $6x10^{23}$ eV/cm^3 at 80 K has been reported to predict well the amorphisation dose for a fairly wide range of ions with different masses [Dennis, 1978]. If there would be a athermal recombination-effect like that in metals, one would not expect a simple scaling with different ion masses.

Some examples of defect production as a function of bulk recoil energy in Si and Ge are given in Table 3.1. For all potentials, the data scales fairly well with a simple KP/NRT equation (for the Ge modified Stillinger-Weber (SW) potential, the scaling between 0.4 and 2 keV is not good because in this potential large amorphous zones start to be formed around 2 keV). For instance, for the "Si SW pot" data set an average threshold energy of 34 eV reproduces within the statistical uncertainty all the data points after the electronic energy loss of about 20% is counted out from the recoil energy.

Comparison of the values for the same element, with different potentials, show that there is a serious potential reliability issue, however. There are hopes that computers are soon powerful enough such that DFT MD simulations can be used to reduce this uncertainty.

Table 3.1. Defect (analysed with the Wigner-Seitz cell approach) production in Si and Ge simulated with different interatomic potentials. The data and potential definitions are from [Nordlund, 1998b]

Recoil energy (keV)	Si, SW pot.	Si, Tersoff pot.	Ge, SW pot	Ge, SW mod pot.
0.4	4.1 +- 0.5	8.3 +- 0.2	2.4 +- 0.1	4.6 +- 0.3
2.0	17 +- 1	39 +- 2	12 +- 1	47 +- 2
5.0	43 +- 1	84 +- 2	27 +- 1	141 +- 5

In compound semiconductors, GaAs seems to also have a simple damage buildup behaviour with linear increase of damage [Eisen, 1971; Turos, 1999; Nordlund, 2001]. By contrast, in GaN MD simulations [Nordlund, 2003b] were interpreted in a way that there is some athermal damage recombination (similar to metals) going on in the material. Experiments done at 15 K show that the damage buildup even at low temperatures (where defect mobility is unlikely) is really complicated, having three distinct stages prior to full amorphisation [Wendler, 2002]. MD simulations could not reproduce this behaviour [Nordlund, 2003b].

3.3 Role of ionisation-induced and -enhanced diffusion

It has long been recognised that ionising radiation can affect the diffusivity of point defects in semiconductors [Bourgoin, 1973; Bourgoin, 1978; Stievenard, 1990; Seebauer, 2006]. In general the migration energy for ionised defects is lower than for non-ionised defects due to several mechanisms. Therefore, the possibility of ionisation-stimulated diffusion of point defects and impurities needs to be considered when analysing radiation effects data in semiconductors. In particular, the possibility of athermal close-pair recombination of point defects (Bourgoin-mechanism [Bourgoin, 1978]) may lead to reduced defect production compared to calculated values. Such athermal recombination of point defects due to ionisation is reported in SiC [Weber, 2012; Thomé, 2013].

4. Ionic materials

4.1 Ionisation-induced defect production

Defect production from ionisation has been observed in many insulating materials, most notably alkali halides [Sibley, 1984; Itoh, 2001] and SiO_2 [Devine, 1992; Toulemonde, 2012]. Depending on the material and irradiation spectrum, defect production from radiolysis mechanisms can be larger or smaller than defect production from elastic collision displacements. Additional defect production mechanisms emerge at high electronic stopping powers associated with so-called swift heavy ion irradiation [Toulemonde, 1994; Toulemonde, 2004; Zinkle, 2002].

4.2 Role of ionisation-induced and -enhanced diffusion

Ionising radiation can have a profound influence on the diffusivity of point defects in ceramic insulators [Bourgoin, 1973; Bourgoin, 1978; Chen, 1976; Zinkle, 1997a; Mulroue, 2011]. This can lead to significant mobility of radiation defects in certain ionic materials even at temperatures well below room temperature, and can produce dramatically different microstructures (more efficient self-healing of radiation defects) for high ionisation per displacement environments compared to low ionisation per displacement environments [Krefft, 1977; Krefft, 1978; Zinkle, 1995; Zinkle, 1997; Zinkle, 1997a; Zinkle, 2002; Devanathan, 1998; Kinoshita, 2004; Weber, 2012; Thomé, 2013]. Annealing of defects can also occur during ion beam analysis (e.g. Rutherford backscattering spectrometry) of irradiated ceramics [Zinkle, 1997; Zinkle, 1997a; Schnohr, 2006]. Consideration of ionisation-induced or -enhanced diffusion effects generally needs to be included in the evaluation of experimental defect production measurements.

4.3 Threshold displacement energy experiments and modelling

A moderate amount of experimental information is available on threshold displacement energy surfaces for ionic materials, with MgO and Al_2O_3 being the most extensively studied materials [Zinkle, 1997; Smith, 2003]. Typical crystallographic-averaged values of the displacement energies for the anion and cation sublattices range from ~40 to ~100 eV. In recent years, improvements in molecular dynamics simulations in nonmetals has led to a significant number of studies on displacement energies in oxides including MgO [Park, 2000; Kittiratanawasin, 2010], $MgAl_2O_4$ [Smith, 2005a], CeO_2 [Xiao, 2012], TiO_2 [Thomas, 2005; Robinson 2012], UO_2 [Meis, 2005; Bishop, 2012], ThO_2 [Xiao, 2012], ZrO_2 [Xiao, 2012], zircon [Park, 2001; Moreira, 2009] and $Y_2Ti_2O_7$ pyrochlore [Gao, 2011]. Limited recent experimental studies of threshold displacement energies have also been performed on CeO_2 [Yasunaga, 2008], ZrO_2 [Costantini, 2011], ZnO [Knutsen, 2012], TiO_2 [Smith, 2000], and more complex oxides such as perovskite, titanates and zirconates [Smith, 2003, Smith, 2005].

Figure 4.1. Surviving defect fraction in irradiated Al_2O_3 and Al

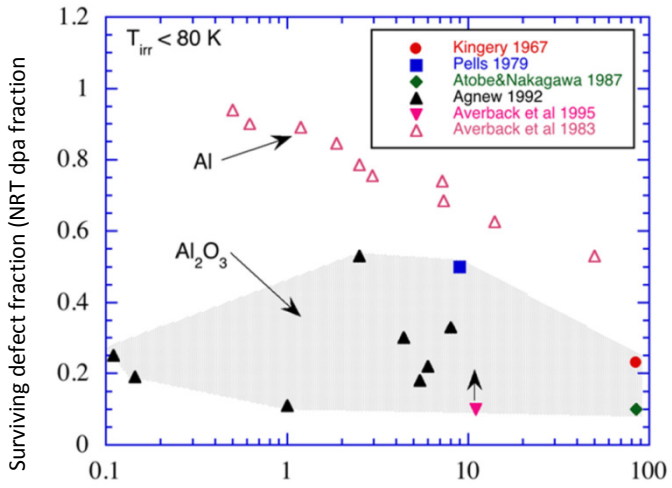

4.4 Defect production ef

There are significantly fewer defect production studies that have been performed on ionic materials compared to metals. This is in part due to the lack of a simple in-situ measurement technique for ionic materials analogous to the electrical resistivity technique that has been a workhorse for defect production measurements in irradiated metals at cryogenic temperatures. Many of the experimental defect production studies on ionic materials have been performed at room temperature, where significant point defect mobility can lead to underestimates of the defect production efficiency [Zinkle, 1997]. In addition, many of the experimental measurements have utilised tools such as optical spectroscopy that are valuable for monitoring specific defects such as F-center monovacancies but are less successful at quantifying the full spectrum of isolated and clustered radiation defects. Typical measured values of defect production efficiency in MgO and Al_2O_3 are 20-50% of the NRT calculated displacement value over a broad range of PKA energies, 0.1-100 keV [Zinkle, 1997; Wendler, 2008], see Figure 4.1, although defect production efficiencies near 100% have been measured in recent ion beam experiments on Al_2O_3 [Schnohr, 2006] and ZnO [Wendler, 2009]. Cleearly further work is needed to resolve the source of these discrepancies. Molecular dynamics simulations of cascades in MgO [Uberuaga, 2005] reported defect production efficiency values of about 50% the calculated NRT value for 2 and 5 keV PKA energies.

4.5 Solute mixing and disordering in multicomponent ceramics

Several studies have examined ion beam mixing and radiation enhanced diffusion effects in ceramics [e.g. Miotello, 1997; vanSambeek, 1998]. Numerous experimental studies have monitored defect accumulation and chemical disordering in irradiated ceramics [Weber, 1998; Kucheyev, 2003; Lian, 2003]. In general, substantial disordering precedes crystalline to amorphous phase transitions in ionic materials. Overall, MD simulations for energetic cascades suggest the degree of atomic mixing per unit of displacement damage is generally lower for ceramics compared to metallic alloys, which might be rationalised on the basis of much higher antisite energies in ionic materials (particularly for anioncation site exchanges).

The quantitative values of disordering are strongly dependent on material, with little mixing observed in $ZrSiO_4$ [Devanathan, 2006] and moderate cation disordering observed in $MgAl_2O_4$ [Smith, 2005a]. MD simulations on MgO [Uberuaga, 2005] have reported peak transient displacements at times near 0.1 ps for 2 and 5 keV cascades, with transient peak Frenkel pair concentrations that are ~20 times higher than the residual defect concentration.

4.6 Amorphisation

At low temperatures where defect migration is inhibited, crystalline to amorphous phase transitions are frequently observed in irradiated ionic materials [Naguib, 1975; Hobbs, 1994; Weber, 1998; Weber, 2000]. The amorphisation can be induced by a variety of mechanisms that depend on the material and bombarding particle, including in-cascade direct impact amorphisation and defect accumulation processes [Weber, 2000; Jagielski, 2009]. For low to medium mass materials that are not susceptible to in-cascade amorphisation, materials with high point defect mobility [Zinkle, 1996] and crystallographic ability to accommodate lattice disorder (such as the fluorite crystal structure) [Sickafus, 2007] tend to exhibit good amorphisation resistance.

5. Carbon-based materials

5.1 Graphitic carbon

Graphite is still of importance as a moderator or reflector in reactor technology. Irradiation of graphite at low temperatures leads to a rise in energy due to the accumulation of defects. This is known as the Wigner energy [Banhart1] which is an important safety issue in nuclear technology. The sudden release of the Wigner energy above 250°C may cause disastrous events such as the Windscale fire in 1957. For this reason, radiation effects and defects in graphite have been subject of numerous studies since a long time [Banhart2; Wullaert, 1964; Kelly, 1981]. However, the situation remained unclear until new nanomaterials on a graphitic basis such as carbon nanotubes or graphene became available. Detailed electron microscopy studies, where electron irradiation and structural characterisation can be carried out at the same time, clarified the picture [Banhart3]. Graphitic nanomaterials, in particular graphene, are now of major technological interest, and radiation effects have to be taken into account in applications in space and zones of high radiation level. Graphene and carbon nanotubes are now subject of detailed characterisation by electron microscopy. Electron irradiation is unavoidable in the electron microscope, but radiation defects have to be avoided nevertheless. This requires detailed knowledge about defect formation and annealing.

It is known that the creation of visible structural defects in graphene or graphite requires a minimum electron energy of approximately 80 keV if the momentum transfer occurs normal to the basal plane of graphite. This corresponds to a displacement threshold of approximately 17 eV (energy of the displaced carbon atom) [Banhart3; Zinkle, 1997]. Due to the presence of conduction electrons, electronic excitations are quenched and do not lead to structural changes under irradiation. The threshold for ballistic displacements shows a large anisotropy in graphite, and the value for in-plane displacements is higher by almost a factor of two. The McKinley-Feshbach formalism [Banhart4] describes the observed ballistic displacement rate rather well. However, lattice vibrations have to be taken into account [Meyer, 2012], leading to a slightly higher displacement rate close to the threshold than predicted by the McKinley-Feshbach theory. It has recently been observed that the threshold energy for displacing atoms at the edges of graphene layers or around existing structural defects is clearly below the bulk threshold. This may lead to an ongoing degradation of graphitic materials starting from edges or defects at electron energies as low as 20 keV [Banhart5]. Since the displacement of even single carbon atoms can be observed *in-situ* in the electron microscope, the situation in graphene is meanwhile well investigated and understood. Graphene is therefore an ideal system to study atom displacements in detail, to test the theoretical concepts, and to determine threshold energies with high precision [Banhart6].

The configuration and behaviour of atomic defects in graphite and graphene is different from other materials [Banhart7]. Due to the high structural flexibility of the graphenic lattice, different ways of reconstructing the hexagonal network and locally changing the

hybridisation of carbon atoms are possible. This allows a relaxation of the lattice via transformations of the Stone-Wales type after the displacement of atoms so that all dangling bonds around defects are saturated. Monovacancies are stable against restructuring of the lattice but have a low migration energy of 1.2–1.4 eV. They may therefore migrate above approximately 250°C and coalesce to form stable and immobile divacancies. This is the most important annealing mechanism in graphitic materials. The formation energy of divacancies (7.2–7.9 eV) is of the same order as of monovacancies (7.3–7.5 eV) so that the defective graphitic lattice at elevated temperatures consists mainly of arrangements of divacancies. Divacancies may occur in different configurations of pentagonal and heptagonal rings and are immobile up to very high temperatures. The reconstruction leads to a variety of new morphologies of graphitic materials that can be induced by careful irradiation at elevated temperatures [Banhart8]. In contrast to vacancies, carbon adatoms are not easily visible by electron microscopy, in particular since their migration energy is as low as 0.4 eV and their thermal displacement accordingly fast, even at room temperature. Therefore, much less is known about "interstitials" in graphitic materials, but the major features of defect production and annealing can be well understood by assuming that vacancies govern the production and dynamics of radiation defects. At temperatures below 250°C, the agglomeration of defects is seen as an ongoing rupture of basal planes, leading eventually to an amorphisation of graphite. This has been confirmed in ion irradiation studies of carbon nanotubes [Banhart9].

5.2 Radiation damage in diamond

Diamond has by far not as many applications as graphitic materials, therefore radiation effects in diamond have not been studied in much detail until now. Displacement thresholds of 30–48 eV have been reported [Zinkle, 1997; Steeds, 2011]; higher than in graphitic materials and due to the dense packing of carbon atoms in the diamond lattice [Banhart10]. This makes diamond somewhat more stable under irradiation and therefore a "radiation-hard" material. This might be useful for applications of diamond in space and environments with high radiation level. The anisotropy of radiation damage is much less than in graphitic materials, due to the lack of open space in the diamond lattice. Although diamond is an insulator with a band gap of 5.5 eV, electronic excitations do not lead to visible structural defects under irradiation. Thus, we have to assume that ballistic displacements are the main source of radiation damage in diamond. The knowledge about radiation damage in diamond is also limited due to the difficulty of studying the behaviour of individual carbon atoms in a densely packed three-dimensional crystal.

6. Amorphous materials

It is a common misconception that radiation damage or defects cannot exist in amorphous materials. There is ample experimental and theoretical evidence that this is not the case. As perhaps the most direct evidence, positron annihilation experiments have clearly detected open-volume defects in amorphous silicon, with characteristics similar to a vacancy in crystalline silicon [Roorda, 1992]. Moreover, these open-volume and other possible defects can be annealed by heating the sample [Roorda, 1992; Roorda, 1999], similar to the well-known characteristics of defects in crystalline materials. The annealing has also been shown to release considerable amounts of heat [Roorda, 1999].

In ionic amorphous materials, such as silica-based glasses, it is well established that color centres correspond to dangling bond or impurity defects, similar to those observed in the corresponding crystalline materials (quartz in the case of silica) [Lieb, 2007; Keinonen, 2008]. Computer simulations have given considerable insight into the nature of defects in amorphous materials. They have shown that both vacancy-like open-volume [Bob; Delaye, 1993; Bob; Delaye, 1993b; Nordlund, 2005] and interstitial-like compressed regions [Nordlund, 2005] can exist in metallic glasses. Simulations have also shown that such defects can have a major role on the plastic flow of the materials [Mayr, 2003] and hence that irradiation can be used to modify the mechanical properties of metallic glasses [Mayr, 2003; Avchaciov, 2012].

Detailed analyses of the motion of atoms in liquids and amorphous materials have shown that a significant fraction of atoms in disordered materials undergo correlated motion that exceeds the mobility expected for a simple Gaussian random walk [Schober, 1993; Donati 1998; Glotzer, 1999; Donati, 1999; Volmayr-Lee, 2002; Giovambattista, 2003], a finding supported which is supported by experiments [Böhmer, 1998; Ehmler, 1998; Zöllmer, 2002; Faupel, 2003]. Fundamentally interesting is that such motion, which is sometimes called atom “strings” (not to be confused with the entirely different concept of strings in particle physics) has been attributed to provide an explanation for why liquids exist [Nordlund, 2005] via the Granato theory of liquids and solids [Granato, 1992].

Although amorphous materials thus share some common characteristics with crystalline ones regarding damage, many aspects are different. For instance, as a single broken bond in a covalently bonded material can be considered a defect [Lieb, 2007], the concept of atom displacements as the source of damage does not necessarily apply, and hence the use of the dpa concept is not very well motivated. In fact it is known that even low-energy electrons with energies of only a few keV can regenerate damage in amorphous zones [Jenčič, 1996; Robinson, 1996], which can be understood to be due to breaking of single bonds by electronic excitation processes [Frantz, 2001].

Due to such complications, it is more naturally to describe damage in amorphous materials with the energy deposition (e.g. in SI units of Gray = Joules of radiation energy/kg of material), similar to the common practice in biological materials [Barcellos-Hoff, 1996b].

7. Use of SRIM to calculate dpa values

7.1 Discussion SRIM damage calculations

Finally, we briefly consider the common usage of the SRIM (Stopping and Range of Ions in Matter [SRIM-2013; SRIMbook], previously known as TRIM for Transport and Range of Ions in Matter [TRIM; ZBL]) for calculating dpa values. The SRIM software has gained wide popularity in the ion irradiation community. The primary reasons are that, on one hand it is free and easy to install and use in Windows operating system, on the other hand it can calculate ion penetration depth profiles for any kind of ion with energies from a few tens of eV to 1 GeV in any material.

The SRIM software treats the ion penetration in a material with the binary collision approximation, i.e. as a series of independent binary collisions. The electronic stopping is used on the ions along its movement path as a frictional force, in principle in the same manner as in MD simulations. The positions of target atoms with which the ions are selected with a Monte Carlo algorithm, i.e. the material is completely random. The only parameters used to describe a material with respect to the selection of the colliding atom positions are the density of the material and the relative elemental composition. The SRIM calculations can be ran in two different modes: “Ion distribution and quick calculation of damage” and “Detailed calculation with full damage cascades”. In the former, only the path of the incoming ion is followed. In the latter, also all knock-on atoms of all generations (primary, secondary, etc.) that have an energy above the threshold energy are followed.

For describing damage production and sputtering, the code also uses materials parameters for lattice binding energy, surface binding energy and displacement energy. The latter is the same concept as the average threshold displacement energy considered extensively in this report, and used to provide estimates of the damage production. SRIM can be used to calculate damage values in several different ways. In the “Ion distribution” mode, the defect numbers are estimated by using the Kinchin-Pease equation for each primary-knock on atom based on its recoil energy. In the “Full cascade” mode, the code keeps track of all displaced atoms and counts them as vacancies (although there is a minor correction due to “replacement collisions” which reduce the vacancy number). Both modes can be used to report the number of vacancies as a function of depth, and in newer versions it is also possible to make 3D damage distributions. The SRIM vacancy number is commonly directly equated with the number of displaced atoms and used to calculate the dpa value. This can be done in two slightly different ways, either using the “Displaced atoms” or the “Vacancies produced” numbers, which differ by the number of replacement collisions. It is also possible to extract the nuclear deposited energy as a function of depth and use this together with the Kinchin-Pease or NRT equation to calculate a number of displaced atoms.

The SRIM damage calculations are problematic in several ways, however. The lack of detailed physics of material thermodynamics and crystal structure naturally limits severely

what kind of information can be obtained from the code, but this is a feature of the physical approximation used (BCA with Monte Carlo collisions) and hence not a problem with the software itself. However, what is genuinely problematic is that the different SRIM calculations can give widely different damage numbers. Hence, if a scientific work reports only a dpa value "obtained from SRIM" without specifying how they are precisely derived from the software, the values obtained are not unique or easily reproducible.

As a simple example, for this report we used the SRIM software version 2013.00 to estimate the damage produced for 10 keV Si irradiation of Si at perpendicular incidence. The physical parameters used for SRIM were the default ones, namely ion mass 27.977 amu, sample Si atom mass 28.086 amu, sample density 2.321 g/cm^3, lattice binding energy 2 eV, surface binding energy 4.7 eV and displacement energy 15 eV. Using these parameters, the "Quick calculation of damage" mode gives a damage level of about 0.75 vacancies/(Å ion) at the damage maximum as a depth of about 8 nm, while the "Full cascade" calculation gives a damage level of about 1.2 displacements/(Å ion) and 1.1 vacancies/(Å ion), see Figure 7.1.

Figure 7.1. Comparison of results obtained with SRIM2013 for an identical irradiation condition of 10 keV Si irradiation of Si using the "Quick damage calculation" (left) and "Full damage cascades" (right) modes

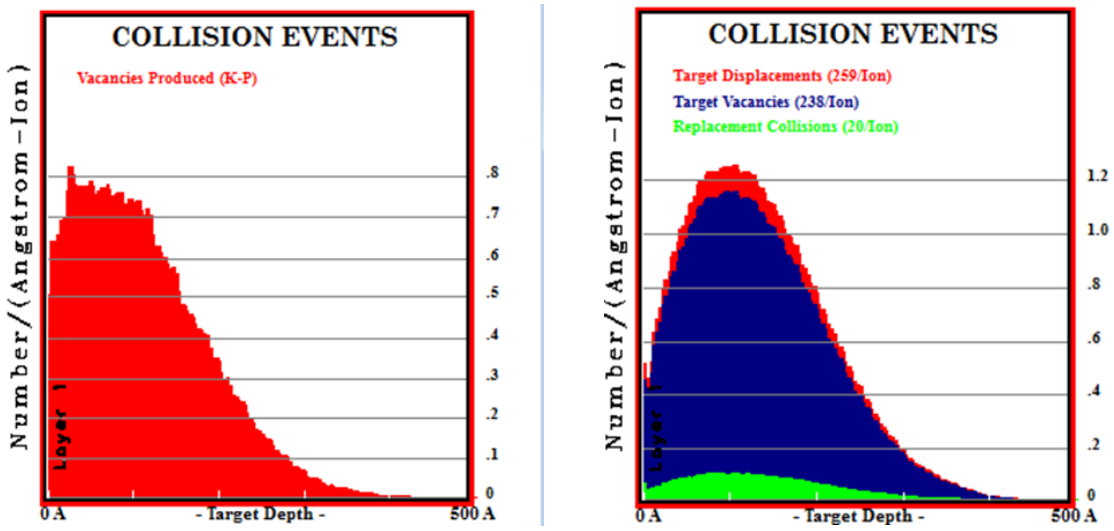

As it is evident in the figures, there is a major difference of about 50% in the damage production numbers obtained with the two models. Moreover, for a calculation of a "dpa" value it is not obvious whether one should use the "Target displacements" or "Target vacancies" values in the full cascade mode. The data for the quick damage calculation had a statistics of about 15 000 ions and the one for the full damage cascades one of about 5 000 ions.

As another example, if these three values are recalculated into a dpa value for an ordinary ion irradiation fluence of 10^{14} ions/cm^2, one obtains (using a volume/atom of 20.0 Å^3 for Si) dpa values of 0.15, 0.22 and 0.24 at the damage maximum.

On the other hand, one can also calculate a dpa value from the energy deposition. Here it is worth noting that SRIM outputs a value of "Energy to recoils" which is not exactly the same thing as total nuclear energy deposition, as it does not give the energy lost to sub-threshold collisions. SRIM outputs the latter quantity separately as "Phonons". Hence the total nuclear deposited energy of the incoming ion is the sum of the "Energy to recoils" and "Phonon" energy depositions. However, to further complicate the issue, the recoils also lose energy to

electronic stopping, and thus for the whole cascade, the nuclear deposited energy is less than the value given by the Energy to recoils file. Since in many cases this additional energy loss to electrons and the fraction of energy lost to phonons can be a substantial fraction of the total, it will also make a major difference if the damage (dpa) values are calculated from the "Energy to recoils" values or the total nuclear energy deposition (which corresponds to e.g. numerical integration of stopping powers).

For the same example case as above, 10 keV Si -> Si, the "energy to recoils" has a value of about 40 eV/(Å ion) at the damage maximum, see Figure 7.2, both in the quick damage and full cascade modes. From this, using the original form of the Kinchin-Pease equation of (Deposited E)/(2 E_d) with the same displacement energy value as in SRIM, E_d=15 eV, one obtains for the fluence 10^{14} ions/cm^2 a dpa value of 40 eV/(Å ion)/(2x15 eV)x0.01 ions/Å^2 x 20.0 Å^3 = 0.27.

Figure 7.2. Comparison of energy deposition results obtained with SRIM2013 for an identical irradiation condition of 10 keV Si irradiation of Si using the "Quick damage calculation" (left) and "Full damage cascades" (right) modes

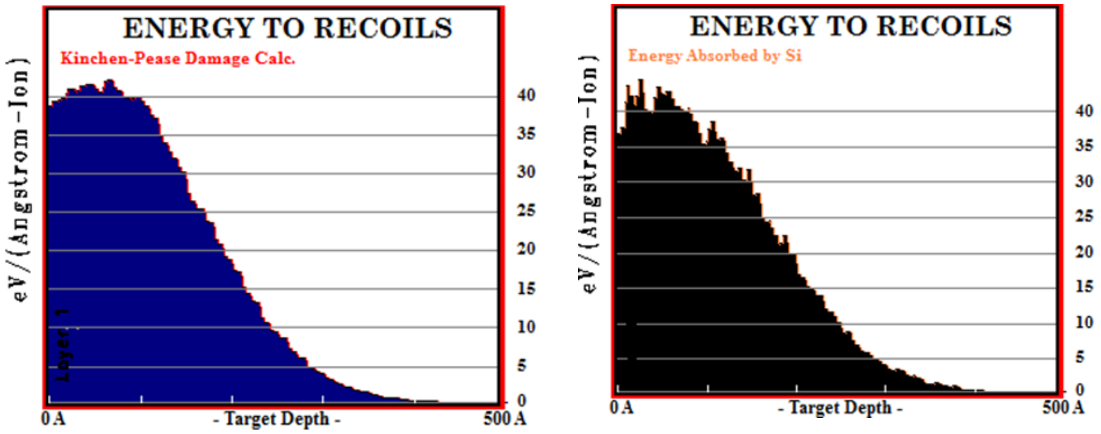

The calculations were the same as those used for Figure 7.1.

Finally, the same calculation can also be done including the phonon contribution, i.e. with the total nuclear deposited energy. In the example case, the energy deposited to phonons at the damage maximum was about 32 eV/(Å ion) in the quick damage calculation mode and 26 eV/(Å ion) in the full cascade mode. If these values are added to the "energy to recoils" value of 40 eV/(Å ion), the dpa calculation gives 0.48 and 0.44, respectively.

Hence we find that depending on the simulation model and definition used, SRIM can give dpa values of 0.15, 0.22, 0.24, 0.27, 0.44 and 0.48 for the same irradiation condition.

Since SRIM is based on the BCA and the Kinchin-Pease approximations, one cannot say that any of these values is definitely "right" or "wrong". If there would be a highly accurate experiment or MD simulation standard value available, one could use this as a reference point to select which SRIM model to use. Unfortunately, as discussed elsewhere in this report, for Si an absolutely reliable reference value does not exist.

7.2 Recipe to calculate NRT-dpa values from SRIM

For Fe a fairly reliable reference can be considered to exist, since MD simulation results of the total Frenkel pair production give consistent results with very different potentials [Björkas, 2007a] (cf. Section 2.2). The NRT-dpa equation gives much higher damage production numbers than MD calculations, as expected. Using the arc-dpa model instead of the NRT-dpa model naturally gives good agreement with the MD defect production, since the arc-dpa model fit includes the same MD data (see top three lines in Table 7.1).

Stoller et al. compared SRIM damage production using different SRIM models and also with MD results in detail in [Stoller, 2013]. They found, similarly to the simple Si example in the previous subsection, that the full cascade model gives higher damage values than the Kinchin-Pease model. The difference in the case of Fe was even higher, about a factor of 2. Some of the results are reproduced in Table 7.1.

Table 7.1. Damage (Number of Frenkel pairs) obtained for 78.7 keV PKA (~50 keV damage energy) in iron with different kinds of calculations. In all SRIM calculations, the displacement energy was set to 40 eV and the lattice binding energy to 0 eV

Simulation/equation	Model	Number of defects	Reference
Reference: Molecular dynamics, 50 keV, 100 K	9 simulations at ~15 ps	168 ± 4 (standard error)	[Stoller, 2013]
NRT model	NRT-dpa eq. with T_{dam}=50 keV	500	[Stoller, 2013]
arc-dpa model	arc-dpa eq. with T_{dam}=50 keV	153	[This work]
SRIM-2008 Kinchin-Pease Quick calculation, 5000 ions	NRT eq. with T_{dam}	540	[Stoller, 2013]
SRIM-2008 Kinchin-Pease Quick calculation, 5000 ions	sum of v_i and v_T from vacancy.txt file	530	[Stoller, 2013]
SRIM-2008 Full Cascade calculation, 5000 ions	NRT Eq. with T_{dam}	572	[Stoller, 2013]
SRIM-2008 Full Cascade calculation, 5000 ions	sum of v_i and v_T from vacancy.txt file	1099	[Stoller, 2013]
SRIM-2008.04 Kinchin-Pease Quick calculation, 10000 ions	NRT eq. with $T_{dam,r}$ based on COLLISON.TXT file	539	[This work]
SRIM-2008.04 Kinchin-Pease Quick calculation, 10000 ions	arc-dpa eq. with $T_{dam,r}$ based on COLLISON.TXT file	218	[This work]

The big difference to the MD results is explained by the athermal damage recombination, which is fully absent from the physics included in SRIM.

Based on considerations of the physics involved and consistency with conventional nuclear energy deposition models, Stoller et al. recommend the following recipe for obtaining dpa values for metals from SRIM [Stoller, 2013] (text adapted by spelling out references to equation numbers):

1. run SRIM using the “Quick” Kinchin and Pease option;
2. choose the recommended displacement threshold energy, for metals from [ASTME521];

3. set the lattice binding energy to zero;
4. compute the damage energy as the sum of the damage energy to target atoms and phonons;
5. use the computed value of T_{dam} to calculate the number of displacements according to the NRT equation which they show to be the most consistent with NRT damage calculations with other models for metals. Since the SRIM vacancy number calculation algorithms are not fully documented, and the source code is not available, the authors of this report concur on using the above recipe for metals.

To summarise this chapter, we find by a simple example and considering [Stoller, 2013] that using SRIM to calculate damage numbers is highly problematic as different models within the code give different results. **This leads us to conclude that when SRIM is used, it is very important to specify the exact SRIM version number and how exactly a "damage", "vacancy" or dpa number is derived from the code.**

7.3 Recipe to calculate arc-dpa values from SRIM outputs

Finally, we do note that the now introduced arc-dpa function can be used in connection with SRIM by utilising the COLLISION.TXT file to obtain a list of all primary recoils, then use the arc-dpa function to calculate the damage for each recoil. If the irradiation condition is such that the primary recoils are well separated, this should give a more accurate damage number than the NRT calculation.

We tested this proposition by rerunning the same SRIM2008 calculation as in [Stoller, 2013] of 78.7 keV Fe recoils in Fe, but to enable using the arc-dpa model, we extracted the damage from the COLLISON.TXT file. This file provides in the Kinchin-Pease calculation model the energy of all primary knock-on atoms. To calculate the damage production properly, one needs to take into account that the electronic stopping should be subtracted out from the primary recoil energy to get the nuclear deposited energy or damage energy of each recoil ($T_{dam,r}$) before using the NRT or arc-dpa equation. To get the correspondence between individual recoil energy E and $T_{dam,r}$, we used the data for $F_{D,n}$ for all recoils shown in Figure 1.2 and fitted a polynomial to this data. We found that an excellent fit up to 300 keV is given by:

$$T_{dam,r}(E) = 0.77678\,E - 0.5882 \cdot 10^{-3}\,E^2 \;(E < 300\ \text{keV})$$

with E given in keV. This energy range is sufficiently high to treat recoil energies obtained for most neutron irradiation conditions. Naturally, for other purposes where even higher-energy recoils are significant, it could be extended to by carrying out additional electronic stopping calculations for higher energies and adding additional polynomial terms to the equation.

Then the damage production per initial ion can be obtained by using this equation to translate the recoil energy into damage energy, and then summing up the damage production of each recoil and dividing by the number of ions with which SRIM was run:

$$N_{FP} = \frac{1}{N_{ions}} \sum_{i=1}^{N_{recoils}} N_{d,arcdpa}\left(T_{dam,r}(E_{recoil})\right)$$

Note that the sum should indeed be over all recoils, but the division over the number of ions simulated. In practice this can be achieved with a simple computer program that parses the recoil lines in the COLLISON.TXT output file.

To check the consistence with the calculations in [Stoller, 2013], we first implemented the damage calculation with the original NRT equation, i.e. $N_d\left(T_{dam,r}(E_{recoil})\right)$. This gave perfect agreement within the statistical uncertainty with the previous Kinchin-Pease calculation in SRIM-2008. Then implementing the arc-dpa calculation, we obtained a value of 218 defects (see Table 7.1). This is quite close to the MD value of 168 defects, confirming that the arc-dpa equation is useful for analytical and numerical estimates of damage production that account for athermal recombination.

The reason that the arc-dpa model value is still lightly higher than the MD value is that at 50 keV there is significant subcascade overlap, and hence there is more recombination than the SRIM-based calculation for each recoil separately would predict.

8. Summary

In this OECD Nuclear Energy Agency report, we have reviewed the current state of understanding of the primary damage production mechanisms in all classes of materials except organic ones.

We described in detail the very useful and widely used standard for estimating the primary damage from neutrons, ions or electrons, namely that proposed by Norgett, Torrens and Robinson in 1975 to evaluate the number of Frenkel pairs formed for a given energy transferred to the primary knock-on atom, and therefore the number of "displacements per atom", or so-called NRT-dpa (or just dpa in short).

As a part of the work, we reviewed critically the range of validity of the dpa, and in particular discuss known shortcomings. We described that the current NRT-dpa standard is fully valid in the sense of a scaled radiation exposure measure, as it is essentially proportional to the radiation energy deposited per volume. As such, it is highly recommended to be used in reporting neutron damage results to enable comparison between different nuclear reactors and ion irradiations. However, in the sense of a measure of damage production the NRT-dpa value has several well-known problems. To partially start to alleviate these problems, for the case of metals we present an "athermal recombination-corrected dpa" (arc-dpa) equation that accounts in a relatively simple functional for the well known issue that the dpa overestimates damage production in metals under energetic displacement cascade conditions, as well as a "replacements-per-atom" (rpa) equation that accounts in a relatively simple functional for the well-known issue that the dpa severely underestimates the actual atom relocations (ion beam mixing) in metals.

Moreover, we present a recommendation for how the dpa value for ion irradiation of metals should be obtained from the widely used SRIM binary collision approximation code.

References

(in alphabetic order by tag)

[Agranovich, 1971] V.M. Agranovitch, V.V. Kirsanov (1971), "Atom-atom collision chain models in a body-centered cubic crystal in a wide temperature range", *Soviet Physics, Solid State*, Volume 12, pp. 1491-2246.

[Allen-Tildesley, 1989] Allen, M.P., D.J. Tildesley (1989), *Computer simulation of liquids*, Oxford University Press, Oxford, England.

[Andersen, 1979] Andersen, H.H. (1979), "The depth resolution of sputter profiling", *Applied Physics*, Volume 18, pp. 131-140.

[Ashcroft-Mermin, 1976] Ashcroft, N.W., N.D. Mermin (1976), *Solid state physics*, Saunders College, Philadelphia.

[ASTME521] ASTM E521, "Standard Practice for Neutron Radiation Damage Simulation by Charged-Particle Irradiation", Annual Book of ASTM Standards, Vol. 12.02, ASTM International, West Conshohocken, PA.

[ASTMFe] ASTM Standard E693-94 (1994), Standard practice for characterising neutron exposure in iron and low alloy steels in terms of displacements per atom (dpa).

[Avchaciov, 2013] Avchaciov, K.A., Y. Ritter, F. Djurabekova, K. Nordlund, and K. Albe (2013), "Controlled softening of $cu_{64}zr_{36}$ metallic glass by ion irradiation", *Applied Physics Letters*, 102:181910.

[Ave0] Siege, S. (1949), *Phys. Rev.* 75, 1823.

[Ave1] Sigmund, P. and Gras-Marti (1981), *Nucl. Instr. and Meth.* 182/183 25.

[Ave2] Parfitt, David C. and Robin W. Grimes (2009), *J. Nucl. Mater.*, 392, 28.

[Ave3] Schwen, D., M. Huang, P. Bellon and R.S. Averback (2009), *J. Nucl. Mater.* 392, 35.

[Ave4] Seitz, F. and J.S. Koehler (1956), *Solid State Physics*, vol. 2, ed. F. Seitz and D. Turnbull, Academic Press, United States, p. 307.

[Ave5] Vineyard, G.H. (1976), Raddiat Eff. 29, 245.

[Ave6] Kim, S.J., M-A. Nicolet, R.S. Averback, and D. Peak (1988), *Phys. Rev.* B 37, 38.

[Ave7] Paine, B.M. and R.S. Averback,

[Averback, 1977] Averback, R.S. and K.L. Merkle (1977), "Radiation-annealing effects in energetic displacement cascades", *Phys. Rev.* B, 16:3860.

[Averback, 1978] Averback, R.S., R. Benedek and K.L. Merkle (1978), "Ion-irradiation studies of the damage function of copper and silver", *Phys. Rev.* B, 18(8):4156.

[Averback, 1998] Averback, R.S. and T. Diaz de la Rubia (1998), "Displacement damage in irradiated metals and semiconductors", *Solid State Physics*, Volume 51, pages 281-402. Academic Press, New York.

[Averback, 1978] Averback, R.S., R. Benedek and K.L. Merkle (1978), "Ion irradiation studies of the damage function of copper and silver", *Phys. Rev.* B, 18 4156-4171.

[Averback, 1983] Averback, R.S. and R. Benedek, K.L. Merkle, J. Sprinkle, L.J. Thompson (1983), "Defect production in ion-irradiated aluminium", *J. Nucl. Mater.*, 113 211-218.

[Averback, 1994] Averback, R.S. (1994), "Atomic displacement processes in irradiated metals", *J. Nucl. Mater.*, 216 49-62.

[Averback, 1998] Averback, R.S. and T. Diaz de la Rubia (1998), "Displacement damage in irradiated metals and semiconductors", *Solid State Physics*, 51 281-402.

[Bacon, 1994] David J. Bacon and Tomas Diaz de la Rubia (1994), Molecular dynamics computer simulations of displacement cascades in metals, J. Nucl. Mat., 216:275--290.

[Banhart1] Telling, R., C.P. Ewels, A.A. El-Barbary and M.I. Heggie (2003), "Wigner defects bridge the graphite gap", *Nature Mater.* 2, 333-337.

[Banhart2] Thrower, P.A., R.M. Mayer (1978), "Point defects and self diffusion in graphite", *Phys. Stat. Sol.* (a) 47 11-36.

[Banhart3] Banhart, F. (1999), "Irradiation effects in carbon nanostructures", *Rep. Progr. Phys.* 62, 1181-1221.

[Banhart4] McKinley, W.A., H. Feshbach (1948), "The Coulomb Scattering of Relativistic Electrons by Nuclei", *Phys. Rev.* 74, 1759-1763.

[Banhart5] Meyer, J.C., F. Eder, S. Kurasch, V. Skakalova, J. Kotakoski, H.J. Park, S. Roth, A. Chuvilin, S. Eyhusen, G. Benner, A.V. Krasheninnikov, and U. Kaiser (2012), "An accurate measurement of electron beam induced displacement cross sections for single-layer graphene", arXiv:1203.2372v1.

[Banhart6] Kotakoski, J., A.V. Krasheninnikov, U. Kaiser and J.C. Meyer (2011), "From point defects in graphene to two-dimensional amorphous carbon, *Phys. Rev. Lett.* 106, 105505.

[Banhart7] Banhart, F., J. Kotakoski and A. Krasheninnikov (2011), Structural defects in graphene", ACS Nano 5, 26-41.

[Banhart8] Krasheninnikov A., Banhart, F. (2007), Engineering of nano-structured carbon materials with electron or ion beams: from oint defects to self-organization, *Nature Mater. 6*, 723-733.

[Banhart9] Lehtinen, O., T. Nikitin, A.V. Krasheninnikov, L. Sun, F. Banhart, L. Kriachtchev and J. Keinonen (2011), "Characterization of ion-irradiation-induced defects in carbon nanotubes, *New J. Phys.* 13, 073004.

[Banhart10] Davies, G. (1994), Properties and Growth of Diamond, INSPEC, London.

[Barcellos-Hoff, 1996b] Barcellos-Hoff, M.H. and T.A. Dix (1996), Redox-mediated activation of latent transforming growth factor-beta 1, Molecular Endocrinology, 10(9):1077-1083.

[Bauer, 1969] Bauer, W., A.I. Anderman, A. Sosin (1969), "Atomic displacement process in gold", *Phys. Rev.* A, 185(3):870.

[BCA] Robinson, M.T., Ian M. Torrens (1974), "Computer simulation of atomic-displacement cascades in solids in the binary-collision approximation", *Phys. Rev.* B, 9(12):5008.

[Beardmore, 1998] Beardmore, K.M., N. Gronbech-Jensen (1998), "An efficient molecular dynamics scheme for the calculation of dopant profiles due to ion implantation" *Phys. Rev.* E, 57:7278.

[Bench, 2000] Bench, M.W., I.M. Robertson, M.A. Kirk, and I. Jenčič (2000), "Production of amorphous zones in GaAs by the direct impact of energetic heavy ions", *J. Appl. Phys.*, 87(1):49-56.

[Berendsen, 1984] Berendsen, H.J.C., J.P. M. Postma, W.F. van Gunsteren, A. DiNola, J.R. Haak (1984), "Molecular dynamics with coupling to external bath", *J. Chem. Phys.*, 81(8):3684.

[Bevington, 1992] Bevington, P.R. (1992), *Data reduction and error analysis for the physical sciences*, McGraw-Hill, New York, United States.

[Birtcher, 1999] Birtcher, R.C., S.E. Donnelly (1999), "Plastic flow produced by single ion impacts on metals", *Nucl. Instr. Meth. Phys. Res*. B, 148:194-199.

[Birtcher, 1978] Birtcher, R.C., R.S. Averback, T.H. Blewitt (1978), "Saturation behavior of cascade damage production using fission fragment and ion irradiations", *J. Nucl. Mater.*, 75 167-176.

[Bishop, 2012] Bishop, C.L., S.T. Murphy, M.J.D. Rushton, R.W. Grimes (2012), "The influence of dipole polarisation on threshold displacement energies in UO2", *Nucl. Instrum. Meth. B*, 274, 195-199.

[Björkas, 2007a] Björkas, C., K. Nordlund (2007), "Comparative study of cascade damage in fe simulated with recent potentials", *Nucl. Instr. Meth. Phys. Res*. B, 259:853.

[Björkas, 2009a] Börkas, C., K. Nordlund (2009), "Assessment of the relation between ion beam mixing, electron-phonon coupling, and damage production in fe", *Nucl. Instr. Meth. Phys. Res*. B, 267:1830-1836.

[Björkas, 2012] Björkas, C., K. Nordlund, and M. J. Caturla (2012), "Influence of the picosecond defect distribution on damage accumulation in irradiated alpha-fe", *Phys. Rev.* B, 85:024105.

[Bob; Delaye, 1993] Delaye, J.M., Y. Limoge (1993), "Molecular dynamics study of vacancy-like defects in a model glass: static behaviour", *J. de Physique I*, 3:2063-2077.

[Bob; Delaye, 1993b] Delaye, J.M., Y. Limoge (1993), "Molecular dynamics study of vacancy-like defects in a model glass: dynamical behaviour and diffusion", *J. de Physique I*, 3:2079-2097.

[Böhmer, 1998] Böhmer, R., R.V. Chamberlin, G. Diezemann, B. Geil, A. Heuer, G. Hinze, S.C. Kuebler, R. Richert, B. Schiener, H. Sillescu, H. W. Spiess, U. Tracht, and M. Wilhelm (1998), "Nature of the non-exponential primary relaxation in structural glass-formers probed by dynamically selective experiments", *J. Non-Cryst. Solids*, 235-237:1-9.

[Bourgoin, 1973] Bourgoin, J.C., J.W. Corbett, H.L. Frisch (1973), Ionization enhanced diffusion, *J. Chem. Phys.*, 59 4042-4046.

[Bourgoin, 1978] Bourgoin, J.C., J.W. Corbett (1978), "Enhanced diffusion mechanisms", *Radiat. Effects*, 36 157-188.

[Brinkman, 1954] Brinkman, J.A. (1954), "On the nature of radiation damage in metals", *J. Appl. Phys.*, 25:961.

[Brown, 1970] Brown, L.M. and Woolhouse G. R (1970), "The loss of coherency of precipitates and the generation of dislocations", *Phil. Mag.*, 21:329-345.

[Broeders, 2004] Broeders, C.H.M., A.Y. Konobeyev (2004), "Defect production efficiency in metals under neutron irradiation", *J. Nucl. Mater.*, 328 197-214.

[Cai, 1998] Cai, D., C.M. Snell, K. M. Beardmore, and N. Gronbech-Jensen (1998), "Simulation of phosphorus implantation into silicon with a single parameter electronic stopping power model. International", *J. Modern Physics C*, 9(3):459.

[Calder, 2010b] Calder, A.F., D. J. Bacon, A. V. Barashev, and Yu (2010), N. Osetsky. X., *Phil. Mag.*, 90:863.

[Car, 1997b] F. Cargnoni, C. Gatti, and L. Colombo (1998), "Formation and annihilation of a bond defect in silicon: an ab-initio quantum-mechanical characterization", Phys. Rev. B, 57:170.

[Caro, 2000b] Caro, M. and A. Caro (2000), "Spectral effects on defect production in the reactor pressure vessel of a pressurized heavy-water reactor", *Phil. Mag. A,* Vol. 80, pp. 1365-1378.

[Caro, 1989] Caro, A. and M. Victoria (1989), "Ion-electron interaction in molecular-dynamics cascades", *Phys. Rev.* A (General Physics), 40(5):2287-91.

[Caro, 1994] Caro, A., M. Alurralde, S. Proennecke and M. Victoria, (1994), "Liquid-drop model and effects of electronic-energy loss on radiation-damage cascades", *Radiation Effects and Defects in Solids*, 129(1-2):105-112.

[Caturla, 1994] Caturla, M.-J., T. Diaz de la Rubia and G. H. Gilmer (1994), "Point defect production, geometry and stability in silicon: a molecular dynamics simulation study", *Mat. Res. Soc. Symp. Proc*., 316:141.

[Caturla, 1995b] Caturla, M.J., T. Diaz de la Rubia and G. H. Gilmer (1995), "Recrystallization of a planar amorphous-crystalline interface in silicon by low energy recoils: a molecular dynamics study", *J. Appl. Phys.*, 77(7):3121.

[Caturla, 1996] Caturla, M.J., L.A. Marques, T. Diaz de la Rubia, G.H. Gilmer (1996), Ion-beam processing of silicon at kev energies: A molecular-dynamics study, *Phys. Rev. B*, 54 (24): 16683, 1996.

[Certain, 2013] Certain, A. (2013), S. Kuchibhatla, V. Shutthanandan, D.T. Hoelzer, T.R. Allen, "Radiation stability of nanoclusters in nano-structured oxide dispersion strengthened (ODS) steels", *J. Nucl. Mater.*, 434 311-321.

[Chason, 1997] Chason, E., S.T. Picraux, M. Poate, J.O. Borland, M.I. Current, T. Diaz de la Rubia, D.J. Eaglesham, O.W. Holland, M.E. Law, C.W. Magee, J.W. Mayer, J. Melngailis and A.F. Tasch (1997), "Ion beams in silicon processing and characterization", *J. Appl. Phys.*, 81(10):6513-6561.

[Chen, 1976] Chen, Y., M.M. Abraham, H.T. Tohver (1976), "Radiation-induced diffusion of hydrogen and deuterium in MgO", *Phys. Rev. Lett.*, 37 1757-1760.

[Chung, 2006] Chung, H.M (2006), Assesment of void swelling in austenitic stainless steel core internals, Volume NUREG/CR-6897; ANL-04/28, Argonne National Laboratory.

[Coltman, 1967] Coltman, R.R., C.E. Klabunde, J.K. Redman (1967), "Survey of thermal-neutron damage in pure metals", *Physical Review*, 156 715-734.

[Coltman, 1975] Coltman, R.R., Jr., C.E. Klabunde, J.K. Redman (1975), "Recovery in stages I and II of thermal and fission neutron irradiated molybdenum", in: M.T. Robinson, F.W.

[Coltman, 1978] Coltman, R.R., C.E. Klabunde, J.K. Redman (1978), "Thermal and fission neutron-produced defect configurations in platinum", *J. Nucl. Mater.*, 69-70 720-723.

[Coltman, 1981] Coltman, R.R. Jr., C.E. Klabunde, J.M. Williams (1981), "Rates of defect production by fission neutrons in metals at 4.7 K", *J. Nucl. Mater.*, 99 284-293.

[Corbett, 1966] Corbett, J.W. (1966), "Electron Radiation Damage" in Semiconductors and Metals, Academic Press, New York.

[Costantini, 2011] Costantini, J.M., F. Beuneu, S. Morrison-Smith, R. Devanathan, W.J. Weber (2011), "Paramagnetic defects in electron-irradiated yttria-stabilized zirconia: Effect of yttria content", *J. Appl. Phys.*, 110 123506.

[Dennis, 1978] Dennis, J.R. and E.B. Hale (1978), "Crystalline to amorphous transformation in ion-implanted silicon: a composite model" *J. Appl. Phys.*, 49:1119.

[Derlet, 2007] Derlet, P., M.D. Nguyen-Manh, and S.L. Dudarev (2007), "Multiscale modeling of crowdion and vacancy defects in body-centered-cubic transition metals", *Phys. Rev.* B, 76:054107.

[Devanathan, 1998] Devanathan, R., K.E. Sickafus, W.J. Weber, M. Nastasi (1998), "Effects of ionizing radiation in ceramics", *J. Nucl. Mater.*, 253 113-119.

[Devanathan, 2006] Devanathan, R., L.R. Corrales, W.J. Weber, A. Chartier, C. Meis (2006), "Atomistic simulation of collision cascades in zircon", *Nucl. Instrum. Meth. B*, 250 46-49.

[Devine, 1992] Devine, R.A.B (1992), "Radiation induced structural changes in amorphous SiO2: I. Point Defects, Jpn", *J. Appl. Phys.*, 31 4411-4421.

[Diaz, 1987] Diaz de la Rubia, T., R.S. Averback, R. Benedek, and W.E. King (1988), "Role of thermal spikes in energetic collision cascades", *Phys. Rev. Lett.*, 59:1930-1933, 1987. See also erratum: *Phys. Rev. Lett.* 60 76.

[Diaz, 1991] Diaz de la Rubia, T. and M.W. Guinan (1991), "New mechanism of defect production in metals: A molecular-dynamics study of interstitial-dislocation-loop formation at high-energy displacement cascades", *Phys. Rev. Lett.*, 66:2766.

[Diaz, 1996] Diaz de la Rubia, T. (1996), "Defect production mechanisms in metals and covalent semiconductors", *Nucl. Instr. Meth. Phys. Res*. B, 120:19.

[Dienes, 1958] Dienes, G.J., A.C. Damask (1958), "Radiation enhanced diffusion in solids", *J. Appl. Phys*., 29 1713.

[Donati, 1998] Donati, C., J.F. Douglas, W. Kob, S.J. Plimpton, P.H. Poole, and S.C. Glotzer (1998), "Stringlike cooperative motion in a supercooled liquid", *Phys. Rev. Lett.*, 80(11):2338.

[Donati, 1999] Donati, C., S.C. Glotzer, P.H. Poole, W. Kob, and S.J. Plimpton (1999), "Spatial correlations of mobility and immobility in a glass-forming lennard-jones liquid", *Phys. Rev.* E, 60(3):3107.

[Draxler, 2005] Draxler, M., S.P. Chenakin, S.N. Markin, and P. Bauer (2005), "Apparent velocity threshold in the electronic stopping of slow hydrogen ions in lif", *Phys. Rev. Lett.*, 95:113201.

[Drosd, 1978] Drosd, R., T. Kosel, J. Washburn (1978), "Temperature dependence of the threshold energy for Frenkel pair production in copper", *J. Nucl. Mater.*, 69-70 804-806.

[Duvenbeck, 2007b] Duvenbeck, A., O. Weingart, V. Buss, and A. Wucher (2007), "Electron promotion and electronic friction in atomic collision cascades", *New J. Physics*, 9:38.

[Ehmler, 1998] Ehmler, H., A. Heesemann, K. Rätzke, F. Faupel, and U. Geyer (1998), "Mass dependence of diffusion in a supercooled metallic melt", *Phys. Rev. Lett.*, 80(22):4919.

[Ehrhart, 1991] Ehrhart, P. (1991), "Properties and interactions of atomic defects in metals and alloys", Volume 25 of Landolt-Bãrnstein, New Series III, chapter 2, page 88, Springer, Berlin.

[Eisen, 1971] Eisen, F.H. (1971), "Iii-v compound review", *Radiation Effects*, 9(3-4):235-42.

[Erginsoy, 1964] Erginsoy, C., G.H. Vineyard, and A. Englert (1964), "Dynamics of radiation damage in a body-centered cubic lattice", *Phys. Rev.*, 133(2):A595.

[Erlebacher, 1999] Erlebacher, J., M.J. Aziz, E. Chason, M.B. Sinclair, and J.A. Floro (1999), "Spontaneous pattern formation on ion bombarded si(001)", *Phys. Rev. Lett.*, 82(11):2330.

[Eyre, 1973] Eyre, B.L. (1973), "Transmission electron microscope studies of point defect clusters in fcc and bcc metals", J. *Phys. F: Metal Phys.*, 3:422-470.

[Faupel, 2003] Faupel, F., Werner F., M.-P. Macht, H. Mehrer, V. Naundorf, K. Rätzke, H.R. Schober, S.K. Sharma and H. Teichler (2003), "Diffusion in metallic glasses and supercooled melts", *Rev. Mod. Phys.*, 75:237-280.

[Faulkner, 1996] Faulkner, R.G. (1996), "Segregation to boundaries and interfaces in solids", *Int. Mater. Rev.*, 41 198-208.

[Fenn-Tyre, 1987] Fenn-Tye, I.A. and A.D. Marwick (1987), "The dependence of cascade mixing in pd on the projectile's mass", *Nucl. Instr. Meth. Phys. Res*., 18:236.

[Flynn, 1988] Flynn, C.P. and R.S. Averback (1988), "Electron-phonon interactions in energetic displacement cascades", *Phys. Rev.* B, 38:7118.

[Frantz, 2001] Frantz, J., J. Tarus, K. Nordlund, and J. Keinonen (2001), "Mechanism of electron-irradiation induced recrystallisation in si", *Phys. Rev.* B, 64:125313.

[Fu, 2004] Fu, Chu-Chun, F. Willaime, and P. Ordejon (2004), "Stability and mobility of mono- and di-interstitials in alpha-fe", *Phys. Rev. Lett.*, 92(17):175503-1.

[Gades, 1995] Gades, H. and H.M. Urbassek (1995), "Simulation of ion-induced mixing of metals", *Phys. Rev.* B, 51:14559.

[Gao, 2011] F. Gao, H.Y. Xiao, and W.J. Weber (2011), "Ab initio molecular dynamics simulations of low energy recoil events in ceramics", *Nucl. Instr. Meth. Phys. Res*. B, 269(14):1693-1697.

[Gao, 1996] Gao, F., D.J. Bacon, A.F. Calder, P.E.J. Flewitt, and T.A. Lewis (1996), "Computer simulation study of cascade overlap effects in alpha-iron", *J. Nucl. Mater.*, 230(1):47.

[Garner, 2005] Garner, F.A., S.I. Porollo, Yu.V. Konobeev and O.P. Maksimkin (2005), "Void swelling of austenitic steels irradiated with neutrons at low temperatures and very low dpa rates", in T.R. Allen, P.J. King, and L. Nelson, editors, *Proceedings of the 12th International conference on environmental degradation of materials in nuclear power system – Water Reactors*, page 439, TMS.

[Gartner, 1995] Gärtner, K. et. al. (1995), "Round robin compbuter simulation of ion transmission through crystalline layers", *Nucl. Instr. Meth. Phys. Res*. B, 102(1-4):183.

[Ghaly, 1994] Ghaly, Mai and R.S. Averback (1994), "Effect of viscous flow on ion damage near solid surfaces", *Phys. Rev. Lett.*, 72(3):364-367.

[Gibson, 1960] Gibson, J.B., A.N. Goland, M. Milgram, and G.H. Vineyard (1960), "Dynamics of radiation damage", *Phys. Rev*, 120(4):1229-1253.

[Giovambattista, 2003] Giovambattista, N.S., V. Buldyrev, F.W. Starr, and H.E. Stanley, (2003), *Phys. Rev. Lett.*, 90:085506.

[Glover, 2000c] Glover, C.J., M.C. Ridgway, A.P. Byrne, K.M. Yu, G.J. Foran, C. Clerc, J.L. Hansen, and A.N. Larsen (2000), "Micro- and macro-structure of implantation-induced disorder" in Ge. *Nucl. Instr. Meth. Phys. Res*. B, 161:1033-1037.

[Glotzer, 1999] Glotzer, S.C. and C. Donati (1999), "Quantifying spatially heterogeneous dynamics in computer simulations of glass-forming liquids", *J. Phys. F: Metals Physics*, 11:A285.

[Goe, 2002] Stefan Goedecker, Thierry Deutsch, and Luc Billard (2002), "A fourfold coordinated point defect in silicon", Phys. Rev. Lett., 88:235501.

[Goldberg, 1993] Goldberg, R.D., R.G. Elliman, J.S. Williams (1993), "The kinetics of self-ion amorphization of silicon, *Nucl. Instr. Meth. Phys. Res.,* B 80 81:596.

[Granato, 1992] Granato, V.A. (1992), "Interstitialcy model for condensed matter states of face-centered-cubic metals, *Phys. Rev. Lettt.,* 68 (7): 974.

[Greenwood, 1994] Greenwood, L.R. (1994), "Neutron interactions and atomic recoil spectra", *J. Nuclear Materials*, 216:29-44.

[Guinan, 1982] Guinan, M.W. (1982), J.H. Kinney, "Resistivity damage rates in fusion neutron irradiated metals at 4.2 K", *J. Nucl. Mater.*, 108&109 95-103.

[Guinan, 1985] Guinan, M.W., J.H. Kinney, R.A. VanKonynenburg (1985), "Defect production and recovery in fcc metals irradiated at 4.2 K", *J. Nucl. Mater.*, 133 and 134 183-193.

[Hashimoto, 2004] Kimura-Hashimoto, A., K. Suenaga, A. Gloter, K. Urita, and S. Iijima (2004), "Direct evidence for atomic defects in graphene layers", *Nature*, 430(7002):870-873.

[Hausmann, 1996] Hausmann, H., A. Pillukat and P. Ehrhart (1996), "Point defects and their reactions in electron-irradiated gaas investigated by optical absorption spectroscopy", *Phys. Rev.* B, 54(12):8527.

[Hensel, 1997] Hensel, H. and H.M. Urbassek (1997), "Implantation and damage under low energy si self-bombardment", *Phys. Rev.* B, 57(13):4756.

[HiggsAtlas] ATLAS Collaboration (2012), "Combined search for the Standard Model Higgs boson using up to 4.9 fb(-1) of pp collision data at root s=7 TeV with the ATLAS detector at the LHC", *Physics Letters B*, 710(1):49-66.

[HiggsCMS] CMS Collaboration, "Combined results of searches for the standard model Higgs boson in pp collisions at root s=7 TeV", *Physics Letters B*, 710(1):26-48, 2012.

[Hobler, 2001] Hobler G. and G. Betz (2001), "On the useful range of application of molecular dynamics simulations in the recoil interaction approximation", *Nucl. Instr. Meth. Phys. Res*. B, 180:203.

[Hobbs, 1994] Hobbs, L.W., F.W. Clinard, Jr., S.J. Zinkle, R.C. Ewing (1994), "Radiation effects in ceramics", *J. Nucl. Mater.*, 216 291-321.

[Hohenstein, 1989] Hohenstein, M., A. Seeger, W. Sigle, "The anisotropy and temperature dependence of the threshold for radiation damage in gold − comparison with other FCC metals", *J. Nucl. Mater.*, 169 (1989) 33-46.

[Holmström, 2008a] Holmström, E., A. Kuronen, and K. Nordlund (2008), "Threshold defect production in silicon determined by density functional theory molecular dynamics simulations", *Phys. Rev.* B, 78(4):045202.

[Holland, 1985] Holland, O.W., J. Narayan and D. Fathy (1985), "Ion beam processes in si", *Nucl. Instr. Meth. Phys. Res*. B, 7/8:243.

[Horak, 1975] Horak, J.A., T.H. Blewitt (1975), "Fast-neutron and thermal-neutron irradiation and annealing of Cu, Ni, Fe, Ti and Pd", *Nucl. Technol*., 27 416-438.

[Hou, 2000] Hou, Q., M. Hou, L. Bardotti, B. Prevel, P. Melinon, and A. Perez (2000), "Deposition of aun clusters on au(111) surfaces., i. atomic-scale modelling", *Phys. Rev.* B, 62(4):2825-2834.

[Hou, 1994] Hou, M. and Z. Pan (1994), "Collision cascades in cu, au and cu3au: a comparison between molecular dynamics and the binary collision approximation", *Nucl. Instr. Meth. Phys, Res. B*, 90:469.

[Hudson, 1975] Hudson, J.A. (1975), "Structural stability during irradiation", *Journal of the British Nuclear Energy Society*, 14 127-136.

[Iseler, 1966] Iseler, G.W., H.I. Dawson, A.S. Mehner, J.W. Kauffman (1966), "Production Rates of Electrical Resistivity in Copper and Aluminum Induced by Electron Irradiation", *Physical Review*, 146 468-471.

[Itoh, 2001] Itoh, N., A.M. Stoneham (2001), *Materials modification by electronic excitation*, Cambridge University Press, Cambridge, United Kingdom.

[Ivanov, 2003] Ivanov, D.S. and L.V. Zhigilei (2003), "Combined atomistic-continuum modeling of short pulse laser melting and disintegration of metal films", *Phys. Rev.* B, 68:064114.

[Jagielski, 2009] Jagielski, J. (2009), L. Thomé, "Multi-step damage accumulation in irradiated crystals", *Appl. Phys. A*, 97 147-155.

[JAPreview2010] Krasheninnikov, A.V. and K. Nordlund (2010), "Ion and electron irradiation-induced effects in nanostructured materials", *J. Appl. Phys.* (Applied Physics Reviews), 107:071301.

[Jenčič, 1996] Jenčič, I. and I.M. Robertson (1996), "Low-energy electron beam induced regrowth of isolated amorphous zones in si and ge", *J. Mater. Res.*, 11(9):2152.

[Ji, 2004] Ji, H.H, M. Yu, H. Shi, X.K. Shi, R. Huang, X. Zhang, J.Y. Zhang, K. Suzuki, and H. Oka (2004), "Molecular dynamics simulation of ion implantation into hafnium dioxide", *Nucl. Instr. Meth. Phys. Res*. B, 226(4):537-542.

[Johnson, 1976] Johnson, R.A. and N.Q. Lam (1976), "Solute segregation in metals under irradiation", *Phys. Rev.* B, 13 4364-4375.

[Jung, 1981] Jung, P. (1981), "Average atomic-displacement energies of cubic metals", *Phys. Rev.* B, 23(2):664.

[Jung, 1973] Jung, P., R.L. Chaplin, H.J. Fenzl, K. Reichelt, P. Wombacher (1973), "Anisotropy of the threshold energy for production of frenkel pairs in copper and platinum", *Phys. Rev.* B, 8 553-561.

[Jung, 1975] Jung, P. G. Lucki (1975), "Damage production by fast electrons in dilute alloys of vanadium, niobium and molybdenum", *Radiat. Effects*, 26 99-103.

[Jung, 1981] Jung, P. (1981), "Average atomic displacement energies of cubic metals", *Phys. Rev.* B, 23 664-670.

[Jung, 1981a] Jung, P. (1981), "On the temperature dependence of the threshold energy for atomic displacement in copper", *Radiat. Effects*, 59 103-104.

[Jung, 1991] Jung, P. (1991), Production of atomic defects in metals, in: H. Ullmaier, et al. (Eds.) Atomic defects in metals, Landolt-Börnstein Database, Vol. 25, Springer.

[Kanjijal, 2001b] Kanjijal, D. (2001), "Swift heavy ion-induced modification and track formation in materials", *Current Science*, 80(12):1560.

[Karaseov, 2009] Karaseov, P.A., A. Yu. Azarov, A.I. Titov, and S.O. Kucheyev (2009), Density of displacement cascades for cluster ions: An algorithm of calculation and the influence on damage formation in zno and gan, Semiconductors, 43:691.

[Karim, 1978] Karim, A.S.A. (1978), M.E. Whitehead, M.H. Loretto, R.E. Smallman, "Electron radiation damage in H.C.P. Metals−I. The determination of the threshold displacement energy in Zn, Cd, Mg and Ti", *Acta Metall.*, 26 975-981.

[Keinonen, 2008] Keinonen, J., F. Djurabekova, K. Nordlund, and K.P. Lieb (2008), "Silicon nanophotonics: Basic principles", Present Status and Perspectives, chapter 14, "Light Emitting Defects in Ion-Irradiated Alpha-Quartz", pp. 379-396, *World Scientific*, Singapore.

[Kenik, 2012] Kenik, E.A., J.T. Busby (2012), "Radiation-induced degradation of stainless steel light water reactor internals", *Mater. Sci. Eng. R*, 73 67-83.

[Kim, 1988] Kim, S.-J., M-A. Nicolet, R.S. Averback and D. Peak (1988), "Low-temperature ion-beam mixing in metals", *Phys. Rev.* B, 37(1):38.

[Kinchin, 1955] Kinchin, G.H. and R.S. Pease (1955), X. *Rep. Prog. Phys*., 18:1.

[King, 1982] King, W.E., R. Benedek, K.L. Merkle and M. Meshii (1982), "Re-examination of the threshold energy surface in copper", in Jin-Ichi Takamura, editor, *Point defects and defect interactions in metals*, p.789.

[Kinchin, 1955] Kinchin, G.H., R.S. Pease (1955), "The displacement of atoms in solids by radiation", *Rep. Prog. Phys.*, 18 1-51.

[King, 1983] King, W.E., K.L. Merkle, M. Meshii (1983), "Threshold energy surface and frenkel pair resistivity for Cu", *J. Nucl. Mater.*, 117 12-25.

[Kinoshita, 2004] Kinoshita, C., K. Yasuda, S. Matsumura (2004), "Effects of simultaneous displacive and ionizing eadiations and of zlectric field on radiation damage in ionic crystals", *Metall. Mater, Trans. A*, 35A 2257-2266.

[Kirk, 1978] Kirk, M.A., T.H. Blewitt (1978), "Atomic rearrangements in ordered fcc alloys during neutron irradiation", *Metall. Mater. Trans. A*, 9 1729-1737.

[Kirk, 1979] Kirk, M.A., L.R. Greenwood (1979), "Determination of the neutron flux and energy spectrum in the low-temperature fast-neutron facility in CP-5, calculations of primary-recoil and damage-energy distributions, and comparisons with experiment", *J. Nucl. Mater.*, 80 159-171.

[Kitagaza, 1985] Kitagawa, K., K. Yamakawa, H. Fukushima, T. Yoshiie, Y. Hayashi, H. Yoshida, Y. Shimomura and M. Kiritani (1985), "Ion-irradiation experiment for the experimental studies of damage evolution of fusion materials", *J. Nucl. Mater.*, 133 and 134:395-399.

[Kittel, 1968] Kittel, Charles (1968), Introduction to *Solid state physics*, John Wiley and Sons, New York, third edition.

[Kittiratanawasin, 2010] Kittiratanawasin, L. (2010), R. Smith, B.P. Uberuaga, K.E. Sickafus, "Displacement threshold and frenkel pair formation energy in ionic systems", *Nucl. Instrum. Meth. B*, 268 2901-2906.

[Klabunde, 1974] Klabunde, C.E., J.K. Redman, A.L. Southern, R.R. Coltman (1974), "Thermal and fission neutron damage in vanadium", *Phys. Status Solidi A*, 21303-307.

[Klabunde, 1982] Klabunde, C.E., R.R. Coltman, Jr. (1982), "Fission neutron damage rates and efficiencies in several metals", *J. Nucl. Mater.*, 108-109, 183-193.

[Knutsen, 2012] Knutsen, K.E., A. Galeckas, A. Zubiaga, F. Tuomisto, G.C. Farlow, B.G. Svensson, A.Y. Kuznetsov (2012), "Zinc vacancy and oxygen interstitial in ZnO revealed by sequential annealing and electron irradiation", *Phys. Rev.* B, 86 121203.

[Koike, 1989] Koike, J., P.R. Okamoto, L.E. Rehn, M. Meshi (1989), "The dose, temperature, and projectile-mass dependence for irradiation-induced amorphization of CuTi, *J. Mater. Res.*, 4 1143-1150.

[Koponen, 1993] Koponen, I. (1993), "Energy transfer between electrons and ions in dense displacement cascades", *Phys. Rev.* B, 47(21):14011.

[Krefft, 1977] Krefft, G.B. (1977), "Ionization-stimulated annealing effects on displacement damage in magnesium oxide", J*ournal of Vacuum Science and Technology*, 14 533-536.

[Krefft, 1978] Krefft, G.B., E.P. EerNisse (1978), "Volume expansion and annealing compaction of ion-bombarded single-crystal and polycrystalline alpha-Al_2O_3", *J. Appl. Phys.*, 49 2725-2730.

[Kucheyev, 2001b] Kucheyev, S.O., J.S. Williams, C. Jagadish, J. Zou, G. Li, and A.I. Titov (2001), "Effect of ion species on the accumulation of ion-beam damage in gan", *Phys. Rev.* B, 64:035202.

[Kucheyev, 2003] Kucheyev, S.O., J.S. Williams, C. Jagadish, J. Zou, C. Evans, A.J. Nelson, A.V. Hamza (2003), "Ion-beam-produced structural defects in ZnO", *Phys. Rev. B*, 67 094115.

[Laaziri, 1999] Laaziri, K., S. Kycia, S. Roorda, M. Chicoine, J.L. Robertson, J. Wang, and S.C. Moss (1999), "High-energy x-ray diffraction study of pure amorphous silicon", *Phys. Rev.* B, 60(19):13520.

[Lam, 1997] Lam, N., P.R. Okamoto, M. Li (1997), "Disorder-induced amorphization", *J. Nucl. Mater.*, 251 89-97.

[Lannoo, 1981] Lannoo, M. and J. Bourgoin (1981), "Point Defects in Semiconductors", Springer, Berlin.

[Lee, 1981] Lee, E.H., P.J. Maziasz, A.F. Rowcliffe (1981), "The structure and composition of phases occurring in austenitic stainless steels in thermal and irradiation environments", in J.R. Holland, L.K. Mansur, D.I. Potter (Eds.) *Phase stability during irradiation*, New York, pp. 191-218.

[Lehmann, 1993] Lehmann, B. and D. Braunig (1993), "A deep-level transient spectroscopy variation for the determination of displacement threshold energies in gaas", *J. Appl. Phys.*, 73(6):2781-5.

[Lennartz, 1977] Lennartz, R., F. Dworschak, H. Wollenberger (1977), "Frenkel pair recombination radius in copper as a function of temperature", *J. Phys. F: Metal Phys*., 7 2011-2019.

[Lian, 2003] J. Lian, J. Chen, L.M. Wang, R.C. Ewing, J.M. Farmer, L.A. Boatner, K.B. Helean, "Radiation-induced amorphization of rare-earth titanate pyrochlores", *Phys. Rev.* B, 68 (2003) 134107.

[Lieb, 2007] Lieb K.P. and J. Keinonen (2007), "Luminescence of ion-irradiated a-quartz", *Contemporary Physics*, 47(5):305.

[Linnros, 1987] Linnros, J. and G. Holmen (1987), "Dose rate dependence and time constant of the ion-beam-induced crystallization mechanism in silicon", *J. Appl. Phys.,* 62(12): 4737.

[Liu, 2000] Liu, B.X., W.S. Lai, Q. Zhang (2000), "Irradiation induced amorphization in metallic multilayers and calculation of glass-forming ability from atomistic potential in the binary metal systems", *Mater. Sci. Eng. R*, 29 1-48.

[Loferski, 1958] Loferski J. and P. Rappaport (1958), "Radiation damage in ge and si detected by carrier lifetime changes: Damage thresholds", *Phys. Rev.*, 111:432.

[Lomer, 1967] Lomer J.N. and M. Pepper (1967), "Anisotropy of defect production in electron irradiated iron", *Phil. Mag.*, 16:119.

[Look, 1999] Look, D.C., J.W. Hemsky and J.R. Sizelove (1999), "Residual native shallow donor in zno", *Phys. Rev. Lett.*, 82(12):2552-2555.

[LSS] Lindhard, J., M. Scharff, and H.E. Shiott (1963), "Range concepts and heavy ion ranges", *Mat. Fys. Medd. Dan. Vid. Selsk*., 33(14):1.

[Lucasson, 1962] Lucasson, P.G. and R.M. Walker (1962), "Production and recovery of electron-induced radiation damage in a number of metals", *Phys. Rev.*, 127:485.

[Lucasson, 1975] Lucasson, P. (1975), "The production of frenkel defects in metals", in M. T. Robinson and F.N. Young Jr., editors, *Fundamental aspects of radiation damage in metals*, pages 42-65, Oak Ridge National Laboratory, United States.

[Lucasson, 1962] Lucasson, P.G., R.M. Walker (1962), "Production and recovery of electron-induced radiation damage in a number of metals", *Physical Review*, 127 485-500.

[Lucasson, 1978] Lucasson, P., A. Lucasson (1978), "Multiple atom displacements in irradiated metals", *Radiat. Effects*, 39 195-204.

[Malerba, 2002] Malerba, L. and J.M. Perlado (2002), "Basic mechanisms of atomic displacement production in cubic silicon carbide: A molecular dynamics study", *Phys. Rev. B*, 65:045202.

[Malerba, 2006] Malerba, L. (2006), "Molecular dynamics simulation of displacement cascades in alpha-fe: a critical review", *J. Nucl. Mater.*, 351:28-38.

[Malerba, 2007] Malerba, L., D.A. Terentyev, G. Bonny, A.V. Barashev, C. Björkas, N. Juslin, K. Nordlund, C. Domain, P. Olsson, R. Chakarova, N. Sandberg, and J. Wallenius (2007), "Modelling of radiation damage in Fe-Cr alloys", *Journal of ASTM International*, 4(6):1-18.

[Malerba, 2010] L. Malerba, M.C. Marinica, N. Anento, C. Björkas, H. Nguyen, C. Domain, F. Djurabekova, P. Olsson, K. Nordlund, A. Serra, D. Terentyev, F. Willaime and C.S. Becquart (2010),

"Comparison of empirical interatomic potentials for iron applied to radiation damage studies", *J. Nucl. Mater.*, 406:19-38.

[Malerba; IAEA, 1970] IAEA (1970), *Neutron fluence measurements*, IAEA Technical Reports Series No. 107.

[Malerba; Jansson, 2013] V. Jansson, L. Malerba, "Simulation of the nanostructure evolution under irradiation in Fe-C alloys", *Journal of Nuclear Materials*, accepted.

[MacFarlane; Kahler, 2010] MacFarlane, R.E. and A.C. Kahler (2010), "Methods for processing ENDF/B-VII with NJOY", *Nuclear Data Sheets* 111, pp. 2739-2890.

[Malerba; Robinson, 1970] Robinson, M.T. (1970), "The Energy dependence of neutron radiation damage in solids", in *Nuclear fusion reactor: Proceedings of international conference* (British Nuclear Energy Society, London), pp. 364-377.

[Malerba; Schultis, 2011] Shultis, J.K. and R.E. Faw (2011), "An MCNP primer", www.mne.ksu.edu/~jks/MCNPprmr.pdf.

[Malerba; Souidi, 2005] Souidi, A., M. Hou, C.S. Becquart, L. Malerba, C. Domain, R.E. Stoller (2011), *Journal of Nuclear Materials* 419 p. 122.

[Marques, 1994] Marques, L.A., M.-J. Caturla, H. Huang, and T. Diaz de la Rubia (1994), "Molecular dynamics studies of the ion beam induced crystallization in silicon", *Mater. Res. Soc. Symp. Proc.*, 396:201.

[Marwick, 1981] Marwick, A.D. (1981), "Solute segregation and precipitate stability in irradiated alloys", *Nucl. Instrum. Meth.*, 182-183 827-843.

[Mattila, 1995] Mattila T. and R.M. Nieminen (1995), "Direct antisite formation in electron irradiation of gaas", *Phys. Rev. Lett.*, 74:2721.

[Maury, 1975] Maury, F., P. Vajda, M. Biget, A. Lucasson, and P. Lucasson (1975), "Anisotropy of the displacement energy in single crystals of molybdenum", *Radiation Effects*, 25:175-185.

[Maury, 1976] Maury, F., M. Biget, P. Vajda, A. Lucasson, and P. Lucasson (1976), "Anisotropy of defect creation in electron-irradiated iron crystals", *Phys. Rev.* B, 14(12):5303.

[Maury, 1978] Maury, F., M. Biget, P. Vajda, A. Lucasson, P. Lucasson, "Frenkel pair creation and stage I recovery in W crystals irradiated near threshold", *Radiat. Effects*, 38 (1978) 53-65.

[Mayr, 2003] Mayr, S.G., Y. Ashkenazy, K. Albe, and R.S. Averback (2003), "Mechanisms of radiation-induced viscous flow: Role of point defects", *Phys. Rev. Lett.*, 90:055505.

[Maziasz, 1989] Maziasz, P.J. (1989), "Formation and stability of radiation-induced phases in neutron-irradiated austenitic and ferritic steels", *J. Nucl. Mater.*, 169 95-115.

[Meis, 2005] Meis, C., A. Chartier (2005), "Calculation of the threshold displacement energies in UO_2 using ionic potentials", *J. Nucl. Mater.*, 341 25-30.

[Merkle, 1976] Merkle, K.L. (1976), "Defect Production by Energetic Particle Bombardment", in N.L. Peterson, S.D. Harkness (Eds.) *Radiation Damage in Metals*, American Society for Metals, Metals Park, OH, pp. 58-94.

[Merkle, 1983] Merkle, K.L., W.E. King, A.C. Baily, K. Haga, M. Meshii (1983), "Experimental determination of the energy dependence of defect production", *J. Nucl. Mater.*, 117 4-11.

[Meyer, 2012] Meyer, J. C., F. Eder, S. Kurasch, V. Skakalova, J. Kotakoski, H.J. Park, S. Roth, A. Chuvilin, S. Eyhusen, G. Benner, A.V. Krasheninnikov, and U. Kaiser (2012). An accurate measurement of electron beam induced displacement cross sections for single-layer graphene. *Phys. Rev. Lett.*, 108:196102.

[Miller, 1991] Miller, LeAnn A., David K. Brice, Anil K. Prinja, and S. Thomas Picraux (1991), "Anisotropic displacement threshold energies in silicon by molecular dynamics simulations", *Mat. Res. Soc. Symp. Proc*., 209:171.

[Miotello, 1997] Miotello, A., R. Kelly (1997), "Revisiting the thermal spike concept in ion-surface interactions", *Nucl. Instrum. Meth, B*, 122 458-469.

[Morita, 1991] Morita, K. (1991), "Metal sputtering and hydrogen retention in metal-carbon composite layer materials", *Fusion Technology*, 19(4):2083-91.

[Moreira, 2009] Moreira, P.A.F.P., R. Devanathan, J.G. Yu, W.J. Weber (2009), "Molecular-dynamics simulation of threshold displacement energies in zircon", *Nucl. Instrum. Meth. B*, 267 3431-3436.

[Motta, 1997] Motta, A.T. (1997), "Amorphization of intermetallic compounds under irradiation - A review", *J. Nucl. Mater.*, 244 227-250.

[Mulroue, 2011] Mulroue, J., D.M. Duffy (2011), "An ab initio study of the effect of charge localization on oxygen defect formation and migration energies in magnesium oxide", *Proc. R. Soc. London, A,* 467 2054-2065.

[Muroga, 1985] Muroga, T., K. Kitajima, S. Ishino (1985), "The effect of recoil energy spectrum on cascade structures and defect production efficiencies", *J. Nucl. Mater.*, 133-134 378-382.

[Nagase, 2012] Nagase, T., T. Sanda, A. Nino, W. Qin, H. Yasuda, H. Mori, et al. (2012), "MeV electron irradiation induced crystallization in metallic glasses: Atomic structure, crystallization mechanism and stability of an amorphous phase under the irradiation", *J. Non-Cryst. Solids*, 358 502-518.

[Naguib, 1975] Naguib, H.M., R. Kelly (1975), "Criteria for bombardment-induced structural changes in non-metallic solids", *Radiat. Effects*, 25 1-12.

[Nakagawa, 2010] Nakagawa S.T. and H.J. Whitlow (2010), "A predictive model for the electronic stopping force for molecular dynamic simulation (I)", *Nucl. Instr. Meth. Phys. Res*. B, 268(19):3287-3290 .

[Nastar, 2012] Nastar, M., F. Soisson (2012), "Radiation-Induced Segregation", in R.J.M. Konings (Ed.) *Comprehensive Nuclear Materials*, Elsevier, Amsterdam , pp. 471-496.

[Nastasi, 1991] Nastasi, M., J.W. Mayer (1991), "Thermodynamics and kinetics of phase transformations induced by ion irradiation", *Materials Science Reports*, 6 1-51.

[NJOY] Puente Espel, F., M.N. Avramova, K.N. Ivanov and S. Misu (2013), "New developments of the MCNP/CTF/NEM/NJOY code system - Monte Carlo based coupled code for high accuracy modelling", *Annals of Nuclear Energy*, 51:18-26.

[Nordlund, 1995] Nordlund K. (1995), "Molecular dynamics simulation of ion ranges in the 1-100 kev energy range", *Comput. Mater. Sci.*, 3:448.

[Nordlund, 1997a] Nordlund, K., N. Runeberg and D. Sundholm (1997), "Repulsive interatomic potentials calculated using hartree-fock and density-functional theory methods", *Nucl. Instr. Meth. Phys. Res*. B, 132:45-54.

[Nordlund, 1997b] Nordlund, K. and R.S. Averback (1997), "Point defect movement and annealing in collision cascades", *Phys. Rev.* B, 56(5):2421−2431.

[Nordlund, 1998a] Nordlund, K and R.S. Averback (1997), "The role of self-interstitial atoms on the high temperature properties of metal", *Phys. Rev. Lett.* 80 (19): 4201-4204.

[Nordlund, 1998b] Nordlund, K., M. Ghaly, R.S. Averback, M. Caturla, T. Diaz de la Rubia and J. Tarus (1998), "Defect production in collision cascades in elemental semiconductors and fcc metals", *Phys. Rev.* B, 57(13):7556-7570.

[Nordlund, 1998c] Nordlund, K., L. Wei, Y. Zhong, and R.S. Averback (1998), "Role of electron-phonon coupling on collision cascade development in ni, pd and pt", *Phys. Rev.* B (Rapid Comm.), 57:13965-13968.

[Nordlund, 1998d] Nordlund, K., M. Ghaly and R.S. Averback (1998), "Mechanisms of ion beam mixing in metals and semiconductors", *J. Appl. Phys.*, 83(3):1238-1246.

[Nordlund, 1999a] Nordlund, K., J. Keinonen, M. Ghaly, and R.S. Averback (1999), "Coherent displacement of atoms during ion irradiation", *Nature*, 398(6722):49-51.

[Nordlund, 1999b] Nordlund K. and R.S. Averback (1999), "Inverse kirkendall mixing in collision cascades", *Phys. Rev.* B, 59:20-23.

[Nordlund, 2005] Nordlund, K., Y. Ashkenazy, R.S. Averback and A.V. Granato (2005), "Strings and interstitials in liquids, glasses and crystals", *Europhys. Lett.*, 71(4):625.

[Nordlund, 2005c] Nordlund, K., J. Wallenius, and L. Malerba (2005), "Molecular dynamics simulations of threshold energies in Fe", *Nucl. Instr. Meth. Phys. Res*. B, 246(2):322-332.

[Nordlund, 2007b] Nordlund, K. (2007), "Molecular dynamics for ion beam analysis", *Nucl. Instr. Meth. Phys. Res*. B, 266:1886.

[Nord, 2002] Nord, J., K. Nordlund and J. Keinonen (2002), "Amorphization mechanism and defect structures in ion beam amorphized si, ge and gaas", *Phys. Rev.* B, 65:165329.

[Nord, 2003a] Nord, J., K. Nordlund, J. Keinonen and K. Albe (2003), "Molecular dynamics study of defect formation in GaN cascades", *Nucl. Instr. Meth. Phys. Res*. B, 202:93.

[Nord, 2003b] Nord, J., K. Nordlund, and J. Keinonen (2003), "A molecular dynamics study of damage accumulation in GaN during ion beam irradiation", *Phys. Rev.* B, 68:184104.

[NRT] Norgett, M.J., M.T. Robinson and I.M. Torrens (1975), "A proposed method of calculating displacement dose rates", Nucl. Engr. and Design, 33(1):50-54.

[NumericalRecipes] Press, W.H., S.A. Teukolsky, W.T. Vetterling, and B.P. Flannery (1995), *Numerical Recipes in C: The Art of Scientific Computing*, Cambridge University Press, New York, second edition.

[Oen, 1973] Oen, O.S. (1973), "Cross sections for atomic displacements in solids by fast electrons", ORNL-4897, Oak Ridge National Laboratory, Oak Ridge, TN, pp. 1-204.

[Okamoto, 1979] Okamoto, P.R., L.E. Rehn (1979), "Radiation-induced segregation in binary and ternary alloys", *J. Nucl. Mater.*, 83 2-23.

[Olsson, 2003] P. Olsson, I.A. Abrikosov, L. Vitos, and J. Wallenius (2003), "Ab initio formation energies of fe-cr alloys", *J. Nucl. Mater*., 321:84.

[Page, 2009] le Page, J., D.R. Mason, C.P. Race and W.M. C. Foulkes (2009), "How good is damped molecular dynamics as a method to simulate radiation damage in metals?" *New J.* Phys., 11:013004.

[Paine, 1985] Paine, B.M., R.S. Averback (1985), "Ion-Beam Mixing- Basic Experiments", *Nucl. Instrum. Meth. Phys, Res. B*, 7-8 666-675.

[Partyka, 2001] Partyka, P., Y. Zhong, K. Nordlund, R.S. Averback, I.K. Robinson, and P. Ehrhart (2001), "Grazing incidence diffuse x-ray scattering investigation of the properties of irradiation-induced point defects in silicon", *Phys. Rev. B*, 64:235207.

[Park, 2000] Park, B., W.J. Weber, L.R. Corrales (2000), "Molecular dynamics simulation of the threshold displacement energy in MgO", *Nucl. Instrum. Meth. B*, 166-167 357-363.

[Park, 2001] B. Park, W.J. Weber, L.R. Corrales, "Molecular-dynamics simulation study of threshold displacements and defect formation in zircon", *Phys. Rev. B*, 64 (2001) 174108.

[Peltola, 2003a] Peltola, J., K. Nordlund, and J. Keinonen (2003), "Explicit phase shift factor stopping model for multi-component targets", *Nucl. Instr. Meth. Phys. Res*. B, 212:118.

[Peltola, 2004] Peltola, J., L.A. Marques, J. Barbolla (2004), « Ion-beam-induced amorphization and recrystallization in silicon, *J. Applied Physics* (96(11): 5947-5976.

[Phythian, 1995] Phythian, W.J., R.E. Stoller, A.J.E. Foreman, A.F. Calder and D.J. Bacon (1995), "A comparison of displacement cascades in copper and iron by molecular dynamics and its application to microstructural evolution", *J. Nucl. Mater.*, 223:245.

[PointDefects] Agullo-Lopez, F., C.R. A Catlow and P.D. Townsend (1988), Point Defects in Materials, Academic, London.

[Posselt, 2000b] Posselt, M. (2000), "Prediction of the morphology of the as-implanted damage in silicon using a novel combination of bca and md simulations", *Materials Science in Semiconductor Processing*, 3(4):317-23.

[Postawa, 2003] Postawa, Z., B. Czerwinski, M. Szewczyk, E.J. Smiley, N. Winograd and B.J. Garrison (2003), "Enhancement of sputtering yields due to c_{60} versus Ga bombardment of ag{111} as explored by molecular dynamics simulations", *Anal. Chem.*, 75:4402-4407.

[Poulin, 1980] Poulin F. and J.C. Bourgoin (1980), "Threshold energy for atomic displacement in electron irradiated germanium", *Rev. Phys. Appl.*, 15(1):15.

[Pronnecke, 1991] Pronnecke, S., A. Caro, M. Victoria, T. Diaz de la Rubia and M.W. Guinan (1991), "The effect of electronic energy loss on the dynamics of thermal spikes in Cu", J. Materials Research, 6(3):483-91.

[Pruneda, 2007] Pruneda, J.M., D. Sanchez-Portal, A. Arnau, J.I. Juaristi and E. Artacho (2007), "Electronic stopping power in lif from first principles", *Phys. Rev. Lett.*, 99:235501.

[Puska, 1998] Puska, M.J., S. Pöykkö, M. Pesola and R.M. Nieminen (1998), "Convergence of supercell calculations for point defects in semiconductors: vacancy in silicon", *Phys. Rev.* B, 58:1318-1325.

[Raman, 1994] Raman, S., E.T. Jurney, J.W. Warner, A. Kuronen, J. Keinonen, K. Nordlund, and D.J. Millener (1994), "Lifetimes in 15n from gamma-ray lineshapes produced in the 2h(14n,pgamma) and 14n(thermal n, gamma) reactions", *Phys. Rev.* C., 50(2):682.

[Ravelosona, 2000] Ravelosona, D., C. Chappert, V. Mathet, H. Bernas (2000), "Chemical order induced by ion irradiation in FePt (001) films", *Applied Physics Letters*, 76 236-238.

[Rieth, 2013] Rieth, M., S.L. Dudarev, S.M. Gonzalez de Vicente, J. Aktaa, T. Ahlgren, S. Antusch, D.E.J. Armstrong, M. Balden, N. Baluc, M.-F. Barthe, W.W. Basuki, M. Battabyal, C.S. Becquart, D. Blagoeva, H. Boldyryeva, J. Brinkmann, M. Celino, L. Ciupinski, J.B. Correia, A. De Backer, C. Domain, E. Gaganidze, C. Garciya-Rosales, J. Gibson, M.R. Gilbert, S. Giusepponi, B. Gludovatz, H. Greuner, K. Heinola, T. Höschen, A. Hoffmann, N. Holstein, F. Koch, W. Krauss, H. Li, S. Lindig, J. Linke, Ch. Linsmeier, P. Lopez-Ruiz, H. Maier, J. Matejicek, T.P. Mishra, M. Muhammed, A. Munoz, M. Muzyk, K. Nordlund, D. Nguyen-Manh, J. Opschoor, N. Ordas, T. Palacios, G. Pintsuk, R. Pippan, J. Reiser, J. Riesch, S.G. Roberts, L. Romaner, M. Rosinski, M. Sanchez, W. Schulmeyer, H. Traxler, A. Urena, J.G. van der Laan, L. Veleva, S. Wahlberg yand M. Walter, T. Weber, T. Weitkamp, S. Wurster, M.A. Yar, J.H. You, and A. Zivelonghi (2013), "Recent progress in research on tungsten materials for nuclear fusion applications in Europe", *Journal of Nuclear Materials*, 432(1-3):482-500.

[Rizza, 2007] Rizza, G., H. Cheverry, T. Gacoin, A. Lamas, and S. Henry (2007), "Ion beam irradiation of embedded nanoparticles: Toward an in situ control of size and spatial distribution", *J. Appl. Phys.*, 101:014321.

[Rizza, 2007b] Rizza, G., A. Dunlop and A. Dezellus (2007), "Behavior of metallic nanoparticles in al matrix under high electronic energy deposition", *Nucl. Instr. Meth. Phys. Res*. B, 256(1):219-223.

[Robinson, 1967] Robinson, M.T. and A.L. Southern (1967), "Sputtering experiments with 1- to 5-Kev Ar+ ions. II. monocrystalline targets of Al, Cu and Au", *J. Appl. Phys.*, 38(7):2969-2973.

[Robinson, 1982] Robinson, M.T. and O.S. Oen (1982), "On the use of thresholds in damage energy calculations", *J. Nucl. Mater.*, 110(2-3):147-149.

[Robinson, 1992] Robinson, M.T. (1992), "Computer simulation studies of high-energy collision cascades", *Nucl. Instr. Meth. Phys. Res*. B, 67:396.

[Robertson, 1996] Robertson, I.M. and I. Jenčič (1996), "Regrowth of amorphous regions in semiconductors by sub-threshold electron beams", *J. Nucl. Mater.*, 239:273-278.

[Roberto, 1977] Roberto, J.B., C.E. Klabunde, J.M. Williams, R.R. Coltman, M.J. Saltmarsh, C.B. Fulmer (1977), "Damage production by high-energy D-Be neutrons in Cu, Nb and Pt at 4.2 degrees K", *Applied Physics Letters*, 30 509-511.

[Robinson, 2012] Robinson, M., N.A. Marks, K.R. Whittle, G.R. Lumpkin (2012), "Systematic calculation of threshold displacement energies: Case study in rutile", *Phys. Rev.* B, 85 104105.

[Roorda, 1992] Roorda, S., R.A. Hakvoort, Veen-A. van, P.A. Stolk, and F.W. Saris (1992), "Structural and electrical defects in amorphous silicon probed by positrons and electrons", *J. Appl. Phys.*, 72(11):5145.

[Roorda, 1999] Roorda, S. (1999), "Low temperature relaxation in amorphous silicon made by ion implantation", *Nucl. Instr. Meth. Phys. Res*. B., Proceedings of the IBMM98 conference.

[Rosenblatt, 1955] Rosenblatt, D.B., R. Smoluchowski, G.J. Dienes (1955), "Radiation induced changes in the electrical resistivity of alpha brass", *J. Appl. Phys.*, 26 1044-1049.

[Roth, 1975] Roth, G., H. Wollenberger, C. Zeckau, K. Lücke (1975), "Energy dependence of the defect production at 78 K and 400 K in electron irradiated copper", *Radiat. Effects*, 26 141-148.

[Ruault, 1984] Ruault, M.O., J. Chaumont, J.M. Penisson and A. Bourret (1984), "High resolution and in situ investigation of defects in bi-irradiated si", *Phil. Mag.* A, 50(5):667.

[Rubia, 1995] Diaz de la Rubia, T. and G.H. Gilmer (1995), "Structural transformations and defect production in ion implanted silicon: A molecular dynamics simulation study", *Phys. Rev. Lett.*, 74(13):2507-2510.

[Russell, 1984] Russell, K.C. (1984), "Phase stability under irradiation", *Prog. Mater. Sci*., 28 229-434.

[Rutherford, 2007] Rutherford, A.M. and D.M. Duffy (2007), "The effect of electron-ion interactions on radiation damage simulations", *J. Phys. Cond. Matter*, 19:496201.

[Samela, 2005] Samela, J., J. Kotakoski, K. Nordlund and J. Keinonen (2005), "A quantitative and comparative study of sputtering yields in Au", *Nucl. Instr. Meth. Phys. Res*. B, 239(4):331-346.

[Samela, 2007] Samela, J., K. Nordlund, J. Keinonen and V.N. Popok (2007), "Comparison of silicon potentials for cluster bombardment simulations", *Nucl. Instr. Meth. Phys. Res*. B, 255:253-258.

[Sandoval, 2009] Sandoval, L. and H.M. Urbassek (2009), "Influence of electronic stopping on sputtering induced by cluster impact on metallic targets", *Physical Review B*, 79(14).

[Schultz, 2007d] Schulz-Ertner, D. and H. Tsujii (2007), "Particle radiation therapy using proton and heavier ion beams", *Journal of Clinical Oncology*, 25(8):953-964.

[Schober, 1993] Schober, H.R., C. Oligschleger and B.B. Laird (1993), "Low-frequency vibrations and relaxations in glasses", *J. of Non-Cryst. Solids*, 156-158:965-968.

[Schilling, 1994] Schilling, W., H. Ullmaier (1994), "Physics of Radiation Damage in Metals", in: B.R.T. Frost (Ed.) *Materials Science and Technology: A comprehensive treatment*, VCH, Weinheim, Germany, pp. 179-241.

[Schnohr, 2006] Schnohr, C.S., E. Wendler, K. Gartner, W. Wesch, K. Ellmer (2006), "Ion-beam induced effects at 15 K in alpha-Al2O3 of different orientations", *J. Appl. Phys.*, 99 123511.

[Seebauer, 2006] Seebauer, E.G. M.C. Kratzer (2006), "Charged point defects in semiconductors", Mater. Sci. Eng. R, 55 57-149.

[Seitz, 1956] Seitz, F. and J.S. Koehler (1956), "Displacement of atoms during irradiation" in *Solid State Physics, Vol. 2, p. 307.*

[Sibley, 1984] Sibley, W.A. (1984), "Radiation damage processes in insulating materials", *Nucl. Instrum. Meth. B*, 1 419-426.

[Sickafus, 2007] Sickafus, K.E., R.W. Grimes, J.A. Valdez, A. Cleave, M. Tang, M. Ishimaru, et al. (2007), "Radiation-induced amorphization resistance and radiation tolerance in structurally related oxides", *Nature Mater.*, 6 217-223.

[Siegel, 1949] Siegel, S. (1949), "Effect of neutron bombardment on order in the alloy Cu_3Au", *Physical Review*, 75 1823-1824.

[Sigle, 1994] Sigle, W., A. Seeger (1994), "Temperature dependence of the threshold energy for atom displacements in Cu", *Phys. Status Solidi A*, 146 57-59.

[Sillanpää, 2000] Sillanpää, J., J. Peltola, K. Nordlund, J. Keinonen and M.J. Puska (2000), "Electronic stopping calculated using explicit phase shift factors", *Phys. Rev. B*, 63:134113.

[Silcox, 1959b] Silcox, J. and P.B. Hirsch (1959), "Dislocation loops in neutron-irradiated copper", *Phil. Mag.*, 4:1356-1374.

[Sizmann, 1978] Sizmann, R. (1978), "The effect of radiation upon diffusion in metals", *J. Nucl. Mater.*, 69-70 386-412.

[Smith, 2001] Smith, B.W. and D.E. Luzzi (2001), "Electron irradiation effects in single wall carbon nanotubes", *J. Appl. Phys.*, 90(7):3509.

[Smith, 1997] Smith, R. (ed.) (1997), "Atomic and ion collisions in solids and at surfaces: theory, simulation and applications", Cambridge University Press, Cambridge, United Kingdom.

[Smith, 2000] Smith, K.L., R. Cooper, M. Colella, E.R. Vance (2000), "Measured displacement energies of oxygen ions in zirconolite and rutile", in: K.P. Hart, G.R. Lumpkin (Eds.) *Scientific Basis for Nuclear Waste Management XXIV, Materials Research Society Symp. Proc.* Vol. 663, pp. 373-379.

[Smith, 2003] Smith, K.L., M. Colella, R. Cooper, E.R. Vance (2003), "Measured displacement energies of oxygen ions in titanates and zirconates", *J. Nucl. Mater.*, 321 19-28.

[Smith, 2005] Smith, K.L., N.J. Zaluzec (2005), "The displacement energies of cations in perovskite ($CaTiO_3$), *J. Nucl. Mater.*, 336 261-266.

[Smith, 2005a] Smith, R., D. Bacorisen, B.P. Uberuaga, K.E. Sickafus, J.A. Ball, R.W. Grimes (2005), "Dynamical simulations of radiation damage in magnesium aluminate spinel", $MgAl_2O_4$", *J. Phys.: Condens. Matter*, 17 875-891.

[Sosin, 1969] Sosin, A., W. Bauer (1969), "Atomic displacement mechanisms in metals and semiconductors", in G.J. Dienes (Ed.) *Studies in Radiation Effects in Solids*, Vol. 3, Gordon and Breach, New York, pp. 153-357.

[Spaepen-Turnbull, 1982] Spaepen, Frans and David Turnbull (1982), "Crystallization processes", Chapter 2, pages 15-42, Academic Press, New York.

[SRIM-2013] Ziegler, J.F., SRIM-2013 software package, available online at http://www.srim.org/.

[SRIMbook] Ziegler, J.F., J.P. Biersack and M.D. Ziegler (2008), SRIM - *The Stopping and Range of Ions in Matter*, SRIM Co., Chester, Maryland, United States.

[Steeds, 2011] Steeds, J.W. (2011), "Orientation dependence of near-threshold damage production by electron irradiation of 4H SiC and diamond and outward migration of defects", *Nucl. Instrum. Meth. B*, 269 1702-1706.

[Stievenard, 1990] Stievenard, D., X. Boddaert, J.C. Bourgoin, H.J. von Bardeleben (1990), "Behavior of electron-irradiation-induced defects in GaAs", *Phys. Rev.* B, 41 5271-5279.

[Stoller, 2013] Stoller, R.E., M.B. Toloczko, G.S. Was, A.G. Certain, S. Dwaraknath, and F.A. Garner (2013), "On the use of srim for computing radiation damage exposure", *Nucl. Instr. Meth. Phys. Res*. B, 310:75.

[Stoller, 2012] Stoller, R.E. (2012), "Primary Radiation Damage Formation", in R.J.M. Konings (Ed.) *Comprehensive Nuclear Materials*, Elsevier, Amsterdam, pp. 293-332.

[Stuchbery, 1999] Stuchbery, A.E. and E. Bezakova (1999), "Thermal-spike lifetime from picosecond-duration preequilibrium effects in hyperfine magnetic fields following ion implantation", *Phys. Rev. Lett.*, 82(18):3637.

[Suzudo; Doran, 1970] Doran (1970), Radiation Effects 2, 249-267.

[Suzudo; English, 2001] English, C.A., S.R. Ortner, G. Gage, et al. (2001), in *Effects of Radiation on Materials*, ASTM STP 1405 151.

[Suzudo; Gao, 1999] Gao, F., D.D. Bacon, A.V. Barashev, H.L Heinisch (1999), Mat. Res. Soc. Symp. Proc. 540, 703-708.

[Suzudo; Heinisch, 1996] Heinisch, H.L., B.N. Singh (1996), *J. Nucl. Mater.* 232, 206-213.

[Suzudo; Ortiz, 2007] Ortiz, C.J. and M.J. Caturla (2007), *Phys. Rev. B*, 75 184101.

[Suzudo; Phythian, 1995] Phythian, W.J., R.E. Stoller, AJ.E. Foreman, A.F Calder, D.J. Bacon (1995), *J. Nucl. Mater.* 223, 245-261.

[Suzudo; Soneda, 1998] Soneda, N., T.D. de la Rubia (1998), *Phil. Mag.* A 78, 995-1019.

[Suzudo; Souidi, 2006] Souidi, A. et al. (2006), *J. Nucl. Mater.* 355, 89-103.

[Suzudo; Suzudo, 2012] Suzudo, T., S.I Golubov, R.E. Stoller, M. Yamaguchi, T. Tsuru, H. Kaburaki (2012), *J. Nucl. Mater.* 423, 40-46.

[Suzudo; Terentyev, 2008] Terentyev, D.A., L. Malerba, P. Klaver, P. Olsson (2008), J. of Nucl. Mater, 382 126-133.

[Suzudo; Lucasson, 2008] Lucas, G. and R. Schäublin (2008), J. Phys.: Condens. Matter 20 415206.

[Szymczak, 1993] Szymczak, W. and K. Wittmaack (1993), " Angular distributions of gold sputtered from a (111) crystal: dependence of spot shapes and of spot and background yields on the primary ion mass and energy an on the target temperature, *Nucl. Instr. Meth. Phys. Res.,* B, 82 (2): 220-33.

[Tan, 1996] M. Tang, L. Colombo, J. Zhu, and T. Diaz de la Rubia (1997), "Intrisic point defects in crystalline silicon: Tight-binding molecular dynamics studies of self-diffusion, interstitial-vacancy recombination and formation volumes", Phys. Rev. B, 55(21):14279.

[Terentyev, 2008b] Terentyev, D. A. T. P. C. Klaver, P. Olsson, M.-C. Marinica, F. Willaime, C. Domain, and L. Malerba (2008), "Self-trapped interstitial-type defects in iron", *Phys. Rev. Lett.*, 100:145503.

[Thomas, 1982] Thomas, G., H. Mori, H. Fujita, R. Sinclair (1980), "Electron irradiation induced crystalline amorphous transitions in Ni-Ti alloys", *Scripta Metall.*, 16 589-592.

[Thomas, 2005] Thomas, B.S., N.A. Marks, L.R. Corrales, R. Devanathan (2005), "Threshold displacement energies in rutile TiO2: A molecular dynamics simulation study", *Nucl. Instrum. Meth. B*, 239 191-201.

[Thomé, 2013] Thomé, L. A. Debelle, F. Garrido, P. Trocellier, Y. Serruys, G. Velisa, S. Miro (2013), "Combined effects of nuclear and electronic energy losses in solids irradiated with a dual-ion beam", *Applied Physics Letters*, 102 141906.

[Thompson, 1973] Thompson, L.J., G. Youngblood, A. Sosin (1973), "Defect retention in copper during electron irradiation at 80 K", *Radiat. Effects*, 20 111-134.

[Torri, 1994] Torri, P., J. Keinonen and K. Nordlund (1994), "A low-level detection system for hydrogen analysis with the reaction 1h(15n,alphagamma)12c", *Nucl. Instr. Meth. Phys. Res*. B, 84:105.

[Toulemonde, 1994] Toulemonde, M., S. Bouffard, F. Studer (1994), "Swift heavy ions in insulating and conducting oxides: tracks and physical processes", *Nucl. Instrum. Meth. B*, 91 108-123.

[Toulemonde, 2004] Toulemonde, M.C. Trautmann, E. Balanzat, K. Hjort, A. Weidinger (2004), "Track formation and fabrication of nanostructures with MeV-ion beams", *Nucl. Instrum. Meth. Phys. Res. B*, 216 1-8.

[Toulemonde, 2011] Toulemonde, M., W.J. Weber, G. Li, V. Shuttanandan, P. Kluth, T. Yang, Y. Wang, Y.W. Zhang (2011), "Synergy of nuclear and electronic energy losses in ion-irradiation processes: The case of vitreous silicon oxide", Physical Review B 83 054106.

[Trikhaus, 1984] Trinkaus H. and W. G. Wolfer (1984), "Conditions for dislocation loop punching by helium bubbles", *J. Nucl. Mater.*, 122 & 123:552--557.

[TRIM] Biersack, J.P. and L.G. Haggmark (1980), "A Monte Carlo computer program for the transport of energetic ions in amorphous targets", Nucl. Instr. Meth., 174:257.

[Turos, 1999] Turos, A., A. Stonert, B. Breeger, E. Wendler, W. Wesch, and R. Fromknecht (1999), "Low temperature transformations of defects in gaas and algaas", *Nucl. Instr. Meth. Phys. Res*., 148:401-405.

[Uberuaga, 2005] Uberuaga, B.P., R. Smith, A.R. Cleave, G. Henkelman, R.W. Grimes, A.F. Voter, K.E. Sickafus (2005), "Dynamical simulations of radiation damage and defect mobility in MgO", *Phys. Rev.* B, 71 104102.

[Urban, 1982] Urban K., B. Saile, N. Yoshida and W. Zag (1982), "The temperature dependence of the displacement threshold energy in f.c.c. and b.c.c. metals", in Jin-Ichi Takamura, editor, *Point Defects and Defect Interactions in Metals*, page 783. North Holland, Amsterdam.

[Urban, 1981] Urban, K. and N. Yoshida (1981), "The threshold energy for atom displacement in irradiated copper studied by high-voltage electron microscopy", *Philos. Mag. A*, 44 1193-1212.

[Vajda, 1977] Vajda, P. (1977), "Anisotropy of electron radiation damage in metal crystals", *Rev. Mod. Phys*., 49:481.

[vanSambeek, 1998] Van Sambeek, A.I., R.S. Averback, C.P. Flynn, M.H. Yang, W. Jager (1998), "Radiation enhanced diffusion in MgO", *J. Appl. Phys.*, 83 7576-7584.

[Vehse, 1968] Vehse, W. E., W. A. Sibley, F. J. Keller and Y. Chen (1968), "Radiation damage in zno single crystals", *Phys. Rev.*, 167(3):828.

[Vitvoskii, 1977] Vitovskii, N.A., D. Mustafakulov, and A.P. Chekmareva (1977), "Threshold energy for the displacement of atoms in semiconductors", *Sov. Phys. Semicond*., 11(9):1024-1028.

[Vollmayr, 2002] Vollmayr-Lee, K., W. Kob, K. Binder and A. Zippelius (2002), *J. Chem. Phys.*, 116:5158.

[Wakai, 1995] Wakai, E., A. Hishinuma, Y. Kato, H. Yano, S. Takai, K. Abiko (1995), "Radiation-induced alpha' phase formation on dislocation loops in Fe-Cr alloys during electron irradiation", J. Phys. IV, 5 277-286.

[Wallner, 1988] Wallner, G., M.S. Anand, L.R. Greenwood, M.A. Kirk, W. Mansel, W. Waschkowski (1988), "Defect production rates in metals by reactor neutron irradiation at 4.6 K", *J. Nucl. Mater.*, 152 146-153.

[Weber, 1998] Weber, W.J., R.C. Ewing, C.R.A. Catlow, T. Diaz de la Rubia, L.W. Hobbs, C. Kinoshita, et al. (1998), "Radiation effects in crystalline ceramic phases relevant to the immobilization and disposition of nuclear waste and weapons plutonium", *J. Mater. Res.*, 13 1434-1484.

[Weber, 2000] Weber, W.J. (2000), "Models and mechanisms of irradiation-induced amorphization in ceramics", *Nucl. Instrum. Meth. Phys. Res. B*, 166 98-106.

[Weber, 2012] Weber, W.J., Y.W. Zhang, L.M. Wang (2012), "Review of dynamic recovery effects on ion irradiation damage in ionic-covalent materials", *Nucl. Instrum. Meth. B*, 277 1-5.

[Wendler, 2003] Wendler, E., A. Kamarou, E. Alves, K. Gärtner and W. Wesch (2003), "Three-step amorphisation process in ion-implanted gan at 15 k", *Nucl. Instr. Meth. Phys. Res*. B, 206:1028.

[Wendler, 2004] Wendler, E., W. Wesch, E. Alves and A. Kamarou (2004), "Comparative study of radiation damage in GaN and InGaN by 400 keV Au implantation", *Nucl. Instr. Meth. Phys. Res*. B.

[Wendler, 2008] Wendler, E., K. Gärtner, W. Wesch (2008), "Comparison of ion-induced damage formation in (110) and (100) MgO", *Nucl. Instrum. Meth. B*, 266 2872-2876.

[Wendler, 2009] Wendler, E., O. Bilani, K. Gärtner, W. Wesch, M. Hayes, F.D. Auret, et al. (2009), "Radiation damage in ZnO ion implanted at 15 K", *Nucl. Instrum. Meth. Phys. Res. B*, 267 2708-2711.

[Willaime, 2001] Willaime, F. (2001), "Impact of electronic structure calculations on the study of diffusion in metals. Revue de Metallurgie", 98(12):1065-71.

[Williams, 1998] Williams, J.S. (1998), Ion implantation of semiconductors, Mater. Sci. Eng. A, 253 8-15.

[Winters, 1992] Winters, H. F. and J. W. Coburn (1992), "Surface science aspects of etching reactions". *Surf. Sci. Rep*, 14:161.

[Windl, 1998] Windl, W., T.J. Lenosky, J.D. Kress, and A.F. Voter (1998), "First-principles investigation of radiation induced defects in si and sic", *Nucl. Instr. and Meth.* B, 141:61-65.

[Wollenberger, 1970] Wollenberger, H.J. (1970), "Production rates of Frenkel defects during low temperature irradiations", in A. Seeger, et al. (Eds.) *Vacancies and Interstitials in Metals*, North-Holland, Amsterdam, pp. 215-254.

[Wurm, 1969] Wurm, J. (1969), "Determination of the displacement function in Al and Cu from the measurement of the activation at low temperature electron irradiation", Kernforschungsanlage Julich, Rept. No. Jul-581-FN.

[Xiaglong, 2002] Xianglong, Yuan and A. N. Cormack (2002), "Efficient algorithm for primitive ring statistics in topological networks", *Comput. Mat. Sci.*, 24:343.

[Xiao, 2012] Xiao, H.Y., Y. Zhang, W.J. Weber (2012), "Ab initio molecular dynamics simulations of low-energy recoil events in ThO_2, CeO_2, and ZrO_2", *Phys. Rev.* B, 86 054109.

[Xu, 2013] Xu, H., R. E. Stoller, Y. N. Osetsky, and D. Terentyev (2013), "Solving the puzzle of < 100 > interstitial loop formation in bcc iron", *Phys. Rev. Lett.*, 110:265503.

[Yasunaga, 2008] Yasunaga, K., K. Yasuda, S. Matsumura, T. Sonoda (2008), "Electron energy-dependent formation of dislocation loops in CeO_2", *Nucl. Instrum. Meth. Phys. Res. B*, 266 2877-2881.

[Zag, 1983] Zag, W., K. Urban (1983), "Temperature dependence of the threshold energy for atom displacement in irradiated molybdenum", *Phys. Status Solidi A*, 76 285-295.

[Zarkadoula, 2013] Zarkadoula, E., R. Devanathan, W.J. Weber, M. Seaton, I.T. Todorov, K. Nordlund, M.T. Dove, and K. Trachenko (2013), "Uncovering the hidden damage in irradiated zirconia", *Phys. Rev.* B.

[ZBL] Ziegler, J.F., J.P. Biersack and U. Littmark (1985), "The Stopping and Range of Ions" in *Matter. Pergamon*, New York.

[Zeb, 2012] Zeb, M. Ahsan, J. Kohanoff, D. Sanchez-Portal, A. Arnau, J.I. Juaristi, and E. Artacho (2012), "Electronic stopping power in gold: The role of d electrons and the h=he anomaly", *Phys. Rev. Lett.*, 108:225504.

[Zhu, 1995] Zhu, Huilong, R.S. Averback and M. Nastasi (1995), "Molecular dynamics simulations of a 10 kev cascade in beta-nial", *Phil. Mag.* A, 71(4):735.

[Zinkle, 1993] Zinkle, S.J. and B.N. Singh (1993), "Analysis of displacement damage and defect production under cascade damage conditions", *J. Nucl. Mater.*, 199(3):173-191.

[Zinkle1988] Zinkle, S.J. (1988), "Electrical resistivity of small dislocation loops in irradiated copper", *J. Phys. F: Metal Phys*., 18 377-391.

[Zinkle1993] Zinkle, S.J., B.N. Singh (1993), "Analysis of displacement damage and defect production under cascade damage conditions", *J. Nucl. Mater.*, 199 173-191.

[Zinkle, 1995] Zinkle, S.J. (1995), "Effect of irradiation spectrum on the microstructural evolution in ceramic insulators", *J. Nucl. Mater.*, 219 113-127.

[Zinkle, 1996] Zinkle, S.J., L.L. Snead (1996), "Influence of irradiation spectrum and implanted ions on the amorphization of ceramics", *Nucl. Instrum. Meth. B*, 116 92-101.

[Zinkle, 1997] Zinkle, S.J., C. Kinoshita, "Defect production in ceramics", *J. Nucl. Mater.*, 251 (1997) 200-217.

[Zinkle, 1997a] Zinkle, S.J., "Irradiation spectrum and ionization-induced diffusion effects in ceramics", in I.M. Robertson, et al. (Eds.) Microstructure Evolution During Irradiation, Materials Research Society, Pittsburgh, 1997, pp. 667-678.

[Zinkle, 2012] Zinkle, S.J (2012), Radiation-Induced Effects on Microstructure, in: R.J.M. Konings (Ed.) Comprehensive Nuclear Materials, Elsevier, Amsterdam, pp. 65-98.

[Zinkle, 2002] Zinkle, S.J., V.A. Skuratov, D.T. Hoelzer (2002), "On the conflicting roles of ionizing radiation in ceramics", *Nucl. Instrum. Meth. B*, 191 758-766.

[Zinkle3] Wang, L.M., S.X. Wang, R.C. Ewing, A. Meldrum, R.C. Birtcher, P. Newcomer Provencio, et al. (2000), "Irradiation-induced nanostructures", *Mater. Sci. Eng. A,* 286 72-80.

[Zinkle5] Singh, B.N., S.J. Zinkle (1993), "Defect accumulation in pure FCC metals in the transient regime: a review", *J. Nucl. Mater.*, 206 212-229.

[Zinkle6] Zinkle, S.J., C. Kinoshita (1997), *Defect production in ceramics*, *J. Nucl. Mater.*, 251 200-217.

[Zinkle,Stoller, 2012] Stoller (2012), Comp. Nucl. Materials.

[Zöllmer, 2002] Zöllmer, V., K. Rätzke, F. Faupel, A. Rehmet, and U. Geyer (2002), "Evidence of diffusion via collective hopping in metallic supercooled liquids and glasses", *Phys. Rev.* B (R), 65:220201.

Appendix: Expert Group on Primary Radiation Damage

Chair

NORDLUND, Kai (Finland)

Members

MALERBA, Lorenzo (Belgium)

BANHART, Florian (France)

SIMEONE, David (France)

WILLAIME, Francois (France)

OKITA, Taira (Japan)

SONEDA, Naoki (Japan)

SUZUDO, Tomoaki (Japan)

CATURLA, Maria Jose (Spain)

BACON, David J. (United Kingdom)

DUDAREV, Sergei (United Kingdom)

WEBB, Roger (United Kingdom)

AVERBACK, Robert (Bob) S. (United States)

GARNER, Frank A. (United States)

STOLLER, Roger E. (United States)

WEBER, William (United States)

ZINKLE, Steven J. (United States)

Scientific Secretary

MASSARA, Simone (OECD/NEA)